

A comprehensive study of new hybrid models for ANFIS with five meta-heuristic algorithms (IWO, DE, FA, PSO, BA) for spatial prediction of groundwater spring potential mapping

Khabat Khosravi¹, Mahdi Panahi^{*2}, Dieu Tien Bui^{*3}

1-Department of watershed management engineering, Faculty of Natural Resources, Sari Agricultural Science and Natural Resources University, Sari, Iran. (E-mail: khabat.khosravi@gmail.com)

2- Department of Geophysics, Young Researchers and Elites Club, North Tehran Branch, Islamic Azad University, Tehran, Iran. (E-mail: panahi2012@yahoo.com)

3- Geographic Information System Group, Department of Business and IT, University College of Southeast Norway, Gullbringvengen 36, 3800 Bø i Telemark, Norway. (E-mail: Dieu.T.Bui@usn.no)

Abstract

Groundwater is one of the most valuable natural resources in the world; therefore developing advanced tools for sustainable management of the groundwater is highly necessary. One of the most important tools for the management of the groundwater is groundwater potential map (GPM). The current study's aim is to proposed and verified new artificial intelligence methods for spatial prediction of groundwater spring potential mapping at Koohtasht-Nourabad plain, Lorestan province, Iran. These methods are new hybrids of Adaptive Neuro-Fuzzy Inference System (ANFIS) with five meta-heuristic algorithms, Invasive Weed Optimization (IWO), Differential Evolution (DE), Firefly (FA), Particle Swarm Optimization (PSO), and Bees (BA) algorithm. Accordingly, a total of 2463 springs were identified and collected, and then, divided in two subsets randomly, including 70% (1725 locations) of the total springs were used for training models, whereas the remaining 30% (738 spring locations) were utilized for the model evaluation. Thirteen groundwater conditioning factors, slope degree, slope aspect, altitude, plan curvature, stream power index (SPI), topographic wetness index (TWI), terrain roughness index (TRI), distance from fault, distance from river, land-use/land-cover, rainfall, soil order, and lithology were prepared for modeling. In the next step, the Stepwise Assessment Ratio Analysis (SWARA) method was employed to quantify the degree of relevance of these conditioning factors and the springs. The global performance of these derived models was assessed using the Area Under the curve (AUC). In addition, the Freidman and Wilcoxon signed rank test were carried out to check and confirm the best model in this study. The result showed that these models has high performance; however, the ANFIS-DE mdel has the highest prediction capability (AUC = 0.875), followed by the ANFIS-IWO model, the ANFIS-FA model (0.873), the ANFIS-PSO model (0.865), and the ANFIS-BA model (0.839). The results of this research can be useful for decision makers to sustainable management of groundwater resources.

Key words: Groundwater spring, ANFIS-DE, ANFIS-IWO, ANFIS-FA, ANFIS-PSO, ANFIS-BA, Iran.

1. Introduction

Groundwater is defined as the water in a saturated zone which fills rock and pore spaces (Berhanu et al., 2014; Fitts, 2002), whereas groundwater potential is the possibility of groundwater occurrence in an area (Jha et al., 2010). The occurrence of groundwater in an aquifer is affected

by various geo-environmental factors including lithology, topography, geology, fault and fracture and its connectivity, drainage pattern and land-use/land-cover (Mukherjee, 1996). Geological strata acts like a conduit and reservoir for groundwater while storage and transmissivity influence the suitability of exploitation of groundwater in a given geological formation. Downhill and depression slopes impart runoff and improve recharge and infiltration, respectively (Waikar and Nilawar, 2014).

Groundwater, which serves as a major source of drinking water to communities, agricultural and industrial sectors, is one of the most precious natural resources in the world (David Keith Todd and Mays, 1980) due to its consistent temperature and widespread availability, low vulnerability to pollution, low development cost, and drought dependability (Jha et al., 2007). Globally, 1.5 billion people are dependent on groundwater, solely for drinking purposes, and about 38% of the irrigated lands depend on the groundwater itself (Siebert et al., 2013). Due to population growth, the demand of water is constantly increased. A major challenge now is how to have sustainable management system of groundwater to preserve and ensure continuous supply with regards to the water demand. One of the most important measures for the groundwater resource management is to collect adequate knowledge on spatial and temporal distribution of groundwater, its quantity as well as its quality.

For the case of Iran, Approximately two-third of the land is covered by deserts. As a result, similar to other arid regions, the main sources of water supply for drinking and other are the groundwater (Nosrati and Van Den Eeckhaut, 2012). Agriculture, which is one of the most prominent economic sectors in Iran, and especially, in the study area, is still be limited due to water scarcity (Zehtabian et al., 2010). Groundwater in Iran supplies around 65% of the water use-up and the remaining 35% is supplied by surface water (Rahmati et al., 2016). One of the most important measures to responsible for the increase of fresh-water is to identify groundwater potential zoning, an essential tool for performing a successful groundwater determination, protection, and management program (Ozdemir, 2011a).

There are a number of methods for groundwater exploitation in traditional approaches including drilling as well as geological, geophysical, and hydrogeological methods. Yet, they are time-consuming, costly (David Keith Todd and Mays, 1980; Israil et al., 2006; Jha et al., 2010; Sander et al., 1996; Singh and Prakash, 2002). Recently, the application of geographic information systems (GIS) and remote sensing (RS) has become an effective procedure for groundwater potential mapping (Fashae et al., 2014) due to their ability in handling huge amount of spatial data, and their applicability for being used efficiently in various fields, including water resources management. In more recent years, some probabilistic models such as frequency ratio (Oh et al., 2011), multi-criteria decision analysis (MCDA) (Kaliraj et al., 2014) (Rahmati et al., 2015) weights-of-evidence (WofE) (Pourtaghi and Pourghasemi, 2014), logistic regression (LR) (Ozdemir, 2011b; Pourtaghi and Pourghasemi, 2014), evidential belief function (EBF) (Nampak et al., 2014; Pourghasemi and Beheshtirad, 2015), decision tree (DT) (Chenini and Mammou, 2010), artificial neural network model (ANN) (Lee et al., 2012), and Shannon's entropy (Naghbi et al., 2015) have been considered for groundwater potential mapping. Bivariate and multivariate statistical models have disadvantages in measuring the relationship between groundwater occurrence and conditioning factors (Tehrany et al., 2013; Umar et al., 2014), whereas MCDA technique is source of bias due to expert opinion. Traditional modeling approaches are mainly based on linear or additive modeling that is not consistent with natural process in the environment

(Clapcott et al., 2013). In recent year, machine learning has proven efficient due to ability to handle non-linear structure data from various sources with different scales. In addition, machine learning requires no statistical assumptions. Among machine learning, ANN is considered as the most widely used model for environmental modeling due to its computational efficiency (Bui et al., 2016; Ghalkhani et al., 2013; Rezaeianzadeh et al., 2014). However, the ANN model has a number of weaknesses such as poor prediction and error in modeling process (Bui et al., 2016); therefore, hybrid models have been proposed. Among hybrid frameworks, ensemble of fuzzy logic and Adaptive Neuro-Fuzzy Inference System (ANFIS) was reported efficient due to its high accuracy (Güçlü and Şen, 2016; Lohani et al., 2012; Shu and Ouada, 2008) (Chang and Tsai, 2016). It should be noted that even though ANFIS model has a higher accuracy than the two other model individually (Mukerji et al., 2009; Nayak et al., 2005), it has some disadvantages since it is weak in finding the best weight parameters affecting the prediction accuracy (Bui et al., 2016). Thus, these weights can be optimized to enhance the prediction accuracy of ground water models with the use of machine learning optimization algorithm.

The main aim of the current study is to carry out groundwater spring potential mapping (GSPM) in Koohdasht-Nourabad plain, Iran using ANFIS model combined with new metaheuristic algorithms, Invasive Weed Optimization (IWO), Differential Evolution (DE), Firefly, Particle Swarm Optimization (PSO), and Bees algorithm (BA). Consequently, the new models have ability to solve the weakness of the traditional ANFIS model. Another goal of the present study is drawing a comparison between prediction capabilities of these five new hybrid models in groundwater potential modeling in the study area as well. Since no such studies have been published so far in the study area, the current study is the pioneer work in this subject.

2. Case study description

Koohdasht-Nourabad Plain is located in the west part of the Lorestan province, Iran. It lies between 33°3' 28 and 34° 22' 55 N latitudes and between 46° 50' 19 and 48° 21' 18 E longitudes (Fig. 1). The region is located in the semi-arid area with mean annual precipitation of about 450 mm (Lorestan Weather Bureau report, 2016). The plain covers around 9531.9 km² with the population of 362,000 people (according to 2016 census). The primary occupation of most people living in the region is agriculture with groundwater is the main source. The altitude of the study area varies between 531 m and 3175 m above the sea level, while the maximum and minimum slope is 0° and 64°, respectively. Geologically, the study area is located in Zagros structural zone of Iran and is mostly covered by Quaternary and Cretaceous-Paleocene geologic time scale. The dominant land-use/land-cover of the study area is moderate forest (20%) and rocks covers the smallest area percentage (0.0007%). The residential areas also covers about 3% of the Koohdasht-Nourabad plain. Rock crop/Inceptisols are the dominant soil types in the study area, covering about 51% of the study area.

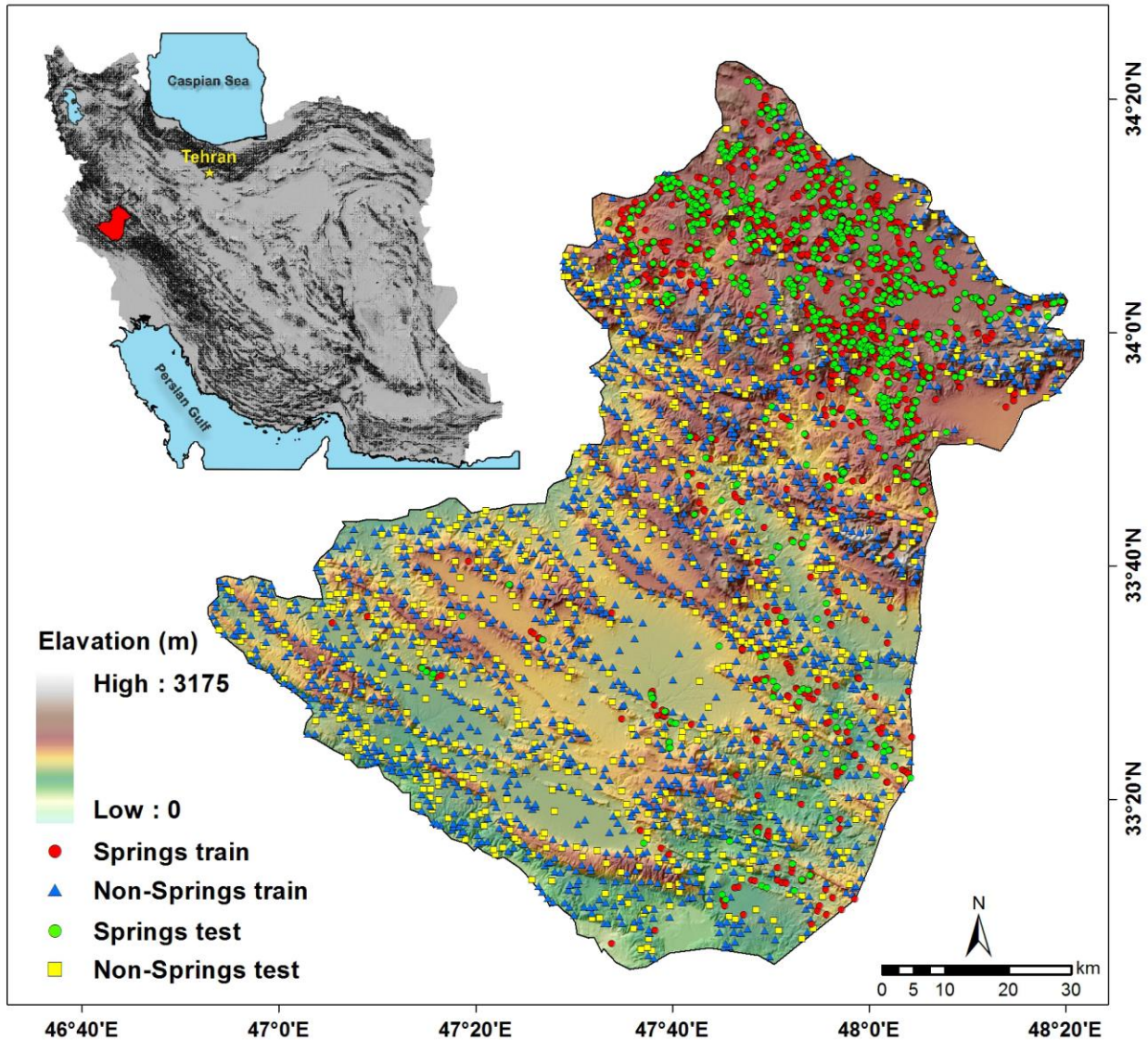


Fig.1. Groundwater well locations with DEM of the study area

3. Methodology

The methodological approach is shown in Fig 2..

3.1. Data preparation

3.1.1. Groundwater spring inventory map

In groundwater modeling, spatial relationship between groundwater springs and conditioning factors should be analyzed and assessed to determine the best subset of these factors. In Koohdasht-Nourabad plain, a total of 2463 springs were provided by Iranian Water Resources Management. In which, most of the spring locations were checked during extensive field surveys with GPS hand hole.

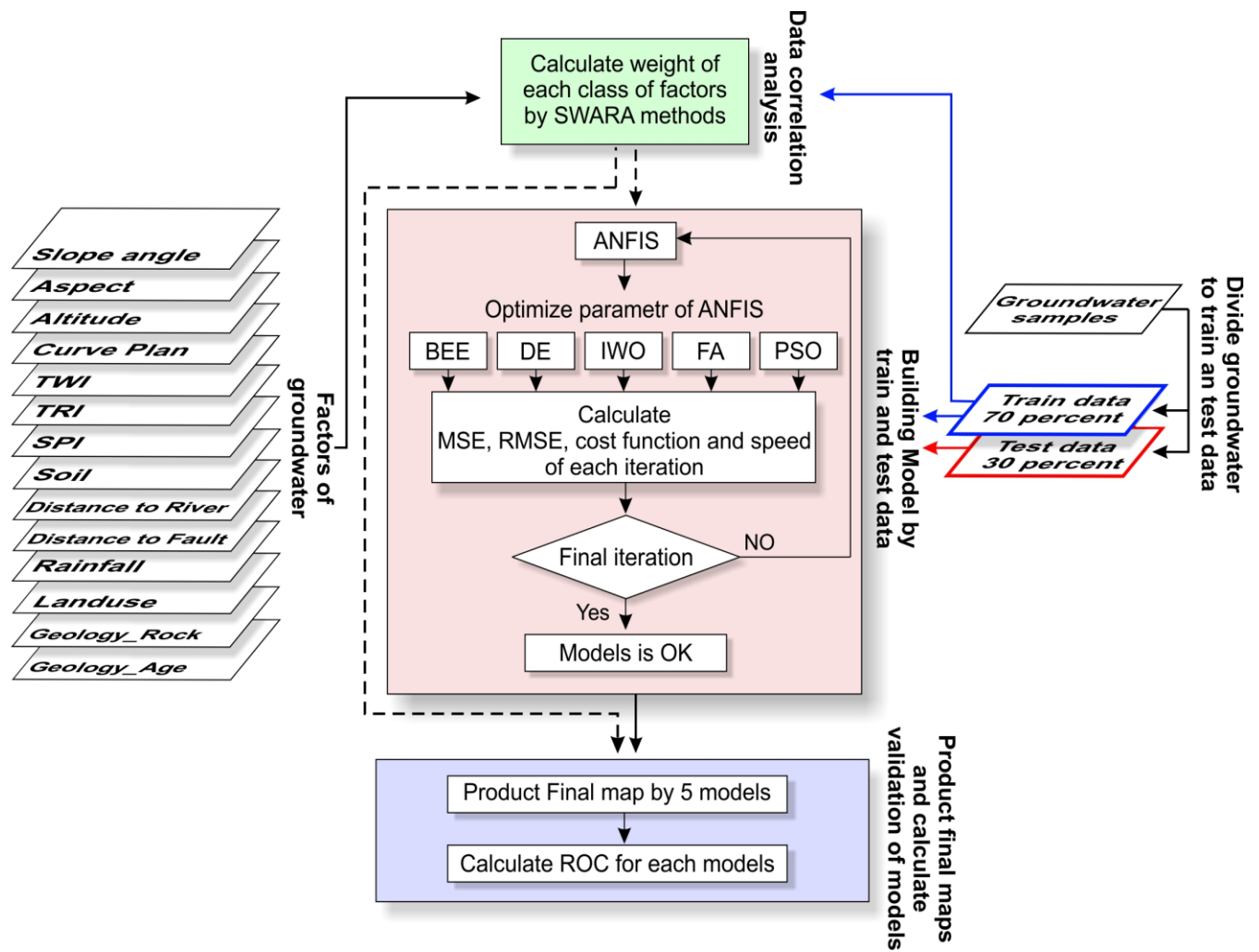


Fig.2. Conceptual modelling adopted in the current study

3.1.2. Construction of the training and validation datasets

Spatial prediction of groundwater potential mapping using machine learning model is considered as a binary classification with two classes, spring and non-spring. Therefore, a total of 2463 non-spring locations were randomly generated using the random point tool in ArcGIS10.2. According to Chung and Fabbri (Chung and Fabbri, 2003), it is possible to validate the model performance using a cross validation method that splits the dataset for the two parts. The first part is used for building model called training dataset and the other part is utilized for validating the model performance named as testing dataset (Pham et al., 2017a). In this study, a ratio of 70/30 was selected randomly for generating the training and testing the dataset (Pourghasemi et al., 2013a; Pourghasemi et al., 2012; Pourghasemi et al., 2013b; Xu et al., 2012). Accordingly, both spring location and non-spring location have been divided into two groups for the training (1725 location) and the validating (738 location) purposes (Fig 1).

Finally, both the training and the testing datasets were converted to raster format and then overlaid with 13 groundwater conditioning factors to extract their attribute values, where the spring pixels were assigned to "1" and non-spring pixels were assigned to "0" (Bui et al., 2015).

3.1.3. Groundwater conditioning factor analysis

3.1.3.1. Selection of the Groundwater conditioning factor and multi-collinearity analysis

After the initial selection of the conditioning factors, these factors should be assessed for multi-collinearity problems. Multi-collinearity takes place when two or more non-independence conditioning factors are highly correlated or in other words inter-dependent (Li et al., 2010). Several methods have been proposed to diagnose multi-collinearity, and among them, Variance Inflation Factor (VIF) and Tolerance are widely used in environmental modeling (Bui et al., 2016; O'brien, 2007). Factors with VIF greater than 5 and tolerance less than 0.1 indicate multi-collinearity problems existed (Bui et al., 2011; O'brien, 2007).

In the current study, 13 conditioning factors have been selected including slope degree, slope aspect, altitude, plan curvature, stream power index (SPI), topographic wetness index (TWI), Terrain roughness index (TRI), distance from fault, distance from river, land-use/land-cover, rainfall, soil order, and lithology units. These factors have been determined based literature review, characteristics of the study area, and data availability (Mukherjee, 1996; Nampak et al., 2014; Oh et al., 2011; Ozdemir, 2011a). In fact, no agreement is reached on which the factors to be used for modeling. The process of converting continuous variables into categorical classes were carried out based on our frequency analysis of springs location (Khosravi et al., 2018; Ahmadisharaf et al., 2016) in order to define the class intervals (Bui et al., 2011).

Digital Elevation Model (DEM) has been downloaded from ASTER global DEM with 30x30 m grid size. Based on the DEM, slope degree, slope aspect, altitude, plan curvature, SPI, TWI and TRI were derived. Slope degree of the study areas varies between 0-64 degree. Slope factor has a direct impact on the runoff generation and groundwater recharge. As the lower the slope, the lower runoff generation and the higher groundwater recharge. The slope degree has been divided in five categories using the quantile classification scheme (Tehrany et al., 2013; Tehrany et al., 2014), including 0-5.5, 5.5-12.11, 12.11-19.4, 19.4-28.7, 28.7-64.3 degree (Fig 3a). Slope aspect is selected because it affects the groundwater potential through solar radiation. In the study area, the north aspect receives a lower sun light, and as a result, is less wet and low evapotranspiration. The slope aspect has been provided in 5 different classes including, flat, north, west, south and east (Fig 3b). The third conditioning factor is altitude. Altitude was divided into five classes using the quantile classification scheme, including 531-1070, 1070-1385, 1385-1703, 1703-2068 and 2068-3175 m (Fig.3c). Plan curvature used with three classes, namely concave (≤ -0.05), flat ($-0.05-0.05$), and convex (>0.05) (Fig.3d) (Pham et al.2017). SPI is related to erosive power of surface runoff, whereas TWI links to amount of the flow that accumulates at any point in the catchment.. SPI, TWI and TRI were constructed using the Automated Geoscientific Analyses tool in SAGA-GIS 2.2 software and finally divided into five classes. They are 0-48664, 48664-227099, 227099-583969, 583969-1330153, 1330153-4136452 (Fig.3e) for SPI. For TWI, these classes are 2.1-4.6, 4.6-5.6, 5.6-6.6, 6.6-7.9, 7.9-11.9 (Fig.3f) and for TRI, these classes are 0-8.7, 8.7-18.2, 18.2-29.9, 29.9-46.6, 46.6-185 (Fig.3g).

Distance from fault and river factors have been generated using fault and river of the study area using the multiple ring-buffer tool in ArcGIS10.2. with five classes including: 0-200, 200-500, 500-1000, 1000-2000 and >2000 m (Fig. 3h and Fig. 3i). Lithology plays a key role in determining the groundwater potential occurrences due to different infiltration rate of formation that has been considered in some previous studies (Adiat et al., 2012; Nampak et al., 2014; Pradhan, 2009).

198 Land-use/land-cover of the study area has been provided through Landsat 7 Enhanced Thematic
199 Mapper plus (ETM+) images downloaded from the US Geological Survey (USGS) and supervised
200 image classification techniques (Lillesand et al., 2014). Finally, the accuracy of the land-use/land-
201 cover map has been controlled by filed surveys.

202 For the case of land-use/land-cover, twenty five types were recognized including agriculture,
203 garden, dense-forest, good rangeland, poor forest, waterway, mixture of garden and agriculture,
204 mixture of agriculture with dry farming, mixture of agriculture with poor-garden, dry farming,
205 follow, dense rangeland, very poor forest, mixture of waterway and vegetation, mixture of
206 moderate forest and agriculture, mixture of moderate rangeland and agriculture, mixture of poor
207 rangeland and follow, mixture of low forest and follow, wood-land, moderate forest, moderate
208 rangeland, poor rangeland, bare soil and rock, urban and residential, mixture of very poor forest,
209 and rangeland have been identified and assigned to code 1 to 25 respectively (Fig.3j).

210 As the major source of recharge to the groundwater, rainfall has been provided via mean annual
211 historical rainfall data of past 15 years (2000–2015) using 4 rain-gauge stations in the study area.
212 Inverse distance weighted (IDW) method has been used for deriving the rainfall map with five
213 categories including: 300-400, 400-500, 500-600, 600-700, 700-800 mm (Fig 3k). The soil
214 properties directly affect the water infiltration rate as well as groundwater recharge. The 1:50,000
215 soil map of Lorestan province obtained from the Iranian Water Resources Department (IWRD)
216 has been used for the analysis. The soil map was in a polygon format which needed to be converted
217 to grid. The most dominant feature of the study area is rock outcrop/Entisols, rock
218 outcrop/Inceptisols, Inceptisols, Inceptisols/Vertisols and Badlands (Fig.3l).

219

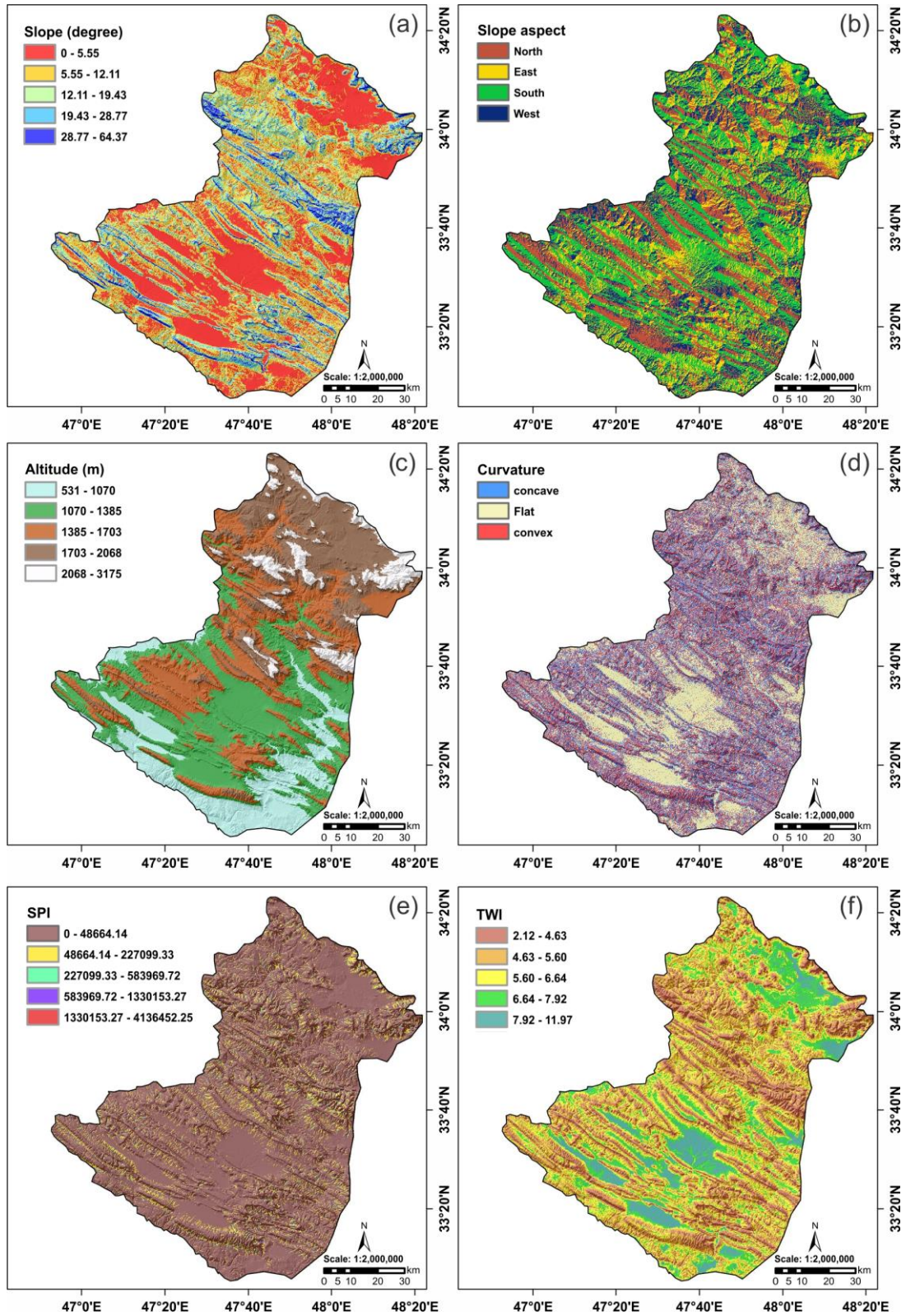
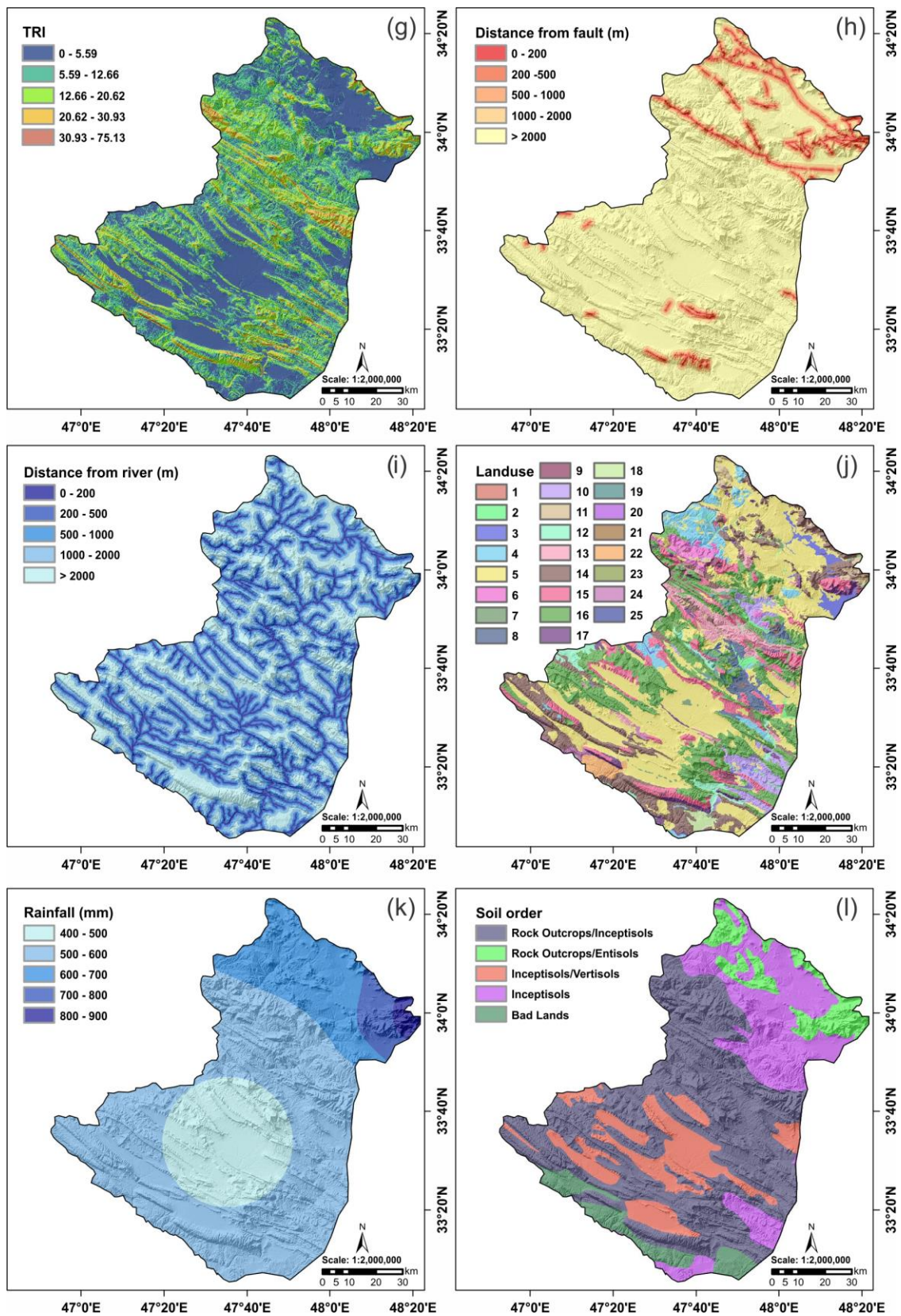


Fig.3. Thematic Groundwater conditioning factor in the study area: slope degree(a), slope aspect (b), altitude (c), **plan** curvature (d), SPI (e), TWI (f), TRI (g), distance from fault (h), distance from river (i), land-use/land-cover (j), rainfall (k), soil order (l), and lithology units (m).



224

225 Fig.3.Continued

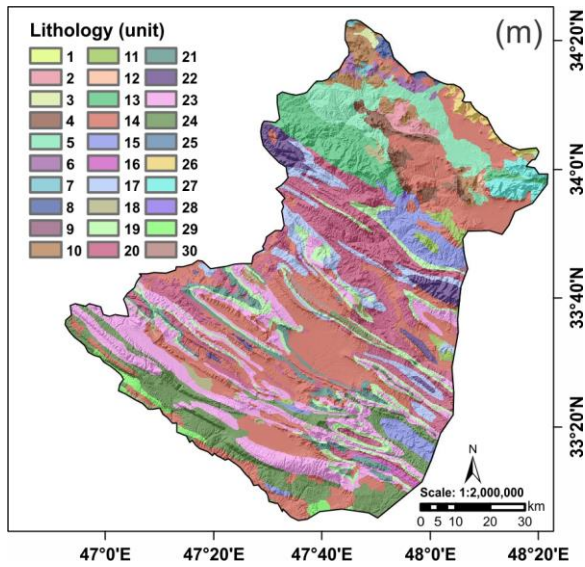


Fig.3. Continued

Finally, all the aforementioned groundwater conditioning factors for modeling purposes were converted to a raster grid with $30\text{ m} \times 30\text{ m}$ in the ArcGIS 10.2 software. Lithology (unit) has a high influence on infiltration; thus, it has been considered in the current study. Lithology for the study area has been constructed in scale of 1:100000, which was provided by Iranian Department of Geology Survey (IDGS). Accordingly, thirty classes were used including: OMq, PeEf, PIQc, K1bl, Plc, pd, TRKubl, TRJvm, MPlfgp, OMql, Plbk, E2c, TRKurl, Qft2, MuPlaj, KEpd-gu, Kgu, Qft1, Ekn, KPeam, PeEtz, Kbgp, EMas-sb, Mgs, TRJlr, Klsol, JKbl, Kur, OMas and Mmn and assigned to code 1 to 30 respectively (Fig.3m).

3.2. Spatial relationship between spring location and conditioning factors

Step-wise Assessment Ratio Analysis (SWARA), a Multi-Criteria Decision Making (MCDM) was first introduced by Keršulienė (Keršulienė et al., 2010) was used due to both simple and rooted on experts' views SWARA has received great attention in various fields in the last five years (Alimardani et al., 2013; Hong et al., 2017). In SWARA, the expert allocates the highest and lowest rank from the most and least valuable criterion, respectively. Afterwards, the all-inclusive ranks are specified by the average value of ranks. The phases of method are as the following:

Phase one (for evolving decision making models): first, the experts define the problem solving criteria. By using the practical knowledge of the experts, the priority for each criteria are determined as well and the criteria are organized in descending order finally.

Phase two (regarding to each parameter's ranking): the following trend is employed for calculation of the weight in each criteria:

Starting from the second criterion, the respondent explains the relative importance of the criterion j in relation to the $(j - 1)$ criterion, and for each particular criterion as well. As Keršulienė

mentioned, this process specifies the Comparative Importance of the Average Value, S_j as follows (Keršulienė et al., 2010):

$$S_j = \frac{\sum_i^n A_i}{n} \quad (1)$$

where n is the number of experts; A_i explicates the offered ranks for each factor by the experts; j stands for the number of the factor.

Subsequently, the coefficient K_j is determined as follows:

$$K_j = \begin{cases} 1 & j = 1 \\ S_j + 1 & j > 1 \end{cases} \quad (2)$$

Recalculation of weight Q_j is as the following:

$$Q_j = \frac{X_{j-1}}{K_j} \quad (3)$$

The relative weights of the evaluation criteria are calculated by the following equation:

$$W_j = \frac{Q_j}{\sum_{j=1}^m Q_j} \quad (4)$$

where W_j shows the relative weight of j -th criterion, and m stands for the total criteria number.

3.3. Groundwater spring prediction modelling

In this research, five new hybrid models namely ANFIS-DE, ANFIS-IWO, ANFIS-FA, ANFIS-PSO, ANFIS-BA were utilized for the analysis of determination of groundwater potential zonation in the study areas and for comparison between their prediction capabilities.

3.3.1. Adaptive Neuro-Fuzzy Inference System

Adaptive Neuro-Fuzzy Inference System (ANFIS) is obtained from the combination of Artificial Neural Network (ANN) and fuzzy logic (Jang, 1993). ANFIS has been proven more efficient than the two mentioned models in various fields (Bui et al., 2016). This is because ANN has the automatic ability but is not able to explain how to get the output from decision making. Fuzzy logic, on the other hand, is the reverse of ANN by generating output from fuzzy logical decision without the ability of self-operating learning (Aghdam et al., 2017; Chen et al., 2017b; Phootrakornchai and Jiriwibhakorn, 2015). Consequently, ANFIS was proposed to solve nonlinear and complex problems in one framework (Rezakazemi et al., 2017). This model has been used in date processing, fuzzy control and others fields (Zengqiang et al., 2008). The members of ANFIS are the function parameters from dataset for describing the system behavior (Jang, 1993). ANFIS applies to Takagi-Sugeno-Kang (TSK) fuzzy model with two rules of “If-Then” with two inputs x_1 and x_2 , and one output f (Takagi and Sugeno, 1985), as follows:

$$\text{Rule 2 1: if } x_1 \text{ is } A_1 \text{ and } x_2 \text{ is } B_1, \text{ then } f_1 = p_1 x_1 + q_1 x_2 + r_1 \quad (5)$$

281 Rule 1: if x_2 is A_2 and x_2 is B_2 , then $f_2 = p_2x_2 + q_2x_2 + r_2$ (6)

282 Jang's ANFIS consists of feed-forward neural network with six distinct layers. Detailed
 283 description of ANFIS can be seen in (Jangs, 1993).

284 3.3.2. Meta-heuristic optimization

285 The main goal of this phase is to find the optimal antecedent and the consequent parameters of
 286 the ANFIS model using IWO, DE, FA, PSO, and Bee algorithms. Fig.4 illustrates a general
 287 methodological flow of ANFIS
 288

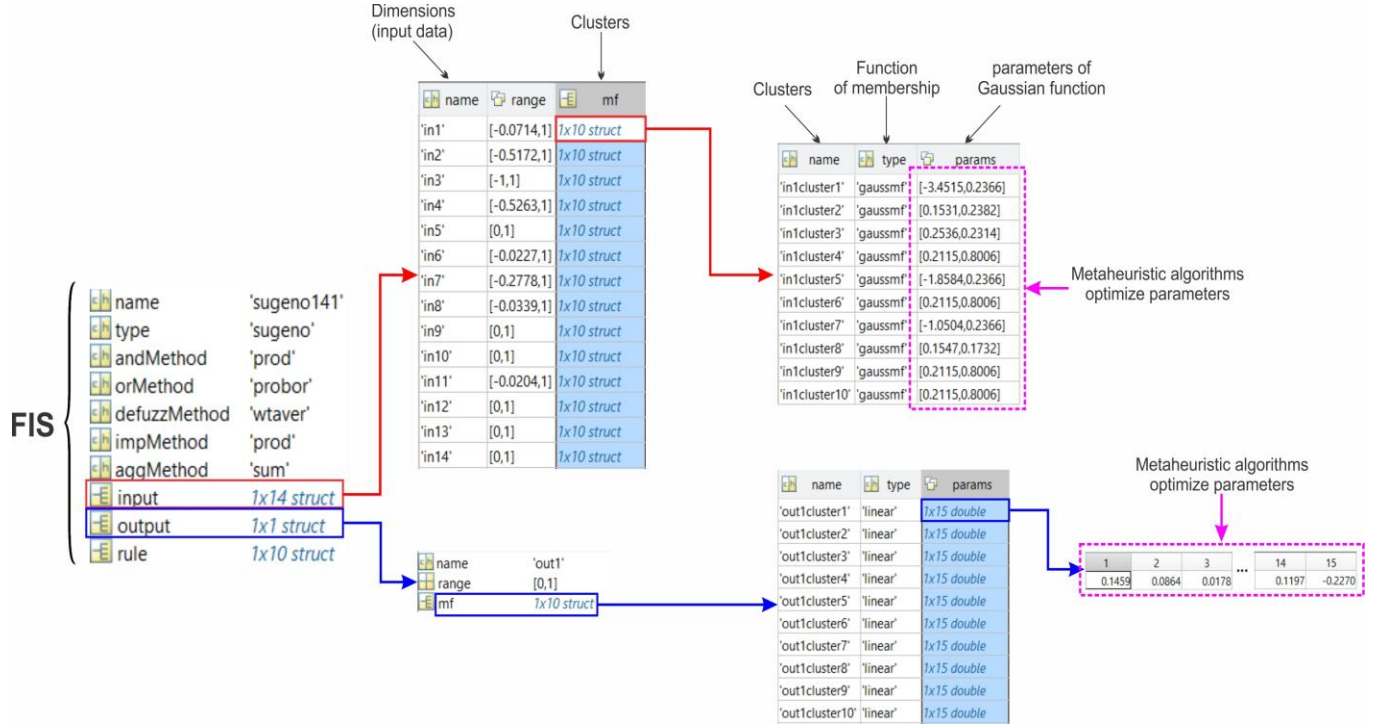


Fig.4. General methodological flow of ANFIS

292 3.3.2.1. IWO algorithm

293 Invasive weed optimization (IWO) is one of the metaheuristic algorithms which mimics the
 294 colonizing behavior of weeds. Its design is based on the way to find proper place for growth and
 295 reproduction of weeds by Mehrabian and Locus (Mehrabian and Lucas, 2006). One characteristic
 296 of this algorithm is its simplified structure; the number of input parameters is low and has strong
 297 robustness. Furthermore, it is easy to understand and the same merit causes it to be used for solving
 298 difficult nonlinear optimization problems (Ghasemi et al., 2014; Naidu and Ojha, 2015; Zhou et
 299 al., 2015). Moreover, by comparing the results of IWO algorithm and other algorithms like SFLA
 300 and PSO for solving optimization problems, IWO algorithm can compete with other ones
 301 (Ghasemi et al., 2014). This algorithm consists of 4 parts as following:

302 1- Initialization

Random spread of some limited weeds in searching area with dimension D is considered as the initial population of solutions.

2- Reproduction

Weeds are able to reproduce some seeds in accordance with their fitness during their growth. In other words, the number of produced seeds from S_{min} value for weeds starts with Worst fitness and then increases in linear fashion to S_{max} for them with best fitness.

3- Spatial dispersal

Produced seeds are distributed in the searching area randomly in a way that is located close to their families with normal distribution, their mean equal to zero, and different variances. Moreover, standard deviation decreases in each iteration from σ_{min} to σ_{max} and is calculated by the following non-linear equation:

$$\sigma_{iter} = \frac{(iter_{max}-iter)^n}{(iter_{max})^n} (\sigma_{min} - \sigma_{max}) + \sigma_{max} \quad (7)$$

where $iter_{max}$ is the last iteration, σ_{iter} is the standard deviation of iteration, and n is the non-linear index considered between 2 and 3 (Saravanan et al., 2013).

4- Competitive exclusion

All weeds and their seeds combine in order to make up the population of next generation. If the population exceeds a definite maximum, those weeds with lower fitness will be removed. The reproduction mechanism and the competition provide breeding opportunity for proper weeds. If they generate fitter offspring, the offspring can survive the competition.

5- Termination Condition

Step 2 to 4 were repeated to reach its maximum defined value and the weeds with the best fitness will be the nearest condition to optimal solution.

3.3.2.2. DE algorithm

DE is another popular algorithm used as an evolutionary algorithm in recent years used for finding global optimal answers in a problem with continuous space (Chen et al., 2017a; Das et al., 2009). This method was first introduced by Storn and Price (Storn and Price, 1997). It is very similar to genetic algorithm that produces next optimum generation by three operators: mutation, crossover, and selection. This algorithm starts by producing random population in which each individual of population is a symbol of solution to the problem. Vector $X_i^G = (x_{1,i}^G, x_{2,i}^G, x_{3,i}^G, \dots, x_{D,i}^G)$ shows each individual of population $i = \{0,1,2, \dots, NP\}$ is a number of each individual, in which D stands for the search dimension or in other words, is a component problem and $G = \{0,1,2, \dots, G_{max}\}$ generation time that G_{max} is the total number of generations. By assuming the maximum and minimum of every dimension of searching space, there are $X_L = \{x_{1,L}, x_{2,L}, \dots, x_{D,L}\}$ and $X_U = \{x_{1,U}, x_{2,U}, \dots, x_{D,U}\}$, respectively; initial population is defined as the following (Storn and Price, 1997):

$$x_{j,i}^0 = x_{j,L} + rand(0,1) \cdot (x_{j,U} - x_{j,L}) \quad (8)$$

340 where $\text{rand}(0,1)$ is a uniformly distributed random number in $[0, 1]$

341 3.3.2.2.1. Mutation

342 The first operator in DE algorithm is mutation, which produces mutant vector $V_i^G =$
343 $(V_i^G, V_2^G, \dots, V_D^G)$ by using each individual which is called target vector. Four well-known mutant
344 operators that are used are as the following:

345 DE/rand/1 : $V_i^G = X_{r1}^G + F \cdot (X_{r2}^G - X_{r3}^G)$

346 DE/rand/2 : $V_i^G = X_{r1}^G + F \cdot (X_{r2}^G - X_{r3}^G) + F \cdot (X_{r4}^G - X_{r5}^G)$

347 DE/best/1 : $V_i^G = X_{best}^G + F \cdot (X_{r1}^G - X_{r2}^G)$

348 DE/best/2 : $V_i^G = X_{best}^G + F \cdot (X_{r1}^G - X_{r2}^G) + F \cdot (X_{r3}^G - X_{r4}^G)$

349 DE/current-to-rand/1 : $V_i^G = X_i^G + F \cdot (X_{r1}^G - X_i^G) + F \cdot (X_{r2}^G - X_{r3}^G)$

350 DE/current-to-rand/1 : $V_i^G = X_i^G + F \cdot (X_{best}^G - X_i^G) + F \cdot (X_{r1}^G - X_{r2}^G)$ (9)

351 $r1, r2, r3, r4$, are the integer numbers that have been chosen randomly from $[0, NP]$ and the
352 condition of $r1 \neq r2 \neq r3 \neq r4$ exists. F is the Scale factor that determines the mutation scale. It
353 is generally selected as a random number from $[0,1]$. X_{best}^G is an individual that has the best fitness
354 value in G generation.

355 3.3.2.2.2. Crossover

356 The purpose of this step is to produce trail vector (U_{ij}) . Thus, this operator is defined by replacing
357 some elements of the target vector X_i^G with mutant vector V_i^G as the following (Storn and Price,
358 1997):

359
$$U_{ij} = \begin{cases} V_{ij}^G & \text{if } \text{rand}[0,1] \leq CR \text{ or } j = j_{rand} \\ X_{ij}^G & \text{otherwise} \end{cases} \quad (10)$$

360 where $i \in \{1, 2, \dots, NP\}$, $j \in \{1, 2, \dots, D\}$, j_{rand} , is a random number from $[1, D]$ and CR is the
361 crossover rate which is uniformly distributed random number in $[0,1]$.

362 3.3.2.2.3. Selection

363 Selection is characterized by comparing fitness value of U_{ij} trail vector with the target vector (X_i^G)
364 and choosing the best ones as the next generation (Storn and Price, 1997).

365
$$X_i = \begin{cases} U_i^G & \text{if } f(U_i^G) \leq f(X_i) \\ X_i^G & \text{otherwise} \end{cases} \quad (11)$$

366

367 3.3.2.3. FA algorithm

. Firefly algorithm has been defined by Yang in Cambridge University (Yang, 2009) as an evolutionary algorithm. In recent years, many researches in different fields have taken advantage of this algorithm for optimization. This algorithm is known as meta-heuristic algorithm that is originated from flashing and communication behavior of fireflies (Yang, 2009; Yang, 2010). Like in every other swarm intelligence algorithm, where their components are known as solutions for the problems, in this algorithm each firefly is a solution and its light intensity is the objective function value. In other words, a firefly with more light intensity is known as a solution. On the other hand, this firefly attracts more fireflies.

Generally, FA algorithm follows three idealized rules as below:

1- All firefly species are unisex, with each of them attracting other fireflies without considering their gender (Amiri et al., 2013).

2- Attractiveness of a firefly is related to its light intensity. Thus, from two flashing firefly species, the one with lower light intensity moves toward the other one with higher light intensity. It should be noted that the distance between fireflies is significant because the farther they are from each other, the dimmer the light gets and the attractiveness declines exponentially (Gandomi et al., 2013). Moreover, if the light intensity of fireflies were the same; they would move randomly (Senapati and Dash, 2013).

3- Light intensity of a firefly is defined as an objective function value and must be optimized.

In order to design FA, two substantial issues are needed to be defined: light intensity variation (I) and the attractiveness' formulation(β). Fireflies' attractiveness is determined by their light intensity or brightness. In addition, brightness is associated with the objective function. The light intensity $I(r)$ varies with the distance r monotonically and exponentially as:

$$I(r) = I_0 e^{-\gamma r^2} \quad (12)$$

where I is the original light intensity, γ is the fixed light absorption coefficient and r is the distance between the two fireflies. Also, attractiveness rate is defined as below:

$$\beta = \beta_0 e^{-\gamma r^2} \quad (13)$$

where β_0 is the attractiveness when $r=0$. Also, the distance between two fireflies i and j with X_i and X_j is determined by the following equation:

$$r_{ij} = \|X_i - X_j\| = \sqrt{\sum_{k=1}^d (X_{i,k} - X_{j,k})^2} \quad (14)$$

where d is the number of the problem dimensions and $X_{i,k}$ is the k - th element of the i - th firefly. Also, the movement of a firefly i which is attracted to another attractive firefly j , is determined by (Yang, 2009):

$$X_i = X_i + \beta_0 e^{-\gamma r_{ij}^2} (X_j - X_i) + \alpha (rand - \frac{1}{2}) \quad (15)$$

In Eq. (21), the first and the second terms determines the attraction. However; the third term is regarded as a randomization with α , which is the step parameter, and ultimately, the rand is a random number generator which is uniformly distributed in a range from 0 to 1.

3.3.2.4. PSO algorithm

PSO was first designed by Eberhart and Kennedy (Eberhart and Kennedy, 1995). Sensible characteristics of this algorithm include being powerful for optimizing the non-linear problems, its quick convergence, and relatively low calculations. These characteristics have made distinctions between this algorithm and other algorithms (Cheng et al., 2010). Thus, PSO algorithm in those problems that need optimization has a special place among researches. This algorithm has been inspired by the way the birds and fish use their collective intelligence for finding the best way to get food (Kennedy, 2011; Kennedy and Eberhart, 1995). Therefore, each bird implemented in this algorithm acts as a particle that is in fact a representative of solution to problems. These particles find the optimum answers for the problem by searching in “n” dimension space whereas “n” is the number of problem's parameters. For this purpose, particles were scattered randomly in considered space at the beginning of algorithm implementation. Then, the positioning in each iteration can improve by using equation 1 and 2 and finding better situations in that iteration and the best position of particles vector addition. Assuming that $x_i^t = (x_{i1}^t, x_{i2}^t, \dots, x_{in}^t)$ and $v_i^t = (v_{i1}^t, v_{i2}^t, \dots, v_{in}^t)$ are the position and velocity of the “i – th” particle in “t th” iteration, respectively. Then, position and velocity of “i th” particle in “(i + 1) th” iteration is calculated by summing equation 1-2 (Eberhart and Kennedy 1995).

$$\begin{aligned} v_i^{t+1} &= \omega v_i^t + c_1 r_1 (p_i^t - x_i^t) + c_2 r_2 (g_i^t - x_i^t) \quad \text{with } -v_{max} \leq v_i^{t+1} \leq v_{max} \\ x_i^{t+1} &= x_i^t + v_i^{t+1} \end{aligned} \quad (16)$$

where x_i^t is the last position of “i th” particle, p_i^t the best found position by “i th” particle, g_i^t the best found location by particles, r_1, r_2 the random number between 1 and 0. ω, c_1 and c_2 the inertia weight, cognitive coefficient, and social coefficient, respectively. In order to value them, many papers have been presented (Olsson, 2010) and finally the following equation has been used (Nieto et al., 2015).

$$\omega = \frac{1}{2 \ln 2} \quad \text{and} \quad c_1 = c_2 = 0.5 + \ln 2 \quad (17)$$

It is noteworthy that the algorithm continues until the best found position by each particles unifies with the best found position of particles. In other words, all particles accumulate in one position and actually the answer to the problem is optimized.

3.3.2.5. Bee algorithm

One of the meta-heuristic algorithms designed according to bee swarm-based is Bee Algorithm. This algorithm which was first introduced by Pham (Pham et al., 2005; Pham et al., 2011) is inspired by foraging behavior of bees' colonies in search of food sources (flower patches) located near the hive. In the beginning, evenly distributed scout bees are scattered randomly in different directions to identify flower patches. After that, scout bees come back to hive and start a specific dance called waggle dance. This dance is for communicating with others in order to share the information of

discovered flower patches. This information indicates direction, distance, and nectar quality of the flower patches. All the information helps the colony to have proper evaluation of all flower patches. After evaluation, scout bees come back to the location of discovered flower patches with other bees named recruit bees. Regarding the distance and the amount of nectar, different number of recruit bees are assigned to each flower patch. In other words, those flower patches with better nectar quality dedicate more recruit bees to themselves. Following that, recruit bees evaluate the quality of flower patches when performing the harvest process so that they leave the flower patches if they have low quality. Conversely, if the flower patch quality is good, it will be announced during the next waggle dance. Before implementing the BA algorithm, the following parameters need to be defined:

The number of scout bees (n), the number of patches selected out of n visited points (m), the number of best patches out of m selected patches (e), the number of bees recruited for e best patches (nep), the number of bees recruited for other ($m-e$) selected patches (nsp), the size of patches (ngh) and the stopping criterion.

At first, “ n ” number of scout bees with uniform distribution is scattered in search space randomly. Then, the algorithm starts to evaluate the fitness of those seen places by scout bees in order to define and select suitable bees as elite bees.

The sites of elite bees are selected from local search and the algorithm implements the neighborhood searches within the selected bees’ sites for the best ones where more bees exist. Only the proper bee is chosen to survive the next bee population in each site and other bees are allocated around the search space randomly to find new potential solutions. These steps continue until the algorithm convergences.

3.4. Model’s performance assessment

Forecasting error as the quantitative approaches, define as the difference between the observed and estimated values which have been used for determination of the accuracy of the performed models. In the current study the model prediction capabilities for each hybrid model in terms of spatial groundwater prediction was evaluated using Mean Squared Error (MSE) as follows (Tien Bui et al, 2016):

$$MSE = \frac{\sum_{i=1}^n (O_i - E_i)^2}{N} \quad (18)$$

where O_i and E_i are observation (target) and prediction (output) values in both training and testing dataset and N is the total samples in the training or the testing dataset.

3.5. Model’s performance validation and comparisons

According to Chung and Fabbri (Chung and Fabbri, 2003), validation is one of the most important steps in any spatial prediction modeling and without validation, the result of the models do not have any scientific significance. Prediction capability of these five spatial groundwater models must be evaluated using both success-rate and prediction-rate curves (Hong et al., 2015). Success-rate curves show how suitable the built model is for the groundwater potential assessment or for the evaluation of the

goodness of fit (Gaprindashvili et al., 2014). Success-rate curves have been constructed using groundwater potential maps and the number of spring locations used in training dataset (Pradhan et al. 2010). Prediction rate curves which show the probabilities of the groundwater occurrences demonstrate how good the model is or evaluate the prediction power of the models. Therefore, it can be used for model prediction capabilities (Brenning, 2005). The construction procedure of prediction rate is similar to the success rate which the testing dataset (were not used in the training phase) has been used for instead of training dataset. The area under the curve (AUC) of success and prediction rate is the base for evaluation of model prediction power or assessment accuracy of the groundwater potential models quantitatively (Khosravi et al., 2016a; Khosravi et al., 2016b; Pham et al., 2017b). The AUC value varies from 0.5 to 1; the higher the AUC, the better the prediction capability of models.

3.6. Inferential statistics

3.6.1-Freidman test

As the conditioning factors have been classified into different classes, non-parametric test has been used in the current study. Non-parametric statistical procedures such as Freidman test (Friedman, 1937) have been used regardless of statistical assumptions (Derrac et al., 2011) and do not need the data to be normally distributed. The main aim of this test is to find whether there is a significant difference between the performed models or not. In other words, performing multiple comparisons to detect significant differences between the behaviors of two or more models (Beasley and Zumbo, 2003). The null hypothesis (H0) is that there are no differences among the performance of the groundwater potential models. The higher the P-value, the higher the probability that the null hypothesis is not true since if the p-value is less than the significance level ($\alpha=0.05$), the null hypothesis will be rejected.

3.6.2 Wilcoxon signed-rank test

The most important drawback of Freidman test is that it only illustrates whether there is any difference between the models or not, and does not have the ability to show pairwise comparisons among performed model. Therefore, another non-parametric statistical test named Wilcoxon signed-rank test have been performed. To evaluate the significance of differences between the performed groundwater potential models, the P value and Z value have been used.

4. Result and analysis

4.1. Multi-collinearity diagnosis

Result of multi-collinearity analysis is shown in Table 1. Result has revealed that as VIF is less than 5 and the tolerance is greater than 0.1, there isn't any multi-collinearity problem among conditioning factors and all of factors are independent.

Table.1. Multi-collinearity analysis for conditioning factors

No	Groundwater conditioning factors	Collinearity Statistics	
		Tolerance	VIF

1	Slope degree	0.231	2.401
2	Slope aspect	0.206	4.270
3	Altitude	0.801	2.097
4	Plan curvature	0.513	1.446
5	SPI	0.410	1.689
6	TWI	0.541	2.113
7	TRI	0.328	1.939
8	Distance from fault	0.408	2.25
9	Distance from river	0.212	3.126
11	Land-use/land-cover	0.296	3.891
12	Rainfall	0.298	1.686
13	Soil order	0.205	4.039
10	Geology (Unit)	0.215	4.150

517

518 4.2. Determination of the most important parameters

519 The most common method of information gain ratio (IGR) was applied to identification of the
520 most important conditioning factors. Result shows that all thirteen conditioning factors are
521 effective on groundwater occurrences as the land-use/landcover factor has the most important
522 impact on groundwater (IGR=0.502) followed by lithology (IGR=0.465), rainfall (IGR=0.421),
523 TWI (IGR=0.400), soil (IGR=0.370), TRI (IGR=0.337), slope degree (IGR=0.317), altitude
524 (IGR=0.287), distance to river (IGR=0.139), aspect (IGR=0.066), plan curvature (IGR=0.0548),
525 distance to fault (IGR=0.0482) and SPI (IGR=0.0323).

526 4.3. Spatial relationship between springs and the conditioning factors by SWARA method

527 The spatial correlation between springs and the conditioning factor has been shown in Table 2. For
528 the slope, the class of 0-5.5 degree shows the highest probability (0.45) on spring groundwater
529 occurrences and there is a contrary correlation between slope degree and SWARA values. As the
530 slope degree increases, the probability of spring occurrence has reduced. In the case of slope
531 aspect, the east aspect (0.44) has the most impact on spring occurrences followed by north (0.22),
532 west (0.177), south (0.15) and flat (0.12) in the Koohdasht- Nourabad plain. According to
533 calculated results, in terms of altitude, the springs are the most abundant in the altitude of 1703-
534 2068 m (0.6) and the least abundant in the altitude of 1070-1385 m (0.04). The SWARA model is
535 high in flat areas (0.4), followed by concave (0.38) and convex (0.2). For SPI, the highest SWARA
536 value is found for the classes of 583969-1330153 (0.46), followed by the classes of 227099-
537 583969(0.0.23) and 48664-227099 (0.19). In the case of the TWI, the SWARA values decrease
538 when the TWI reduces, while the highest TWI belongs to the classes of 6.6-7.9 (0.47), and the
539 lowest is for 2.1-4.6 (0.02). There is an adverse relationship between TRI and SWARA value, and

as the TRI increases, the SWARA value reduces. The highest and the lowest values of SWARA also belongs to classes 0-8.7 (0.54) and 46.6-185 (0.001), respectively. For distance from the fault, distance less than 2000 m has the highest impact on spring occurrences and with increase in the distance (greater than 2000 m), the probability of spring occurrences has reduced. The highest SWARA value belongs to distance from the fault of 500-1000 m (0.29) and the lowest value is for greater than 2000 m (0.1). For the distance to river, it can be seen that the class of 0-200 m has the highest correlation with the spring occurrence (0.46) and there is a contrary relationship between spring occurrence and SWARA values; as the more the distance from the river, the lower the spring occurrence probability. In the case of land use, the highest SWARA values are shown for garden areas (0.219), followed by mixture of garden and agriculture (0.17), agricultural areas (0.12), whereas the lowest SWARA is for bare soil and rock (0.00063). The rainfall between 500 and 600 mm has the highest SWARA value with 0.61 and the lowest SWARA belongs to 300-400 mm (0.02). The Inceptisols have the highest SWARA values (0.5) followed by rock outcrop/Entisols (0.39), rock outcrop/Inceptisols (0.056), Inceptisols/Vertisols (0.028), and Badlands (0.014). The highest probability respectively belongs to the highly porous and very good water reservoir karstic oligomiocene and cretaceous pure carbonate formation (OMq and K1bl), the young and poorly consolidated highly porous detrital rock units (PeEf and Plq) and the unconsolidated quaternary alluvium (PlQc).

Table.2. Spatial correlation between conditioning factors and the spring locations by SWARA methods

Factors	Classes	Comparative importance of average value K_j	Coefficient $K_j = S_j + 1$	$w_j = (X(j-1))/k_j$	weight $w_j / \text{sigma } w_j$
Slope (degree)	0 - 5.55		1.000	1.000	0.454
	5.55 - 12.11	0.300	1.300	0.769	0.349
	12.11 - 19.43	1.500	2.500	0.308	0.140
	19.43 - 28.77	2.000	3.000	0.103	0.047
	28.77 - 64.37	3.500	4.500	0.023	0.010
Slope aspect	East		1.000	1.000	0.448
	North	1.000	2.000	0.500	0.224
	West	0.300	1.300	0.385	0.172
	South	0.100	1.100	0.350	0.156
	Flat	0.8	1.05	0.31	0.121
Altitude (m)	1703 - 2068		1.000	1.000	0.608
	1385 - 1703	2.200	3.200	0.313	0.190
	2068 - 3175	0.800	1.800	0.174	0.106
	531 - 1070	1.000	2.000	0.087	0.053
	1070 - 1385	0.200	1.200	0.072	0.044

	Flat		1.000	1.000	0.408
Plan curvature	concave	0.050	1.050	0.952	0.388
	convex	0.900	1.900	0.501	0.204
	583969.72 - 1330153.27		1.000	1.000	0.466
SPI	227099.33 - 583969.72	1.000	2.000	0.500	0.233
	48664.14 - 227099.33	0.200	1.200	0.417	0.194
	0 - 48664.14	1.000	2.000	0.208	0.097
	1330153.27 - 4136452.25	10.000	11.000	0.019	0.009
	6.64 - 7.92		1.000	1.000	0.471
TWI	5.60 - 6.64	0.700	1.700	0.588	0.277
	7.92 - 11.97	1.300	2.300	0.256	0.120
	4.63 - 5.60	0.100	1.100	0.233	0.110
	2.12 - 4.63	4.000	5.000	0.047	0.022
	0 - 5.59		1.000	1.000	0.544
TRI	5.59 - 12.66	0.800	1.800	0.556	0.302
	12.66 - 20.62	1.500	2.500	0.222	0.121
	20.62 - 30.93	3.000	4.000	0.056	0.030
	30.93 - 75.13	10.000	11.000	0.005	0.003
	0 - 200		1.000	1.000	0.242
Distance from fault (m)	200 - 500	0.050	1.050	0.952	0.231
	500 - 1000	0.100	1.100	0.866	0.210
	1000 - 2000	0.050	1.050	0.825	0.200
	> 2000	0.700	1.700	0.485	0.118
	0 - 200		1.000	1.000	0.464
Distance from river (m)	200 - 500	1.900	2.900	0.345	0.160
	500 - 1000	0.050	1.050	0.328	0.152
	1000 - 2000	0.300	1.300	0.253	0.117
	> 2000	0.100	1.100	0.230	0.107
	Garden		1.000	1.000	0.219
Land-use/land-cover	mixture of garden and agriculture	0.282	1.282	0.780	0.171
	agriculture	0.340	1.340	0.582	0.128

	mixture of poor rangeland and follow	0.419	1.419	0.410	0.090
	follow	0.233	1.233	0.333	0.073
	mixture of moderate rangeland and agriculture	0.294	1.294	0.257	0.056
	mixture of very poor forest	0.124	1.124	0.229	0.050
	mixture of waterway and vegetation	0.549	1.549	0.148	0.032
	moderate forest	0.205	1.205	0.122	0.027
	mixture of agriculture with dry farming	0.064	1.064	0.115	0.025
	wood-land	0.030	1.030	0.112	0.024
	good rangeland	0.043	1.043	0.107	0.023
	rangeland	0.333	1.333	0.080	0.018
	poor rangeland	0.030	1.030	0.078	0.017
	poor forest	0.210	1.210	0.065	0.014
	moderate rangeland	0.281	1.281	0.050	0.011
	bare soil and rock	0.237	1.237	0.041	0.009
	dense rangeland	0.278	1.278	0.032	0.007
	dense-forest	10.000	11.000	0.003	0.001
	waterway	0.000	1.000	0.003	0.001
	mixture of agriculture with poor-garden	0.000	1.000	0.003	0.001
	very poor forest	0.000	1.000	0.003	0.001
	mixture of moderate forest and agriculture	0.000	1.000	0.003	0.001
	mixture of low forest and follow,	0.000	1.000	0.003	0.001
	urban and residential	0.000	1.000	0.003	0.001
	600 - 700		1.000	1.000	0.617
	700 - 800	2.200	3.200	0.313	0.193
	800 - 900	0.600	1.600	0.195	0.121
	500 - 600	1.500	2.500	0.078	0.048
	400 - 500	1.300	2.300	0.034	0.021
Rainfall (mm)					
Soil order	Rock Outcrops/Entisols		1.000	1.000	0.509

	Rock Outcrops/Inceptisols	0.300	1.300	0.769	0.392
	Inceptisols	5.900	6.900	0.111	0.057
	Inceptisols/Vertisols	1.000	2.000	0.056	0.028
	Bad Lands	1.000	2.000	0.028	0.014
	OMq		1.000	1.000	0.133
	PeEf	0.309	1.309	0.764	0.101
	PlQc	0.253	1.253	0.610	0.081
	K1bl	0.113	1.113	0.548	0.073
	Plc	0.014	1.014	0.541	0.072
	pd	0.059	1.059	0.511	0.068
	TRKubl	0.223	1.223	0.417	0.055
	TRJvm	0.027	1.027	0.406	0.054
	MPlfgp	0.048	1.048	0.388	0.051
	OMql	0.015	1.015	0.382	0.051
	Plbk	0.081	1.081	0.353	0.047
	E2c	0.291	1.291	0.274	0.036
	TRKurl	0.059	1.059	0.258	0.034
Lithology (unit)	Qft2	0.335	1.335	0.194	0.026
	MuPlaj	0.100	1.100	0.176	0.023
	KEpd-gu	0.080	1.080	0.163	0.022
	Kgu	0.566	1.566	0.104	0.014
	Qft1	0.064	1.064	0.098	0.013
	Ekn	0.109	1.109	0.088	0.012
	KPeam	0.027	1.027	0.086	0.011
	PeEtz	0.328	1.328	0.065	0.009
	Kbgp	0.445	1.445	0.045	0.006
	EMas-sb	0.310	1.310	0.034	0.005
	Mgs	0.626	1.626	0.021	0.003
	TRJlr	10.000	11.000	0.002	0.000
	Klsol	0.000	1.000	0.002	0.000
	JKbl	0.000	1.000	0.002	0.000

Kur	0.000	1.000	0.002	0.000
OMas	0.000	1.000	0.002	0.000
Mmn	0.000	1.000	0.002	0.000

559

560 **4.4. Application of ANFIS ensemble models and model's assessment**

561 In the current study, hybrids of ANFIS model and five meta-heuristic algorithms were designed,
562 constructed and implemented in MATLAB 8.0 software. These models are trained using the
563 training dataset were applied in building the model. Methods of these models are like this: gained
564 weights by SWARA method for each conditioning factor was fed as the input for training dataset.
565 Also, the spring and non-springs were assigned to 1 and 0 respectively, entered into a hybrid model
566 as an output. It can find and model the relationships between input and output data and the
567 modeling accuracy is calculated by statistical methods. The prediction ability of the five hybrid
568 models with training dataset as a target and estimated springs pixel as an output (in a training
569 phase) and testing dataset (in a validation phase) was shown in Fig.5 and Fig.6.

570 MSE indicates how much output of each hybrid's model is close to real rate. As it can be seen in
571 Fig. 5, MSE of ANFIS-IWO, ANFIS-DE, ANFIS-FA, ANFIS-PSO, and ANFIS-BA have been
572 calculated for the training step 0.066, 0.066, 0.066, 0.049, and 0.09, respectively. This shows that
573 compared to other models, ANFIS-PSO had the best performance while ANFIS-BA had the worst
574 one for training step. However, it should be noted that training step is not adequate for determining
575 the best model for MSE optimization, and MSE level for testing phase needs to be reviewed.
576 According to the results shown in Fig.5, values of MSE – 0.060, 0.060, 0.045, and 0.09 –
577 relate to the hybrid models; ANFIS-IWO, ANFIS-FA, ANFIS-PSO, and ANFIS-BEE have been
578 calculated and indicate that the best performance is for ANFIS-PSO, the worst for ANFIS-BA.

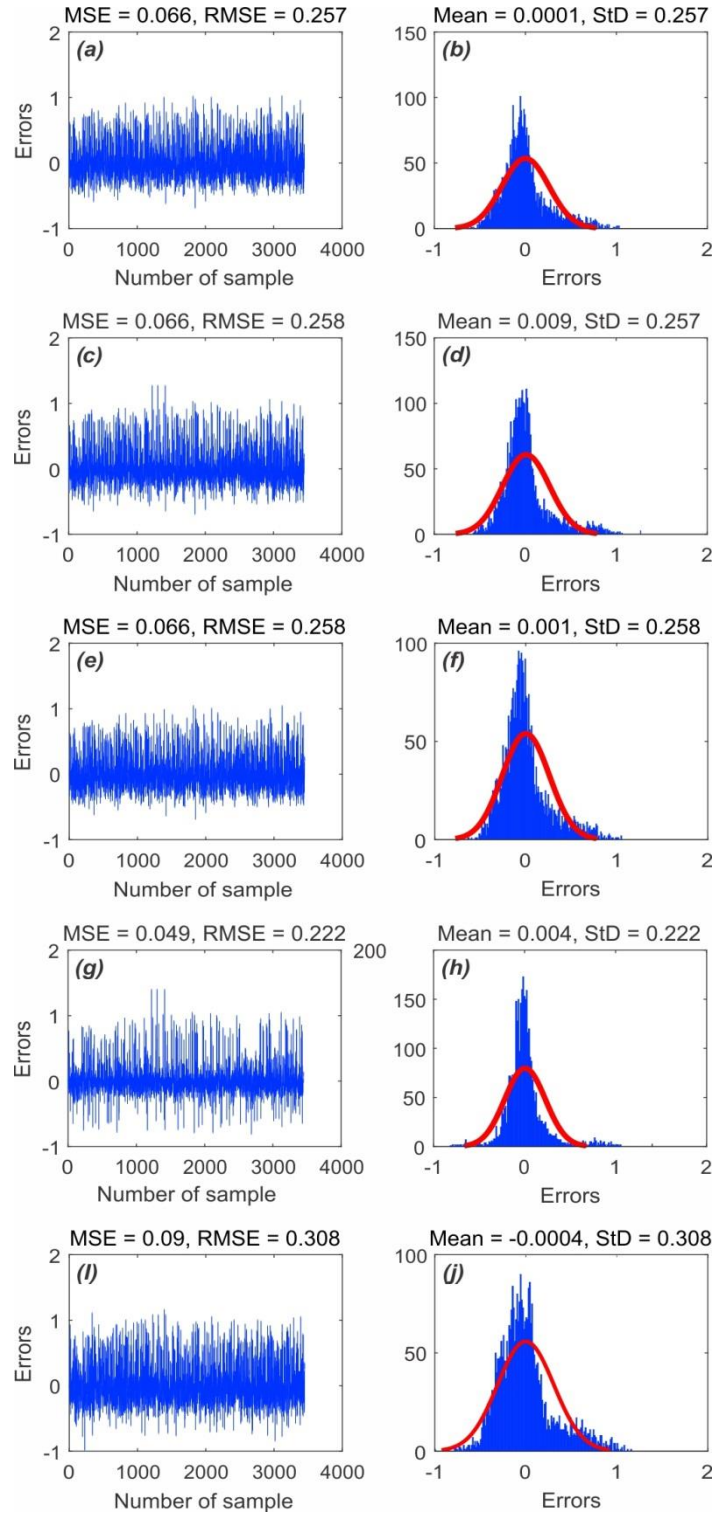


Fig.5. MSE and RMSE values in the training dataset of: a) ANFIS-IWO, c) ANFIS-DE, e) ANFIS-FA, g) ANFIS-PSO i) ANFIS-BA frequency errors of train data samples of b) ANFIS-IWO, d) ANFIS-DE, f) ANFIS-FA, h) ANFIS-PSO j) ANFIS-BA

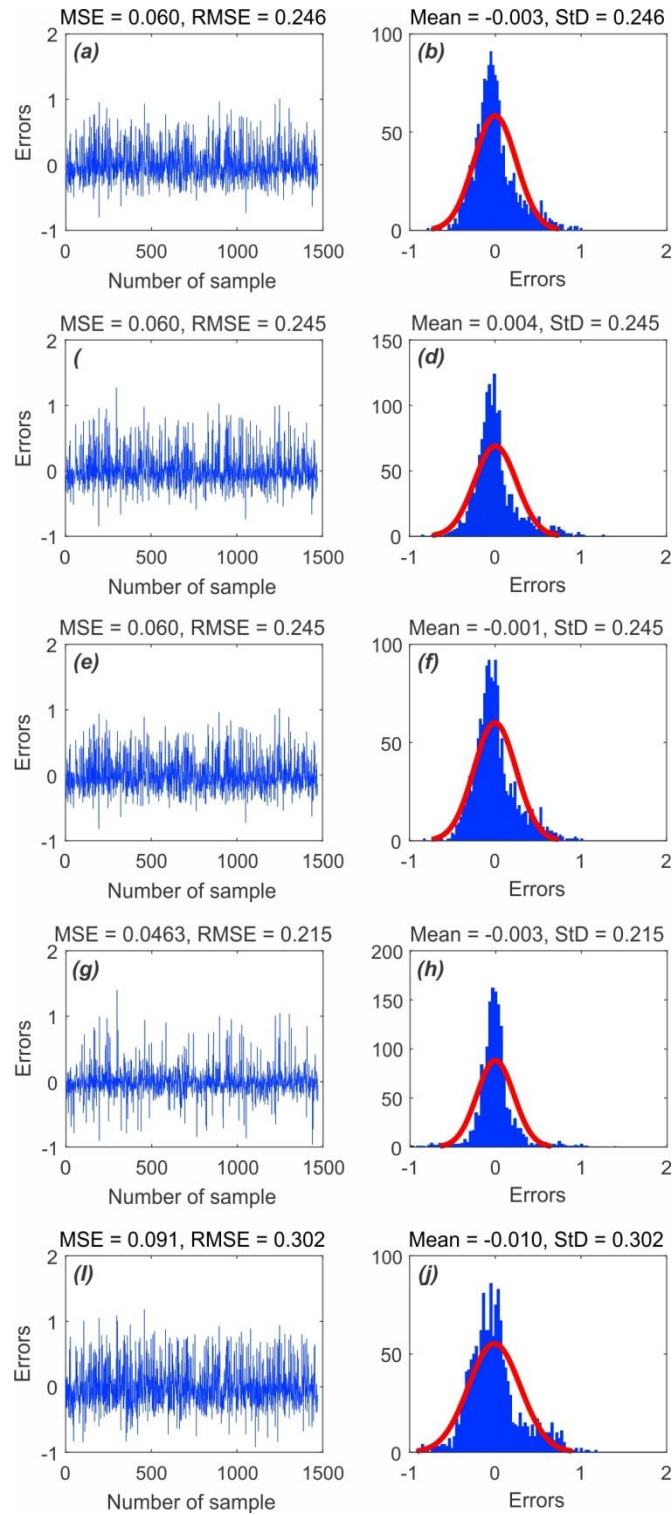


Fig.6. MSE and RMSE values of the validation data samples of a) ANFIS-IWO, c) ANFIS-DE, e) ANFIS-FA, g) ANFIS-PSO l) ANFIS-BA frequency errors of test data samples of b) ANFIS-IWO, d) ANFIS-DE, f) ANFIS-FA, h) ANFIS-PSO j) ANFIS-BA

However, it must be noticed that in addition to accuracy, determining the speed of used models has recently found significance. To accomplish this, therefore, the processing time of 1000 iteration is calculated for each model where the amounts of 8036, 547, 22111, 1050, and 6993 seconds are related to ANFIS-IWO, ANFIS-DE, ANFIS-FA, ANFIS-PSO, and ANFIS-BA, respectively (Fig. 7). As a result, it can be concluded that ANFIS-DE has had the minimum time of processing speed compared to other models and ANFIS-FA has had the maximum time.

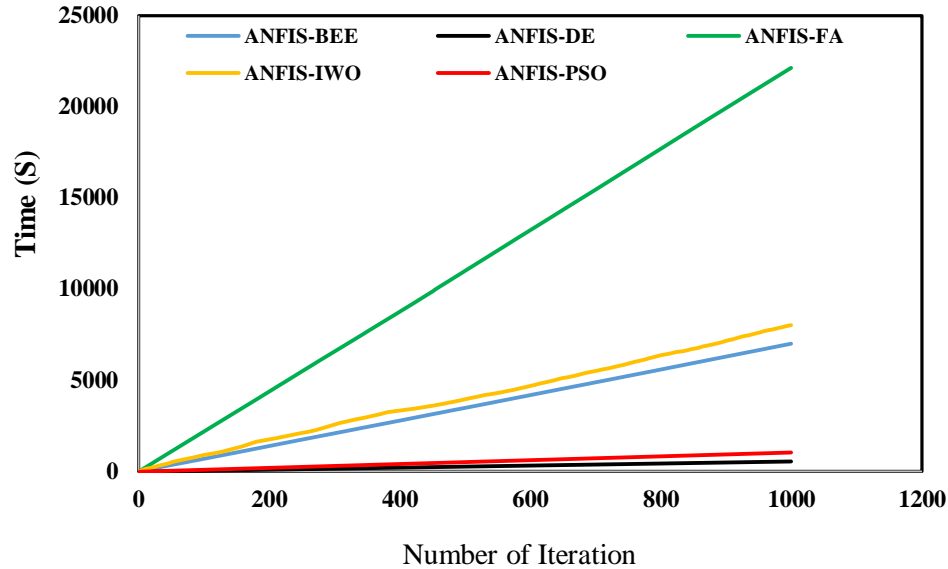


Fig. 7. Processing time used for training the models

On the other hand, it is possible to test how each model achieves convergence in learning. By drawing a diagram, cost function values have been calculated in each iteration of convergence graph for all five models as depicted in Fig.8. The results show that cost function values of ANFIS-DE and ANFIS-BA become constant in 30 and 95 iterations. This indicates a rapid convergence of every model. On the other side, ANFIS-PSO, ANFIS-IWO, and ANFIS-FA achieved convergence in 650, 650, and 360 iterations, respectively that indicates the low speed of these methods in reaching convergence.

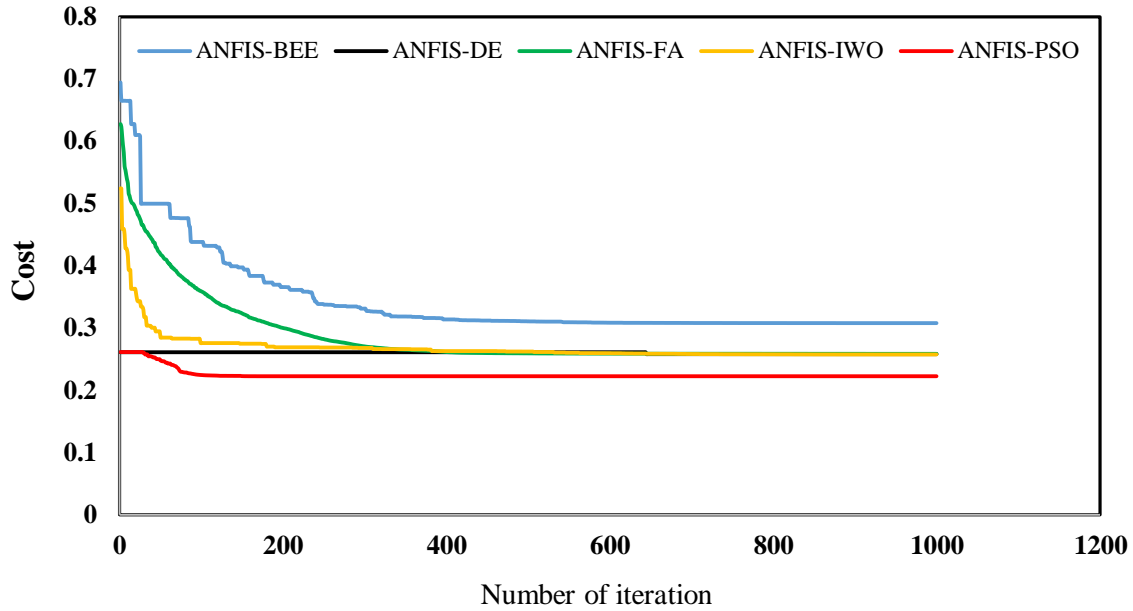


Fig.8. Convergence plot of the models

4.5. Preparation of groundwater spring potential maps using ANFIS hybrid models

In this study, SWARA values were standardized between 0-1 and were then transformed to MATLAB software. Following that, ANFIS hybrid models of ANFIS with IWO, DE, FA, PSO and BA algorithms were constructed using training dataset and standardized SWARA values. In the next step, the built models were used for estimating the groundwater spring index (GSI), which was assigned to whole the pixels of the study area and finally, the groundwater spring potential mapping was developed from groundwater spring indices. At first, each pixel was assigned to a unique groundwater spring index. In second step, all indices were exported in ArcGIS10.2 software and were utilized in the construction of the groundwater spring potential mapping. Ultimately, the archived maps were divided into five potential classes, namely very low, low, moderate, high and very high based on quantile classification scheme. Therefore, based on the five hybrid model, five maps of groundwater spring potential were prepared (Figs.9 a-e). There are six methods, namely manual, equal interval, geometric interval, quantile, natural break and standard deviation for classification based on the different purposes. The selection of the best method depends on the characteristics of the data and the distribution of the groundwater spring indexes in a histogram (Ayalew and Yamagishi, 2005). If the distribution of the indexes in the histogram is normal or close to normal, two methods of Equal interval and standard deviation are used. However, if the indexes have a positive or negative skewness, the quantile or natural break classification is proper for indexes classification (Akgun, 2012). In this research, the histogram was checked and the results revealed that quantile method was better than other methods for indexes classification.

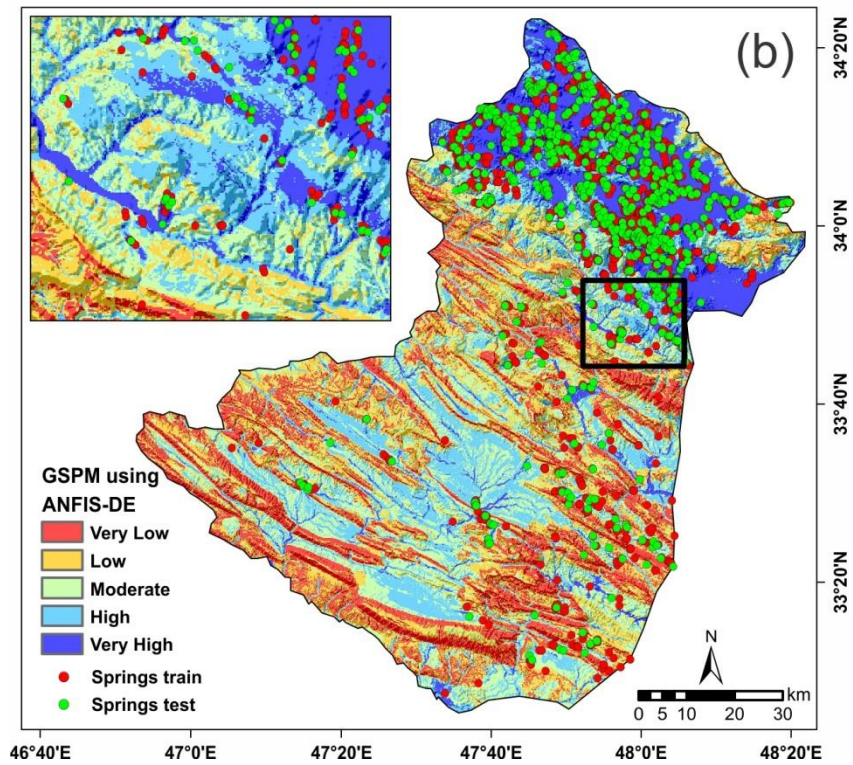
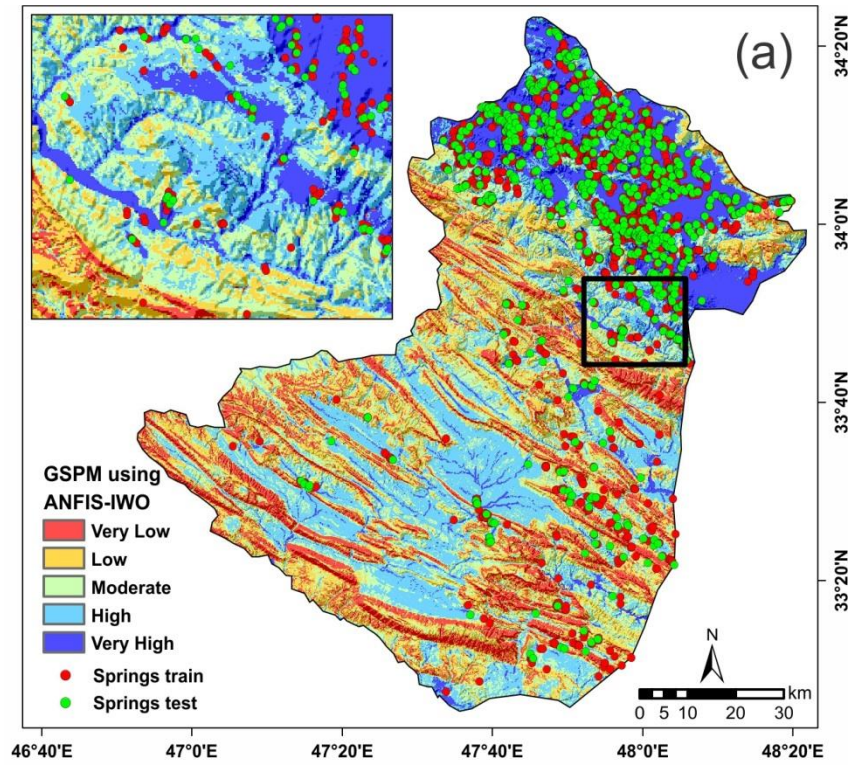


Fig.9. Groundwater spring potential mapping using ANFIS-IWO (a), ANFIS-DE (b), ANFIS-FA (c), ANFIS-PSO (d) and ANFIS-BA (e).

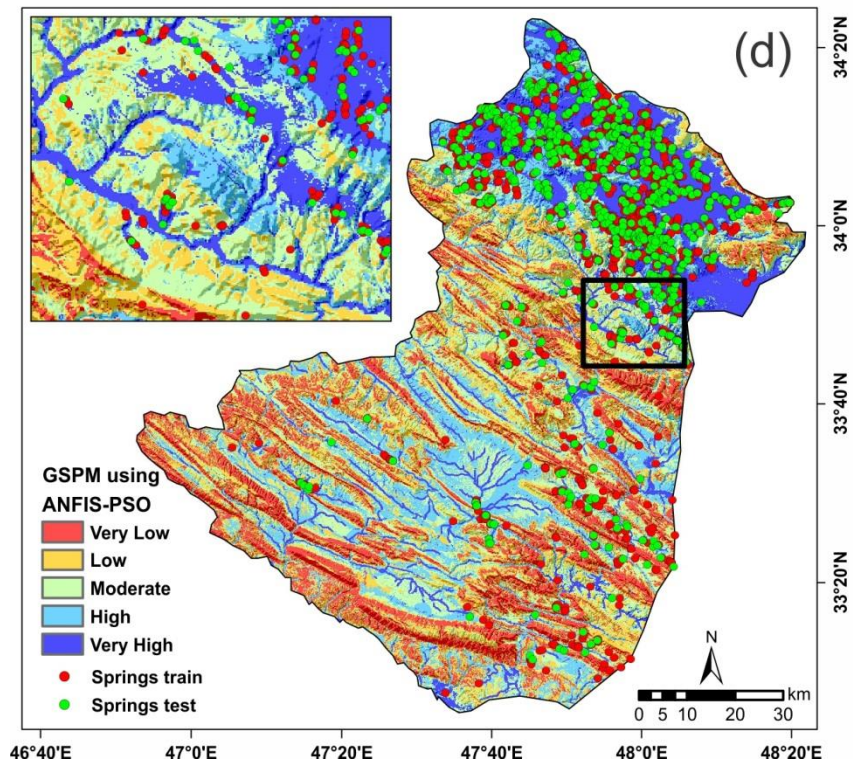
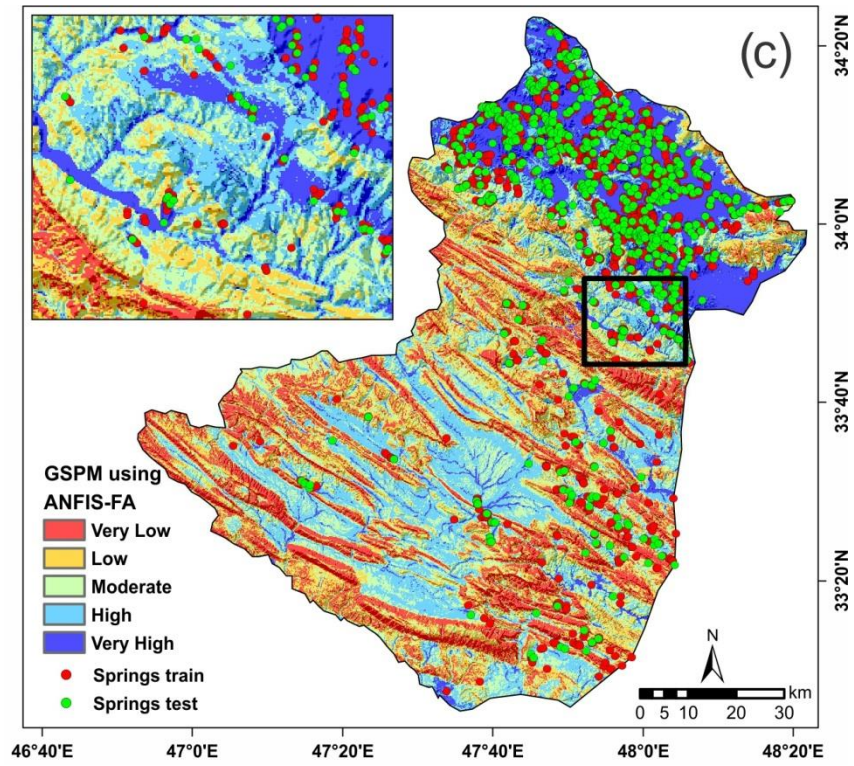


Fig.9. Continued

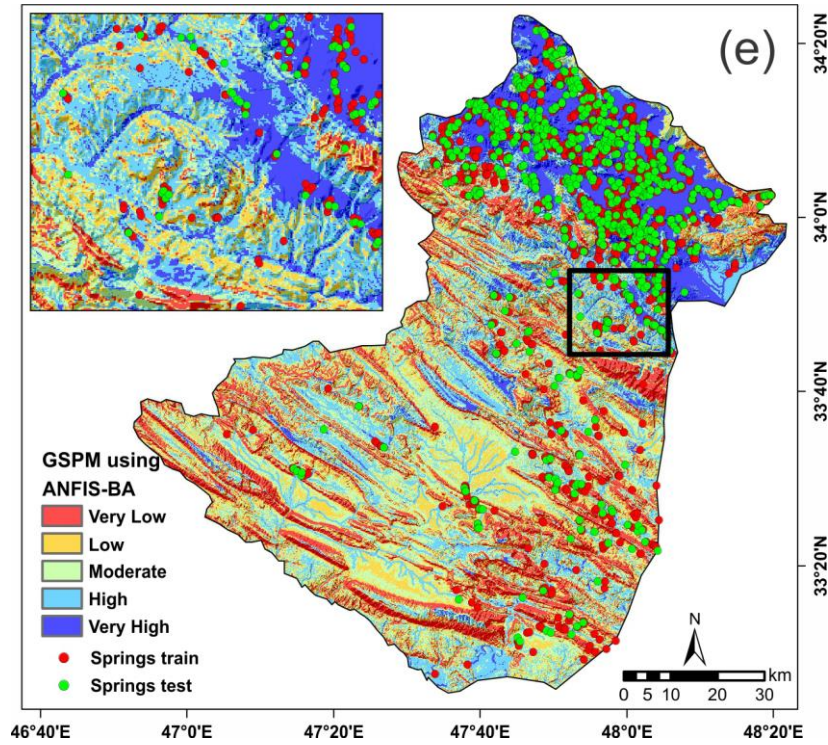


Fig.9. Continued

4.6. Validation and comparisons of the groundwater spring potential map

The prediction ability and reliability of the five achieved maps have been evaluated by both the training and the validating dataset. The results of the success rate revealed that the ANFIS-DE had the highest AUC value of 0.883 followed by ANFIS-IWO and ANFIS-FA (0.882), ANFIS-PSO (0.871) and ANFIS-BA (0.852) (Fig.10a). The results exhibited that all five models had a very good prediction capability but the ANFIS-DE has the highest prediction rate (0.873) followed by NFIS-IWO and ANFIS-FA (0.873), ANFIS-PSO (0.865) and ANFIS-BA (0.839), respectively (Fig.10b).

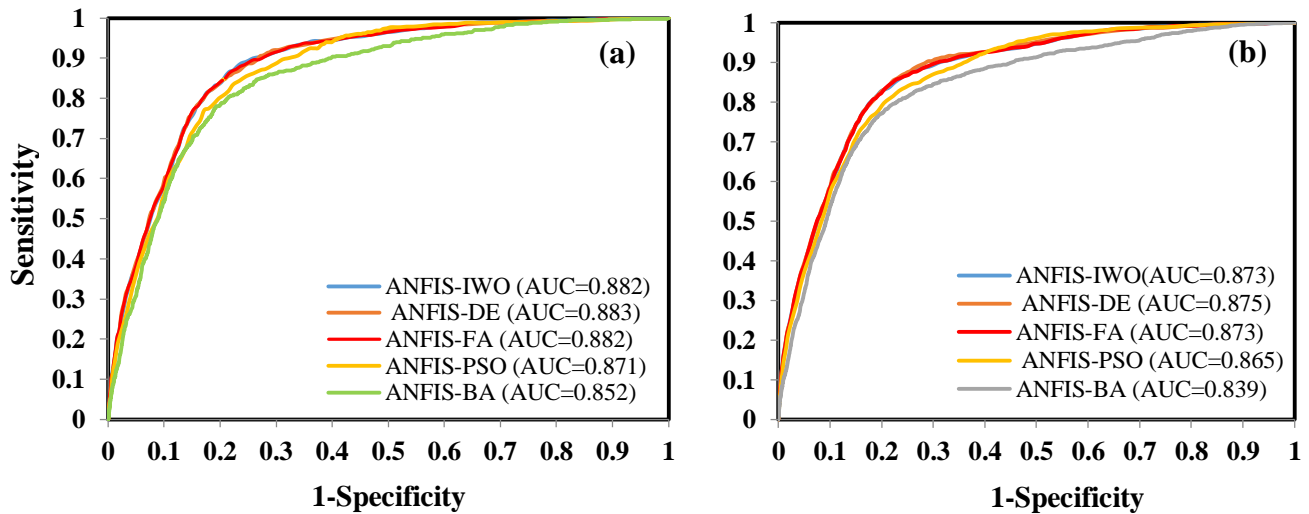


Fig.10. Success rate (a) and prediction rate (b) curves for the five performed models

4.7. Non-parametric statistical tests

The two tests of Freidman and Wilcoxon signed rank have been performed to determine whether there are any statistically significant differences between the models performance or not. The result of Freidman test revealed that (Table.3) as Sig and chi-square values were less than 0.05 and greater than 3.84, respectively, null hypothesis has been rejected. The result also indicated that there was statistically a significant difference between prediction capabilities of these five models.

Table.3. The result of Freidman test

NO	Performed models	Mean rank	Chi-square	Sig
1	ANFIS-DE	3.04	64.84	0.00
2	ANFIS-IWO	3.13		
3	ANFIS-FA	2.98		
4	ANFIS-PSO	2.72		
5	ANFIS-BA	3.12		

To show the pairwise differences between models performance, the Wilcoxon signed rank test was carried out and result were shown in Table 4. Result of the Wilcoxon signed-rank test showed that both P-values and z were far from the standard values of 0.05 and (from -1.96 to + 1.96), respectively except for ANFIS-FA vs. ANFIS-DE and ANFIS-PSO vs. ANFIS-DE. This indicates that there are statistically significant differences between models performance except for ANFIS-FA vs. ANFIS-DE and ANFIS-PSO vs. ANFIS-DE.

Table.4. The result of Wilcoxon signed rank test

NO	Pairwise comparison	Z-Value	P-Value	Significance
1	ANFIS-DE vs. ANFIS-BA	-3.97	0.00	Yes
2	ANFIS-FA vs. ANFIS-BA	-2.37	0.017	Yes
3	ANFIS-IWO vs. ANFIS-BA	-2.35	0.018	Yes
4	ANFIS-PSO vs. ANFIS-BA	-3.04	0.002	Yes
5	ANFIS-FA vs. ANFIS-DE	-1.32	0.185	No
6	ANFIS-IWO vs. ANFIS-DE	-3.96	0.00	Yes
7	ANFIS-PSO vs. ANFIS-DE	-0.841	0.41	NO
8	ANFIS-IWO vs. ANFIS-FA	-3.19	0.001	Yes
9	ANFIS-PSO vs. ANFIS-FA	-1.90	0.057	Yes

10	ANFIS-PSO vs. ANFIS-IWO	-2.44	0.015	Yes
----	-------------------------	-------	-------	-----

4.8. Percentage area

The percentage area of each class of final map resulting from five hybrid models has been represented in Fig.11. According to results, as ANFIS-DE is more accurate in groundwater spring prediction capabilities, the percentage areas of very low, low, moderate, high and very high groundwater spring potential are about 19.06, 19.88, 21.72, 20.55 and 18.78 % of the study area, respectively.

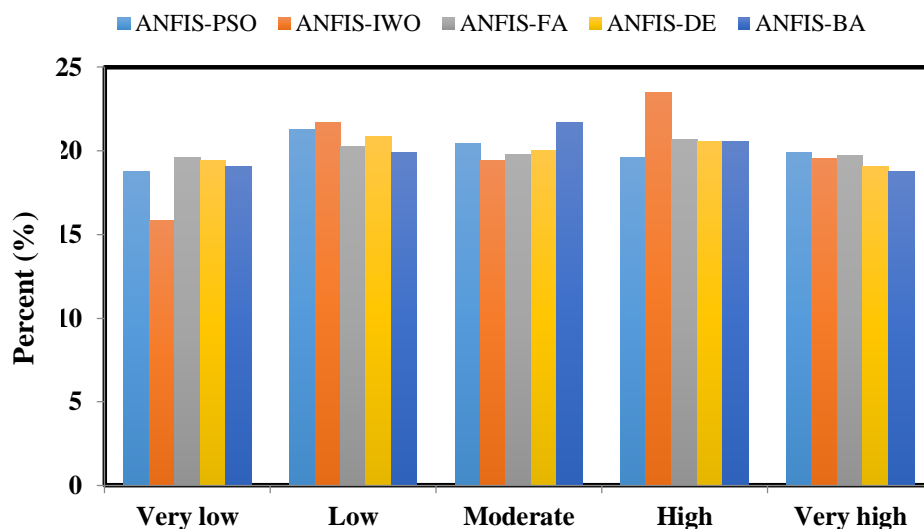


Fig.11. Percentage areas of different groundwater spring potential classes for five models

5. Discussion

5.1. The impact of conditioning factor's classes on GSPM

Assessment of conditioning factor is a necessary step in finding the correlation analysis between spring and conditioning factor. It should be noted that no universal guideline is available regarding the number and size of the classes as well as selecting the conditioning factors. They were selected mostly based on characteristics of the study area and previous similar studies (Xu et al., 2013). As the slope increase, the probability of the water infiltration reduces and runoff generation will increase. Thus, the more the slope, the lowest the spring occurrence probability. According to the result of the SWARA method, the springs almost occur in a middle altitude or mountain slopes (but wells are dug in a low-land area). The flat curvature class retains and infiltrates rainfall. Therefore, the amount of groundwater in these areas is higher than concave or convex curvature. The east aspect has more springs than other aspects. These results are in accordance with Pourtaghi and Pourghasemi (2014), that had explained most springs occurred in the elevation of 1600-1900 m and east slope aspect (with FR method). TWI shows the amount of wetness, and it is obvious that the more the TWI, the higher the springs probability occurrence is. Terrain Roughness Index (TRI) or topographic roughness or terrain ruggedness calculates the sum of change in elevation between a grid cell and its neighborhood, and as the lowest the roughness, the highest spring

potential mapping. The SPI shows the erosive power of the water and mountainous area is higher than plain area. So, As the SPI increases, the spring potential occurrence increases. Rivers are one of the most important sources of groundwater recharge and the nearer to river, the higher probability to springs occurrences. Also, as the rainfall increases, the higher springs incident, but in the current study, some other conditioning factors affected the spring occurrences.

Most of the springs were located in the garden land-use/land-cover. Therefore, it can be stated that the gardens have been established near the springs. Pliocene-Quaternary formation in a geologic time scale is newer and Quaternary formation has a high potential to groundwater springs incident due to high permeability. The fault is discontinuity in a volume of rock. Thus, the nearer to the fault, the higher the spring occurrence probability will be. Inceptisols soils are relatively new and are characterized by having only the weakest appearance of horizons, the most abundant on the Earth (<https://www.britannica.com/science/Inceptisol>) and mostly formed from colluvial and alluvial materials. So, due to high permeability and high rainfall infiltration, they have a high potential for springs occurrences. In the case of lithological unit, there are four suitable rock type as water reservoir based on physical phenomena such as porosity and permeability that consist of: 1. unconsolidated sands and gravels; 2. sandstones; 3. Lime-stones; and 4. basaltic lava flows. In this study area lithological units include sedimentary rocks mostly carbonate and detrital rocks with cover of alluvium and minor soil.

5.2. Advantages/disadvantages of the models and performance analysis

The highest accuracy based on the RMSE in both training and testing dataset belonged to the ANFIS-PSO model. However, based on the AUC for success and prediction rate, the ANFIS-DE model has the highest prediction capability. The problem with RMSE comes from the fact that it is based on the error assessment. But the models should be acted upon holistically based on the abilities. AUC for Receiver operating characteristic (ROC) curves (success and prediction rate curves) is based on the true positive (TP), true negative (TN), false positive (FP) and false negative (FN), it is more accurate than RMSE for comparison (Termeh et al., 2018).

ANFIS is one of the machine learning algorithms that is proper for natural phenomenon modeling due to its non-linear structure. The ANFIS model, which is based on Takagi–Sugeno fuzzy inference system, is a hybrid of ANNs and fuzzy logic. Therefore, it has a potential to capture the benefits of both in a single framework and can be considered as a robust model. The predictions in ANFIS model are based on learning the “if–then” rules between groundwater spring locations and conditioning factors.

Polykretis et al. (Polykretis et al., 2017), applied ANFIS for landslide susceptibility mapping (LSM) in Peloponnese peninsula, Grece and stated that ANFIS model was a robust model. Vahidinia et al. (Vahidnia et al., 2010), applied ANFIS model to LSM in the Mazandaran Province, Iran, and revealed that ANFIS was a flexible and non-linear model and was completely appropriate for building a framework of easy inferences. Isanta Navarro (Isanta Navarro, 2013), applied ANFIS to stability augmentation of an airplane and stated that ANFIS had some advantages including: (1) much better learning ability, (2) need for fewer adjustable parameters than those required in other neural network structure and (3) allowing a better integration with other control design methods by its networks.

Despite several advantages of ANFIS, non-adjutancy of membership function is the biggest disadvantage of this model. Finding the optimal parameter for neural fuzzy model in a membership function is difficult; therefore, the best parameter should be finding other optimization models. This problem was addressed in this paper for being solved by five meta-heuristic algorithms, namely Invasive Weed Optimization, Differential Evolution, Firefly, Particle Swarm Optimization and Bees algorithms. The aim of any optimization is to find values of the variable to gratify the restriction by minimizing or maximizing the objective function. These optimization algorithms are completely new in environmental modeling (especially in groundwater potential mapping) and have been used for natural hazards assessment by a few researchers in landslide susceptibility assessment (Chen et al., 2017a) as well as in flood susceptibility mapping (Bui et al., 2016; Termeh et al., 2018).

In the current study, the results showed that DE algorithm optimized the parameter for neural fuzzy model better than four other algorithms. The main DE algorithm's advantage is its simplicity as it consists of only three parameters called N (size of population), F (mutation parameter) and C (crossover parameter) for controlling the search process (Tvrđik, 2006). Advantages of DE algorithm can be explained as follows: (1) Ability to handle non-differentiable, nonlinear and multimodal cost functions, (2) Parallelizability to cope with computation intensive cost functions, (4) good convergence properties, i.e. consistent convergence to the global minimum in consecutive independent trials, and (5) random sampling and combining vectors in the present population for creating vectors for the next generation.

Finally, it should be noted that each algorithm has some advantages or disadvantages according to the optimization problems which can be summarized as:

Some of the advantages of IWO in comparison to other evolutionary algorithms include the way of reproduction, spatial dispersal, and competitive exclusion (Mehrabian and Lucas, 2006) as well as the fact that seeds and their parents are ranked together and those with better fitness survive and become reproductive (Ahmed et al., 2014). This algorithm can benefit from combined advantages of retaining the dominant poles and the error minimization (Abu-Al-Nadi et al., 2013) and there is no need for continuity or differentiability of the objective function.

Bees algorithm doesn't employ any probability approach, but utilizes fitness evaluation to drive the search (Yuce et al., 2013). This algorithm is implemented with several optimization problems or in other words, BA uses a set of parameters including the number of scout bees in the selected patches, the number of best patches in the selected patches, the number of elite patches in the selected best patches, the number of recruited bees in the elite patches, the number of recruited bees in the non-elite best patches, the size of neighborhood for each patch, the number of iterations and the difference between the value of first and last iterations that makes it powerful. BA also has both local and global search capability and the local search step of the algorithm covers the best locations. BA is really easy to use and available for hybridization combination with other algorithms (Yuce et al., 2013). Another advantage is hiring smart bees since bees (artificial insects) can memorize the location of the best food source and its quality which has been found before. If the new solution has a lower fitness than the best-saved solution in the SB memory, it is replaced with new candidate solution (Gorji-Bandpy and Mozaffari, 2012).

Firefly Algorithm's (FA) advantages are summarized as: (1) handling highly non-linear, multi-modal optimization problems efficiently, (2) not utilizing velocities (3) very high speed of

convergence in finding the global optimized answer (4) ability to be integrated with other optimization techniques as a flexible method, and finally (5) not needing a good initial solution to beginning of its iteration process.

Advantages of Particle Swarm Optimization (PSO) algorithm can be summarized as follows: (1) Particles update themselves with the internal velocity; (2) particles have a memory important to the algorithm, (3) the 'best' particle gives out the information to others, (4) it often produces quality solutions more rapidly than alternative methods, (5) this algorithm simulates bird flocking behavior to achieve a self-evolution system, (6) it automatically searches for the optimum solution in the solution space, (7) (Wan, 2013).

As a result, there isn't any algorithm which works perfectly for all optimization problems, and each algorithm has a different performance accuracy based on different data. New algorithms, therefore, should be applied, tested and finally the most powerful algorithm should be selected; as the conclusion of the research demands.

5.3. Previous works and future work proposal

Some research has been carried out in groundwater well or spring potential mapping using bivariate statistical models (Al-Manmi and Rauf, 2016; Guru et al., 2017; Nampak et al., 2014) using random forest (Rahmati et al., 2016) and using boosted regression tree and classification and regression tree (Naghbi et al., 2016). The ANFIS-metaheuristic hybrid models have not seen used in groundwater potential mapping. However, these hybrid models have proven efficient in flood susceptibility mapping (Bui et al., 2016; Termeh et al., 2018) and landslide susceptibility mapping (Chen et al., 2017a). Tien Bui et al. (Bui et al., 2016) ensemble the ANFIS using two optimization models, namely Genetic (GA) and PSO for the identification of flood prone areas in Vietnam. Razavi Termeh et al. (Termeh et al., 2018), used ANFIS-Ant Colony Optimization, ANFIS-GA and ANFIS-PSO in flood susceptibility mapping of Jahrom basin and stated that ANFIS-PSO had higher prediction capabilities than the two other models. Chen et al (2017) applied three hybrid models, namely ANFIS- Genetic Algorithm (GA), ANFIS-Differential Evolution (DE) and ANFIS-Particle Swarm Optimization (PSO) for identifying the areas prone to landslides in Hanyuan County, China. The results showed that ANFIS-DE had a higher performance (AUC=0.84) followed by ANFIS-GA (AUC=0.82) and ANFIS-PSO (AUC=0.78).

In general, the results of the present study and different researchers revealed that by applying hybrid models, better results could be achieved for any spatial prediction modeling including groundwater potential mapping. The ensembles of ANFIS by meta-heuristic algorithms can be proposed for any spatial prediction modeling such as groundwater potential mapping, flood susceptibility mapping, landslide susceptibility assessment, gully occurrences susceptibility mapping and other endeavors at a regional scale and in other areas.

For future work, it is recommended that (1) the water quality of the Koohdasht-Nourabad plain be investigated and the water quality of areas with high potential be determined for different aspects such as drinking, agricultural and industrial activities, and (2) the groundwater vulnerability assessment should be applied by some common methods including DRASTIC model for which the zones with high potential to groundwater occurrences should be preserved against pollution.

6. Conclusion

Groundwater is the most important natural resource in the world and about 25 percent of all fresh water is estimated as groundwater. Thus, the groundwater potential mapping has been considered as one of the most effective tools for the management of groundwater resources for better exploitation. The conservation and the maps with high accuracy is necessary for decisions. As the natural phenomena are complex, the simple method and statistical models do not have an appropriate result in modeling of the natural phenomena. To solve the problem, the artificial intelligence models have been used for having a reasonable result but these model have some weaknesses, especially in modeling process. To resolve this problem, this study verifies the five new hybrid models of ANFIS with metaheuristic algorithms namely IWO, DE, FA, PSO and BA to increase the prediction capability of the spatial prediction of groundwater potential mapping (1) for solving the weakness of the artificial intelligence models and (2) using non-linear structure of these models which are better for modeling of the complex natural phenomena such as groundwater modeling. The result of this modeling has been evaluated using prediction rate ROC curves and the results showed that all models had very good reasonable results. However, the ANFIS-DE had the highest prediction power (0.875) followed by ANFIS-IWO and ANFIS-FA (0.873), ANFIS-PSO (0.865) and ANFIS-BA (0.839). Thus, the results revealed that the metaheuristic algorithms could optimize the weights parameters of the ANFIS model with high accuracy as the highest advantage of these algorithms

According to the results of the SWARA method, most springs existed in an altitude of 1703-2068 m, flat curvature, east aspect, TWI of 6.6-7.9, TRI of 0-8.7, SPI of 583969-1330153, Inceptisols soil, slope of 0-5.5 degree, 0-200 m distance from river, 500-1000 m distance from fault, rainfall between 500-600 mm, in a garden, in a Pliocene-Quaternary lithological age and OMq lithology unit.

The results of the current study is helpful for Iran Water Resources Management Company (IWRMC) for sustainable management of the groundwater resources. Overall, the maps resulting from these hybrid artificial intelligence algorithms can be applied for better management of the groundwater resources in the study area, and can be used for other areas for groundwater potential assessment or mapping of gully, flood, landslide and other susceptibility uses in the world due to its high precision.

References

- Abu-Al-Nadi DI, Alsmadi OM, Abo-Hammour ZS, Hawa MF, Rahhal JS. Invasive weed optimization for model order reduction of linear MIMO systems. *Applied Mathematical Modelling* 2013; 37: 4570-4577.
- Adiat K, Nawawi M, Abdullah K. Assessing the accuracy of GIS-based elementary multi criteria decision analysis as a spatial prediction tool—A case of predicting potential zones of sustainable groundwater resources. *Journal of Hydrology* 2012; 440: 75-89.
- Aghdam IN, Pradhan B, Panahi M. Landslide susceptibility assessment using a novel hybrid model of statistical bivariate methods (FR and WOE) and adaptive neuro-fuzzy inference system (ANFIS) at southern Zagros Mountains in Iran. *Environmental Earth Sciences* 2017; 76: 237.
- Ahmed A, Al-Amin R, Amin R. Design of static synchronous series compensator based damping controller employing invasive weed optimization algorithm. *SpringerPlus* 2014; 3: 394.

854 Akgun A. A comparison of landslide susceptibility maps produced by logistic regression, multi-criteria
855 decision, and likelihood ratio methods: a case study at İzmir, Turkey. *Landslides* 2012; 9: 93-106.

856 Al-Manmi DAM, Rauf LF. Groundwater potential mapping using remote sensing and GIS-based, in
857 Halabja City, Kurdistan, Iraq. *Arabian Journal of Geosciences* 2016; 9: 357.

858 Alimardani M, Hashemkhani Zolfani S, Aghdaie MH, Tamošaitienė J. A novel hybrid SWARA and VIKOR
859 methodology for supplier selection in an agile environment. *Technological and Economic*
860 *Development of Economy* 2013; 19: 533-548.

861 Alley WM, Reilly TE, Franke OL. Sustainability of ground-water resources. Vol 1186: US Department of
862 the Interior, US Geological Survey, 1999.

863 Alweshah M, Abdullah S. Hybridizing firefly algorithms with a probabilistic neural network for solving
864 classification problems. *Applied Soft Computing* 2015; 35: 513-524.

865 Amiri B, Hossain L, Crawford JW, Wigand RT. Community detection in complex networks: Multi-
866 objective enhanced firefly algorithm. *Knowledge-Based Systems* 2013; 46: 1-11.

867 Ayalew L, Yamagishi H. The application of GIS-based logistic regression for landslide susceptibility
868 mapping in the Kakuda-Yahiko Mountains, Central Japan. *Geomorphology* 2005; 65: 15-31.

869 Beasley TM, Zumbo BD. Comparison of aligned Friedman rank and parametric methods for testing
870 interactions in split-plot designs. *Computational statistics & data analysis* 2003; 42: 569-593.

871 Berhanu B, Seleshi Y, Melesse AM. Surface Water and Groundwater Resources of Ethiopia: Potentials
872 and Challenges of Water Resources Development. Nile River Basin. Springer, 2014, pp. 97-117.

873 Brenning A. Spatial prediction models for landslide hazards: review, comparison and evaluation. *Natural*
874 *Hazards and Earth System Science* 2005; 5: 853-862.

875 Bui DT, Lofman O, Revhaug I, Dick O. Landslide susceptibility analysis in the Hoa Binh province of
876 Vietnam using statistical index and logistic regression. *Natural hazards* 2011; 59: 1413.

877 Bui DT, Pradhan B, Nampak H, Bui Q-T, Tran Q-A, Nguyen Q-P. Hybrid artificial intelligence approach
878 based on neural fuzzy inference model and metaheuristic optimization for flood susceptibility
879 modeling in a high-frequency tropical cyclone area using GIS. *Journal of Hydrology* 2016; 540:
880 317-330.

881 Bui DT, Pradhan B, Revhaug I, Nguyen DB, Pham HV, Bui QN. A novel hybrid evidential belief function-
882 based fuzzy logic model in spatial prediction of rainfall-induced shallow landslides in the Lang
883 Son city area (Vietnam). *Geomatics, Natural Hazards and Risk* 2015; 6: 243-271.

884 Chang F-J, Tsai M-J. A nonlinear spatio-temporal lumping of radar rainfall for modeling multi-step-ahead
885 inflow forecasts by data-driven techniques. *Journal of Hydrology* 2016; 535: 256-269.

886 Chen W, Panahi M, Pourghasemi HR. Performance evaluation of GIS-based new ensemble data mining
887 techniques of adaptive neuro-fuzzy inference system (ANFIS) with genetic algorithm (GA),
888 differential evolution (DE), and particle swarm optimization (PSO) for landslide spatial
889 modelling. *CATENA* 2017a; 157: 310-324.

890 Chen W, Pourghasemi HR, Panahi M, Kornejady A, Wang J, Xie X, et al. Spatial prediction of landslide
891 susceptibility using an adaptive neuro-fuzzy inference system combined with frequency ratio,
892 generalized additive model, and support vector machine techniques. *Geomorphology* 2017b;
893 297: 69-85.

894 Cheng Z, Zhou H, Yang H. Research on MPPT control of PV system based on PSO algorithm. *Control and*
895 *Decision Conference (CCDC)*, 2010 Chinese. IEEE, 2010, pp. 887-892.

896 Chenini I, Mammou AB. Groundwater recharge study in arid region: an approach using GIS techniques
897 and numerical modeling. *Computers & Geosciences* 2010; 36: 801-817.

898 Chung C-JF, Fabbri AG. Validation of spatial prediction models for landslide hazard mapping. *Natural*
899 *Hazards* 2003; 30: 451-472.

900 Clapcott J, Goodwin E, Snelder T. Predictive Models of Benthic Macroinvertebrate Metrics. Prepared for
901 Ministry for the Environment. Cawthron Report, 2013.

902 Das S, Abraham A, Chakraborty UK, Konar A. Differential evolution using a neighborhood-based
 903 mutation operator. *IEEE Transactions on Evolutionary Computation* 2009; 13: 526-553.
 904 David Keith Todd, Mays LW. *Groundwater Hydrology*, 2nd Edition. Wiley, New York 1980.
 905 Derrac J, García S, Molina D, Herrera F. A practical tutorial on the use of nonparametric statistical tests
 906 as a methodology for comparing evolutionary and swarm intelligence algorithms. *Swarm and*
 907 *Evolutionary Computation* 2011; 1: 3-18.
 908 Eberhart R, Kennedy J. A new optimizer using particle swarm theory. *Micro Machine and Human*
 909 *Science*, 1995. MHS'95., Proceedings of the Sixth International Symposium on. IEEE, 1995, pp.
 910 39-43.
 911 Fashae OA, Tijani MN, Talabi AO, Adedeji OI. Delineation of groundwater potential zones in the
 912 crystalline basement terrain of SW-Nigeria: an integrated GIS and remote sensing approach.
 913 *Applied Water Science* 2014; 4: 19-38.
 914 Fitts CR. *Groundwater science*: Academic press, 2002.
 915 Friedman M. The use of ranks to avoid the assumption of normality implicit in the analysis of variance.
 916 *Journal of the american statistical association* 1937; 32: 675-701.
 917 Gandomi AH, Yang X-S, Talatahari S, Alavi AH. Firefly algorithm with chaos. *Communications in Nonlinear*
 918 *Science and Numerical Simulation* 2013; 18: 89-98.
 919 Gaprindashvili G, Guo J, Daorueang P, Xin T, Rahimy P. A new statistic approach towards landslide
 920 hazard risk assessment. *International Journal of Geosciences* 2014; 5: 38.
 921 Ghalkhani H, Golian S, Saghaian B, Farokhnia A, Shamseldin A. Application of surrogate artificial
 922 intelligent models for real-time flood routing. *Water and Environment Journal* 2013; 27: 535-
 923 548.
 924 Ghasemi M, Ghavidel S, Akbari E, Vahed AA. Solving non-linear, non-smooth and non-convex optimal
 925 power flow problems using chaotic invasive weed optimization algorithms based on chaos.
 926 *Energy* 2014; 73: 340-353.
 927 Gorji-Bandpy M, Mozaffari A. Multiobjective optimization of irreversible thermal engine using mutable
 928 smart bee algorithm. *Applied Computational Intelligence and Soft Computing* 2012; 2012: 5.
 929 Güçlü YS, Şen Z. Hydrograph estimation with fuzzy chain model. *Journal of Hydrology* 2016; 538: 587-
 930 597.
 931 Guru B, Seshan K, Bera S. Frequency ratio model for groundwater potential mapping and its sustainable
 932 management in cold desert, India. *Journal of King Saud University-Science* 2017; 29: 333-347.
 933 Hong H, Panahi M, Shirzadi A, Ma T, Liu J, Zhu A-X, et al. Flood susceptibility assessment in Hengfeng
 934 area coupling adaptive neuro-fuzzy inference system with genetic algorithm and differential
 935 evolution. *Science of The Total Environment* 2017.
 936 Hong H, Pradhan B, Xu C, Bui DT. Spatial prediction of landslide hazard at the Yihuang area (China) using
 937 two-class kernel logistic regression, alternating decision tree and support vector machines.
 938 *Catena* 2015; 133: 266-281.
 939 Isanta Navarro R. Study of a neural network-based system for stability augmentation of an airplane.
 940 2013.
 941 Israil M, Al-Hadithi M, Singhal D. Application of a resistivity survey and geographical information system
 942 (GIS) analysis for hydrogeological zoning of a piedmont area, Himalayan foothill region, India.
 943 *Hydrogeology journal* 2006; 14: 753-759.
 944 Jang J-S. ANFIS: adaptive-network-based fuzzy inference system. *IEEE transactions on systems, man, and*
 945 *cybernetics* 1993; 23: 665-685.
 946 Jha MK, Chowdary V, Chowdhury A. Groundwater assessment in Salboni Block, West Bengal (India) using
 947 remote sensing, geographical information system and multi-criteria decision analysis
 948 techniques. *Hydrogeology journal* 2010; 18: 1713-1728.

949 Jha MK, Chowdhury A, Chowdary V, Peiffer S. Groundwater management and development by
 950 integrated remote sensing and geographic information systems: prospects and constraints.
 951 Water Resources Management 2007; 21: 427-467.

952 Kaliraj S, Chandrasekar N, Magesh N. Identification of potential groundwater recharge zones in Vaigai
 953 upper basin, Tamil Nadu, using GIS-based analytical hierarchical process (AHP) technique.
 954 Arabian Journal of Geosciences 2014; 7: 1385-1401.

955 Kennedy J. Particle swarm optimization. Encyclopedia of machine learning. Springer, 2011, pp. 760-766.

956 Kennedy J, Eberhart R. Particle swarm optimization, IEEE International of first Conference on Neural
 957 Networks. Perth, Australia, IEEE Press, 1995.

958 Keršulienė V, Zavadskas EK, Turskis Z. Selection of rational dispute resolution method by applying new
 959 step-wise weight assessment ratio analysis (SWARA). Journal of business economics and
 960 management 2010; 11: 243-258.

961 Khosravi K, Nohani E, Maroufinia E, Pourghasemi HR. A GIS-based flood susceptibility assessment and its
 962 mapping in Iran: a comparison between frequency ratio and weights-of-evidence bivariate
 963 statistical models with multi-criteria decision-making technique. Natural Hazards 2016a; 83:
 964 947-987.

965 Khosravi K, Pourghasemi HR, Chapi K, Bahri M. Flash flood susceptibility analysis and its mapping using
 966 different bivariate models in Iran: a comparison between Shannon's entropy, statistical index,
 967 and weighting factor models. Environmental monitoring and assessment 2016b; 188: 656.

968 Khosravi K, Pham B.T, Chapi K, Shirzadi A, Shahabi H, et al. 2018. A comparative assessment of decision
 969 trees algorithms for flash flood susceptibility modeling at Haraz watershed, northern Iran.
 970 Science of the Total Environment 627, 744-755.

971 Lee M-J, Choi J-W, Oh H-J, Won J-S, Park I, Lee S. Ensemble-based landslide susceptibility maps in Jinbu
 972 area, Korea. Environmental Earth Sciences 2012; 67: 23-37.

973 Li Y-F, Xie M, Goh T-N. Adaptive ridge regression system for software cost estimating on multi-collinear
 974 datasets. Journal of Systems and Software 2010; 83: 2332-2343.

975 Lillesand T, Kiefer RW, Chipman J. Remote sensing and image interpretation: John Wiley & Sons, 2014.

976 Lohani A, Kumar R, Singh R. Hydrological time series modeling: A comparison between adaptive neuro-
 977 fuzzy, neural network and autoregressive techniques. Journal of Hydrology 2012; 442: 23-35.

978 Mehrabian AR, Lucas C. A novel numerical optimization algorithm inspired from weed colonization.
 979 Ecological informatics 2006; 1: 355-366.

980 Mukerji A, Chatterjee C, Raghuwanshi NS. Flood forecasting using ANN, neuro-fuzzy, and neuro-GA
 981 models. Journal of Hydrologic Engineering 2009; 14: 647-652.

982 Mukherjee S. Targeting saline aquifer by remote sensing and geophysical methods in a part of Hamirpur-
 983 Kanpur, India. Hydrogeol J 1996; 19: 53-64.

984 Naghibi SA, Moghaddam DD, Kalantar B, Pradhan B, Kisi O. A comparative assessment of GIS-based data
 985 mining models and a novel ensemble model in groundwater well potential mapping. Journal of
 986 Hydrology 2017; 548: 471-483.

987 Naghibi SA, Pourghasemi HR, Dixon B. GIS-based groundwater potential mapping using boosted
 988 regression tree, classification and regression tree, and random forest machine learning models
 989 in Iran. Environmental monitoring and assessment 2016; 188: 44.

990 Naghibi SA, Pourghasemi HR, Pourtaghi ZS, Rezaei A. Groundwater qanat potential mapping using
 991 frequency ratio and Shannon's entropy models in the Moghan watershed, Iran. Earth Science
 992 Informatics 2015; 8: 171-186.

993 Naidu YR, Ojha A. A hybrid version of invasive weed optimization with quadratic approximation. Soft
 994 Computing 2015; 19: 3581-3598.

995 Nampak H, Pradhan B, Manap MA. Application of GIS based data driven evidential belief function model
 996 to predict groundwater potential zonation. Journal of Hydrology 2014; 513: 283-300.

997 Nayak P, Sudheer K, Rangan D, Ramasastri K. Short-term flood forecasting with a Neurofuzzy model.
 998 Water Resources Research 2005; 41.
 999 Negnevitsky M. Artificial intelligence: a guide to intelligent systems: Pearson Education, 2005.
 1000 Nieto PG, García-Gonzalo E, Fernández JA, Muñiz CD. Hybrid PSO–MARS–based model for forecasting a
 1001 successful growth cycle of the *Spirulina platensis* from experimental data in open raceway
 1002 ponds. Ecological engineering 2015; 81: 534-542.
 1003 Nosrati K, Van Den Eeckhaut M. Assessment of groundwater quality using multivariate statistical
 1004 techniques in Hashtgerd Plain, Iran. Environmental Earth Sciences 2012; 65: 331-344.
 1005 O'brien RM. A caution regarding rules of thumb for variance inflation factors. Quality & Quantity 2007;
 1006 41: 673-690.
 1007 Oh H-J, Kim Y-S, Choi J-K, Park E, Lee S. GIS mapping of regional probabilistic groundwater potential in
 1008 the area of Pohang City, Korea. Journal of Hydrology 2011; 399: 158-172.
 1009 Olsson AE. Particle swarm optimization: Theory, techniques and applications: Nova Science Publishers,
 1010 Inc., 2010.
 1011 Ozdemir A. GIS-based groundwater spring potential mapping in the Sultan Mountains (Konya, Turkey)
 1012 using frequency ratio, weights of evidence and logistic regression methods and their
 1013 comparison. Journal of Hydrology 2011a; 411: 290-308.
 1014 Ozdemir A. Using a binary logistic regression method and GIS for evaluating and mapping the
 1015 groundwater spring potential in the Sultan Mountains (Aksehir, Turkey). Journal of Hydrology
 1016 2011b; 405: 123-136.
 1017 Pham BT, Bui DT, Pourghasemi HR, Indra P, Dholakia M. Landslide susceptibility assessment in the
 1018 Uttarakhand area (India) using GIS: a comparison study of prediction capability of naïve bayes,
 1019 multilayer perceptron neural networks, and functional trees methods. Theoretical and Applied
 1020 Climatology 2017a; 128: 255-273.
 1021 Pham BT, Khosravi K, Prakash I. Application and comparison of decision tree-based machine learning
 1022 methods in landside susceptibility assessment at Pauri Garhwal Area, Uttarakhand, India.
 1023 Environmental Processes 2017b; 4: 711-730.
 1024 Pham D, Ghanbarzadeh A, Koc E, Otri S, Rahim S, Zaidi M. The bees algorithm. Technical note.
 1025 Manufacturing Engineering Centre, Cardiff University, UK 2005: 1-57.
 1026 Pham D, Ghanbarzadeh A, Koc E, Otri S, Rahim S, Zaidi M. The bees algorithm-A novel tool for complex
 1027 optimisation. Intelligent Production Machines and Systems-2nd I* PROMS Virtual International
 1028 Conference (3-14 July 2006). sn, 2011.
 1029 Phootrakornchai W, Jiriwibhakorn S. Online critical clearing time estimation using an adaptive neuro-
 1030 fuzzy inference system (ANFIS). International Journal of Electrical Power & Energy Systems 2015;
 1031 73: 170-181.
 1032 Polykretis C, Chalkias C, Ferentinou M. Adaptive neuro-fuzzy inference system (ANFIS) modeling for
 1033 landslide susceptibility assessment in a Mediterranean hilly area. Bulletin of Engineering
 1034 Geology and the Environment 2017: 1-15.
 1035 Pourghasemi H, Moradi H, Aghda SF. Landslide susceptibility mapping by binary logistic regression,
 1036 analytical hierarchy process, and statistical index models and assessment of their performances.
 1037 Natural hazards 2013a; 69: 749-779.
 1038 Pourghasemi HR, Beheshtirad M. Assessment of a data-driven evidential belief function model and GIS
 1039 for groundwater potential mapping in the Koohrang Watershed, Iran. Geocarto International
 1040 2015; 30: 662-685.
 1041 Pourghasemi HR, Pradhan B, Gokceoglu C. Application of fuzzy logic and analytical hierarchy process
 1042 (AHP) to landslide susceptibility mapping at Haraz watershed, Iran. Natural hazards 2012; 63:
 1043 965-996.

1044 Pourghasemi HR, Pradhan B, Gokceoglu C, Mohammadi M, Moradi HR. Application of weights-of-
 1045 evidence and certainty factor models and their comparison in landslide susceptibility mapping at
 1046 Haraz watershed, Iran. *Arabian Journal of Geosciences* 2013b; 6: 2351-2365.

1047 Poursalehi N, Zolfaghari A, Minuchehr A. A novel optimization method, Effective Discrete Firefly
 1048 Algorithm, for fuel reload design of nuclear reactors. *Annals of Nuclear Energy* 2015; 81: 263-
 1049 275.

1050 Pourtaghi ZS, Pourghasemi HR. GIS-based groundwater spring potential assessment and mapping in the
 1051 Birjand Township, southern Khorasan Province, Iran. *Hydrogeology Journal* 2014; 22: 643-662.

1052 Pradhan B. Groundwater potential zonation for basaltic watersheds using satellite remote sensing data
 1053 and GIS techniques. *Open Geosciences* 2009; 1: 120-129.

1054 Rahmati O, Pourghasemi HR, Melesse AM. Application of GIS-based data driven random forest and
 1055 maximum entropy models for groundwater potential mapping: a case study at Mehran Region,
 1056 Iran. *Catena* 2016; 137: 360-372.

1057 Rahmati O, Samani AN, Mahdavi M, Pourghasemi HR, Zeinivand H. Groundwater potential mapping at
 1058 Kurdistan region of Iran using analytic hierarchy process and GIS. *Arabian Journal of Geosciences*
 1059 2015; 8: 7059-7071.

1060 Rezaeianzadeh M, Tabari H, Yazdi AA, Isik S, Kalin L. Flood flow forecasting using ANN, ANFIS and
 1061 regression models. *Neural Computing and Applications* 2014; 25: 25-37.

1062 Rezakazemi M, Dashti A, Asghari M, Shirazian S. H 2-selective mixed matrix membranes modeling using
 1063 ANFIS, PSO-ANFIS, GA-ANFIS. *International Journal of Hydrogen Energy* 2017.

1064 Sander P, Chesley MM, Minor TB. Groundwater assessment using remote sensing and GIS in a rural
 1065 groundwater project in Ghana: lessons learned. *Hydrogeology Journal* 1996; 4: 40-49.

1066 Saravanan B, Vasudevan E, Kothari D. A solution to unit commitment problem using invasive weed
 1067 optimization algorithm. *Power, Energy and Control (ICPEC), 2013 International Conference on.*
 1068 *IEEE, 2013*, pp. 386-393.

1069 Senapati MR, Dash PK. Local linear wavelet neural network based breast tumor classification using firefly
 1070 algorithm. *Neural Computing and Applications* 2013; 22: 1591-1598.

1071 Shu C, Ouarda T. Regional flood frequency analysis at ungauged sites using the adaptive neuro-fuzzy
 1072 inference system. *Journal of Hydrology* 2008; 349: 31-43.

1073 Siebert S, Henrich V, Frenken K, Burke J. Update of the digital global map of irrigation areas to version 5.
 1074 Rheinische Friedrich-Wilhelms-Universität, Bonn, Germany and Food and Agriculture
 1075 Organization of the United Nations, Rome, Italy 2013.

1076 Singh AK, Prakash SR. An integrated approach of remote sensing, geophysics and GIS to evaluation of
 1077 groundwater potentiality of Ojhala sub-watershed, Mirzapur district, UP, India. *Asian conference*
 1078 *on GIS, GPS, aerial photography and remote sensing, Bangkok-Thailand, 2002.*

1079 Storn R, Price K. Differential evolution—a simple and efficient heuristic for global optimization over
 1080 continuous spaces. *Journal of global optimization* 1997; 11: 341-359.

1081 Takagi T, Sugeno M. Fuzzy identification of systems and its applications to modeling and control. *IEEE*
 1082 *transactions on systems, man, and cybernetics* 1985: 116-132.

1083 Tehrany MS, Pradhan B, Jebur MN. Spatial prediction of flood susceptible areas using rule based
 1084 decision tree (DT) and a novel ensemble bivariate and multivariate statistical models in GIS.
 1085 *Journal of Hydrology* 2013; 504: 69-79.

1086 Tehrany MS, Pradhan B, Jebur MN. Flood susceptibility mapping using a novel ensemble weights-of-
 1087 evidence and support vector machine models in GIS. *Journal of hydrology* 2014; 512: 332-343.

1088 Termeh SVR, Kornejady A, Pourghasemi HR, Keesstra S. Flood susceptibility mapping using novel
 1089 ensembles of adaptive neuro fuzzy inference system and metaheuristic algorithms. *Science of*
 1090 *the Total Environment* 2018; 615: 438-451.

1091 Tvrdík J. Competitive differential evolution and genetic algorithm in GA-DS toolbox. Technical Computing
1092 Prague, Praha, Humusoft 2006: 99-106.

1093 Umar Z, Pradhan B, Ahmad A, Jebur MN, Tehrany MS. Earthquake induced landslide susceptibility
1094 mapping using an integrated ensemble frequency ratio and logistic regression models in West
1095 Sumatera Province, Indonesia. *Catena* 2014; 118: 124-135.

1096 Vahidnia MH, Alesheikh AA, Alimohammadi A, Hosseinali F. A GIS-based neuro-fuzzy procedure for
1097 integrating knowledge and data in landslide susceptibility mapping. *Computers & Geosciences*
1098 2010; 36: 1101-1114.

1099 Waikar M, Nilawar AP. Identification of groundwater potential zone using remote sensing and GIS
1100 technique. *Int J Innov Res Sci Eng Technol* 2014; 3: 1264-1274.

1101 Wan S. Entropy-based particle swarm optimization with clustering analysis on landslide susceptibility
1102 mapping. *Environmental earth sciences* 2013; 68: 1349-1366.

1103 Xu C, Dai F, Xu X, Lee YH. GIS-based support vector machine modeling of earthquake-triggered landslide
1104 susceptibility in the Jianjiang River watershed, China. *Geomorphology* 2012; 145: 70-80.

1105 Xu C, Xu X, Dai F, Wu Z, He H, Shi F, et al. Application of an incomplete landslide inventory, logistic
1106 regression model and its validation for landslide susceptibility mapping related to the May 12,
1107 2008 Wenchuan earthquake of China. *Natural hazards* 2013; 68: 883-900.

1108 Yang X-S. Firefly algorithms for multimodal optimization. *International symposium on stochastic*
1109 *algorithms*. Springer, 2009, pp. 169-178.

1110 Yang X-S. *Nature-inspired metaheuristic algorithms*: Luniver press, 2010.

1111 Yuce B, Packianather MS, Mastrocinque E, Pham DT, Lambiasi A. Honey bees inspired optimization
1112 method: the bees algorithm. *Insects* 2013; 4: 646-662.

1113 Zehtabian G, Khosravi H, Ghodsi M. High demand in a land of water scarcity: Iran. *Water and*
1114 *Sustainability in Arid Regions*. Springer, 2010, pp. 75-86.

1115 Zeng Y, Zhang Z, Kusiak A. Predictive modeling and optimization of a multi-zone HVAC system with data
1116 mining and firefly algorithms. *Energy* 2015; 86: 393-402.

1117 Zengqiang M, Cunzhi P, Yongqiang W. Road safety evaluation from traffic information based on ANFIS.
1118 *Control Conference, 2008. CCC 2008. 27th Chinese. IEEE, 2008*, pp. 554-558.

1119 Zhou Y, Luo Q, Chen H, He A, Wu J. A discrete invasive weed optimization algorithm for solving traveling
1120 salesman problem. *Neurocomputing* 2015; 151: 1227-1236.

1121
1122
1123
1124
1125
1126
1127
1128
1129
1130

A comprehensive study of new hybrid models for ANFIS with five meta-heuristic algorithms (IWO, DE, FA, PSO, BA) for spatial prediction of groundwater spring potential mapping

Khabat Khosravi¹, Mahdi Panahi^{*2}, Dieu Tien Bui^{*3}

1-Department of watershed management engineering, Faculty of Natural Resources, Sari Agricultural Science and Natural Resources University, Sari, Iran. (E-mail: khabat.khosravi@gmail.com)

2- Department of Geophysics, Young Researchers and Elites Club, North Tehran Branch, Islamic Azad University, Tehran, Iran. (E-mail: panahi2012@yahoo.com)

3- Geographic Information System Group, Department of Business and IT, University College of Southeast Norway, Gullbringvengen 36, 3800 Bø i Telemark, Norway. (E-mail: Dieu.T.Bui@usn.no)

Abstract

Groundwater ~~is are~~ one of the most valuable natural resources in the world; ~~therefore developing advanced tools for and their~~ sustainable management ~~of the groundwater~~ is highly necessary. One of the most important ~~methods-tools in-for the~~ management ~~ofing the~~ groundwater is ~~developing~~ groundwater potential mapping (GPM). The current study's ~~aim is to proposed and verified new artificial intelligence methods for spatial prediction of groundwater spring potential mapping at Koohdasht-Nourabad plain, Lorestan province, Iran.~~ These ~~methods are~~ benefits from a new hybrids of Adaptive Neuro-Fuzzy Inference System (ANFIS) with five meta-heuristic algorithms, ~~namely~~ Invasive Weed Optimization (IWO), Differential Evolution (DE), Firefly (FA), Particle Swarm Optimization (PSO), and Bees (BA) algorithms. Accordingly, A-a total ~~number~~ of 2463 springs were identified and collected, and then, divided in two ~~elassessubsets~~ randomly, including 70% (1725 locations) of the total springs were applied-used for ~~model-training models, whereas~~ and the remaining 30% (738 spring locations) ,which were excluded in the training phase, were utilized for the model evaluation. Thirteen groundwater ~~occurrence~~ conditioning factors, ~~namely~~ slope degree, slope aspect, altitude, plan curvature, stream power index (SPI), topographic wetness index (TWI), terrain roughness index (TRI), distance from fault, distance from river, land-use/land-cover, rainfall, soil order, and lithology ~~(units) have beenwere selectedprepared~~ for modeling. In the next step, the Stepwise assessment-Assessment ratio-Ratio analysis-Analysis (SWARA) method was employed applied to quantify the degree of relevance determine the spatial correlation betweenof these springs and conditioning factors and the springs. The global performance of these derived models accuracy of the map achieved after applying these five hybrid models waswas assessed determined using the area Area under-Under the receiver operating ~~characteristic (ROC)-curve (AUC).~~ In addition, the Freidman and Wilcoxon signed rank test were carried out to check and confirm the best model in this study. The result showed that Although the results of these models has high performance; however, performed models are close to each other, butthe ANFIS-DE mdel has the highest prediction capability (AUC = 0.875), followed by the ANFIS-IWO model, andthe ANFIS-FA model (0.873), the ANFIS-PSO model (0.865), and the ANFIS-BA model (0.839). The results of this research can be useful for decision makers to sustainable management of groundwater resources.

Key words: Groundwater spring, ANFIS-DE, ANFIS-IWO, ANFIS-FA, ANFIS-PSO, ANFIS-BA, Iran.

1. Introduction

Groundwater is defined as the water in a saturated zone which fills rock and pore spaces (Berhanu et al., 2014; Fitts, 2002). ~~whereas and~~ groundwater potential is the possibility of groundwater occurrence in an area (Jha et al., 2010). The occurrence of groundwater in an aquifer is affected by various geo-environmental factors including lithology, topography, geology, fault and fracture and its connectivity, drainage pattern and land-use/land-cover (Mukherjee, 1996). ~~As one of the major conditioning factors, geological-Geological~~ strata acts like a conduit and reservoir for groundwater ~~while. S~~ storage and transmissivity ~~of the formation has~~ influence ~~on~~ the suitability of exploitation of groundwater in a given geological formation. Downhill and depression slopes impart runoff and improve recharge and infiltration, respectively (Waikar and Nilawar, 2014).

Groundwater, which serves as a major source of drinking water to communities, ~~for~~ agricultural and ~~for~~ industrial ~~purposesectors~~, is one of the most precious natural resources in the world (David Keith Todd and Mays, 1980) due to its consistent temperature ~~and~~, widespread availability, low vulnerability to pollution, low development cost, and drought dependability (Jha et al., 2007). ~~The life of about Globally, 1.5 billion people are depend~~ ~~sent on upon~~ groundwater, ~~in the world~~ solely for drinking purposes, and about 38% of the irrigated lands depend on the groundwater itself (Siebert et al., 2013). ~~Due to As the~~ population ~~growth, of mankind on earth increases~~, the demand ~~for-of~~ water ~~is~~ constantly increases~~esd~~. ~~The-A~~ major challenge ~~now~~ is ~~how to have~~ sustainable management ~~system~~ of groundwater to preserve and ensure continuous supply with regards to ~~the~~ water demand. One of the most important measures for ~~the~~ groundwater resource management is ~~having-to collect~~ adequate knowledge on spatial and temporal distribution of groundwater, its quantity as well as its quality.

~~For the case of Iran, Approximately, two-third of Iran's are~~ ~~the land~~ is covered by deserts. As a result, similar to other arid regions, the main sources of water supply for ~~drinking and various other uses, especially drinking, depends on are~~ the groundwater (Nosrati and Van Den Eeckhaut, 2012). Agriculture, ~~which~~ is one of the most prominent economic sectors in Iran, and especially, in the study area, ~~is still be~~ limited ~~by~~ ~~due to~~ water scarcity (Zehtabian et al., 2010). Groundwater in Iran supplies around 65% of the water use-up and the remaining 35% is supplied by surface water (Rahmati et al., 2016). One of the most important measures to responsible for ~~the~~ increase ~~in-of~~ fresh-water ~~demand for drinking and agriculture is the-to~~ ~~identifyication-of~~ groundwater potential zoning, ~~as~~ an essential tool for performing a successful groundwater determination, protection, and management program (Ozdemir, 2011a).

There are a number of methods for groundwater exploitation in traditional approaches including drilling as well as geological, geophysical, and hydrogeological methods. Yet, they are ~~not-only~~ time-consuming, ~~and-costly-but uneconomical~~ (David Keith Todd and Mays, 1980; Israil et al., 2006; Jha et al., 2010; Sander et al., 1996; Singh and Prakash, 2002). Recently, the application of geographic information systems (GIS) and remote sensing (RS) has become an effective procedure ~~to-for~~ groundwater potential mapping (Fashae et al., 2014) due to their ability in handling huge amount of spatial data, ~~their easy performance~~ and their applicability for being used ~~efficiently~~ in ~~a lot-of various~~ fields, including water resources management. In more recent years, some probabilistic models such as frequency ratio (Oh et al., 2011), multi-criteria decision analysis (MCDA) (Kaliraj et al., 2014) (Rahmati et al., 2015) weights-of-evidence (WofE) (Pourtaghi and Pourghasemi, 2014), logistic regression (LR) (Ozdemir, 2011b; Pourtaghi and Pourghasemi, 2014), evidential belief function (EBF) (Nampak et al., 2014; Pourghasemi and Beheshtirad,

2015), decision tree (DT) (Chenini and Mammou, 2010), artificial neural network model (ANN) (Lee et al., 2012), and Shannon's entropy (Naghbi et al., 2015) have been ~~used~~ considered for ~~recognition of~~ groundwater potential mapping. ~~The b~~ Bivariate and multivariate statistical models have ~~some~~ disadvantages in measuring the relationship between groundwater occurrence and conditioning factors ~~for the definition of statistical assumptions prior to the study~~ (Tehrany et al., 2013; Umar et al., 2014). ~~whereas~~ MCDA technique is source of bias due to expert opinion. Traditional modeling approaches are ~~also mainly~~ based on linear or additive modeling that is not consistent with natural process in the environment (Clapcott et al., 2013) ~~but,~~ machine in recent year, machine learning has proven efficient models due to ability to hand with non-linear structure handle data from various measurement sources with different scales. In addition, machine learning and makerequires no statistical assumptions; ~~hence being useful for modeling applications such as GPM. Among machine learning,~~ ANN ~~model~~ is considered as the most widely used model for environmental modeling ~~among other machine learning models~~ due to its computational efficiency (Bui et al., 2016; Ghalkhani et al., 2013; Rezaeianzadeh et al., 2014). ~~However,~~ the ANN model has a number of weaknesses such as poor prediction and error in modeling process (Bui et al., 2016); ~~therefore, hybrid models have been proposed. Thus, Among hybrid frameworks, ANN model ensembles withof~~ fuzzy logic ~~model~~ and Adaptive Neuro-Fuzzy Inference System (ANFIS) ~~model, which is a hybrid model proposed and used by some researchers due to was reported efficient due to~~ its high accuracy (Güçlü and Şen, 2016; Lohani et al., 2012; Shu and Ouarda, 2008) (Chang and Tsai, 2016). It should be noted that even though ANFIS model has a higher accuracy than the two other model individually (Mukerji et al., 2009; Nayak et al., 2005), it has some disadvantages since it is weak in finding the best weight parameters affecting the prediction accuracy (Bui et al., 2016). ~~Thus,~~ these weights can be optimized to enhance the prediction accuracy of ground water models recognized using soft computing with the use of machine learning optimization processalgorithm. Optimization problem is the problem of finding the best solution from among a set of all possible solutions.

The main aim of the current study is to carry out groundwater spring potential mapping (GSPM) in Koohdasht-Nourabad plain, Iran using ANFIS model, ~~with some combined with~~ new metaheuristic ~~models algorithms, namely~~ Invasive Weed Optimization (IWO), Differential Evolution (DE), Firefly, Particle Swarm Optimization (PSO), and Bees algorithm (BA). ~~Consequently, the new models which have some ensembles with ANFIS have ability~~ to solve the weakness of the traditional ANFIS model. Another goal of the present study is drawing a comparison between prediction capabilities of these five new hybrid models in groundwater potential modeling in the study area as well. ~~The main difference between the current study and the literature review is that these new hybrid models have not been used before for groundwater potential mapping, but their accuracy in prediction of landslide (Chen et al., 2017a) and flood (Termeh et al., 2018) susceptibility mapping has been confirmed recently.~~ Since no such studies have been published so far in the study area, the current study is the pioneer work in this subject.

2. Case study description

Koohdasht-Nourabad Plain is located in the west part of the Lorestan province, Iran. It lies between 33°3' 28 and 34° 22' 55 N latitudes and between 46° 50' 19 ~~and~~ 48° 21' 18 E longitudes (Fig. 1). The region is located in the semi-arid area with mean annual precipitation of about 450 mm (Lorestan Weather Bureau report, 2016). The plain covers around 9531.9 km² with the population of 362,000 people (according to 2016 census). The primary occupation of most people living in

the region is agriculture farming with groundwater is the main source and water requirements are met through groundwater extraction. The altitude of the study area varies between 531 m and 3175 m above the sea level, while the maximum and minimum slope is 0° and 64°, respectively. Geologically, the study area is located in Zagros structural zone of Iran and is mostly covered by Quaternary and Cretaceous-Paleocene geologic time scale. The dominant land-use/land-cover of the study area is moderate forest (20%) and rocks covers the smallest area percentage (0.000670007%). The residential areas also covers about 3% of the Koohdasht-Nourabad plain. Rock crop/Inceptisoils are the dominant soil types in the study area, covering about 51% of the study area.

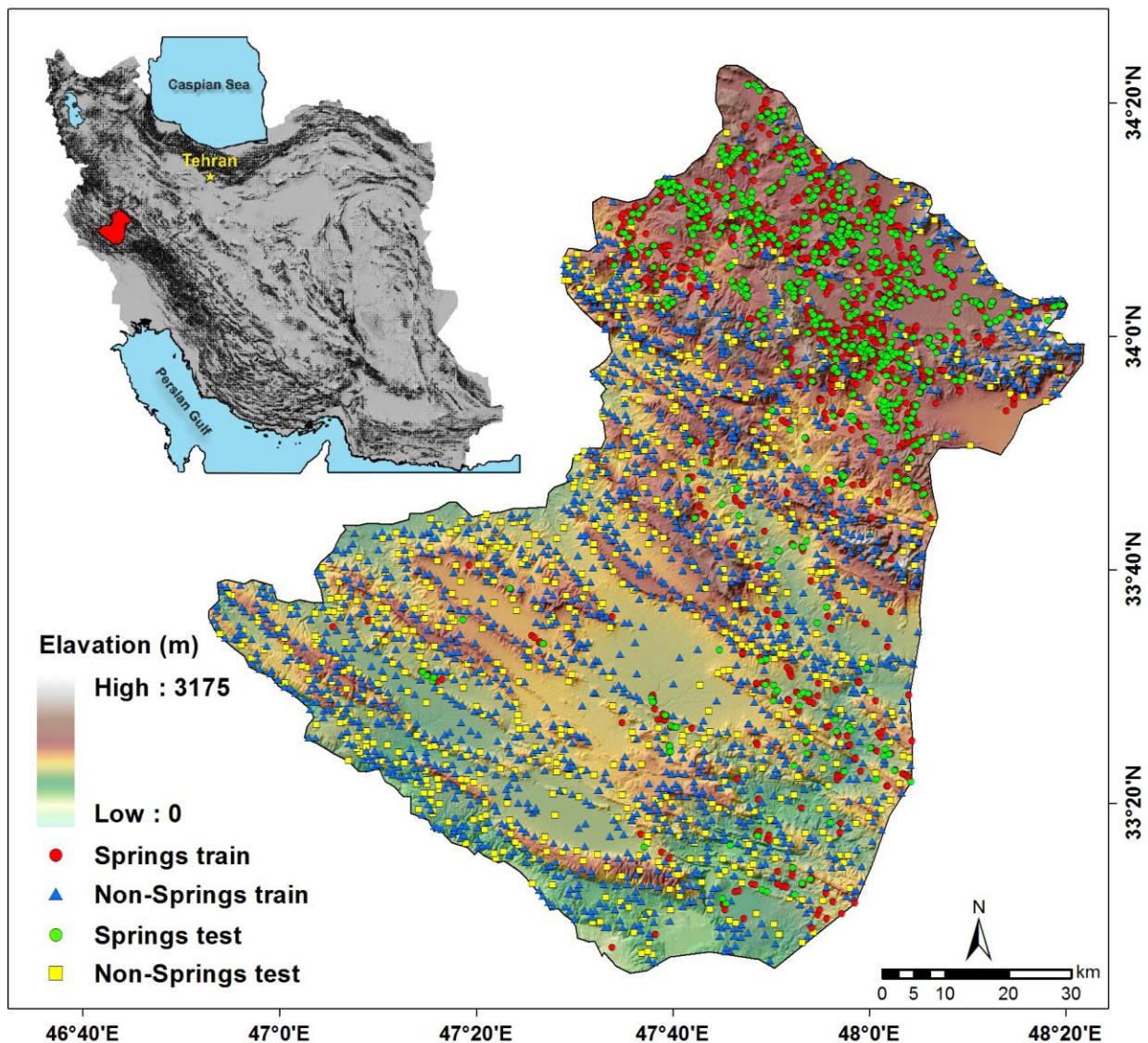


Fig.1. Groundwater well locations with DEM of the study area

3. Methodology

The methodological approach ~~has been~~ is shown in Fig 2. ~~and will be described step by step below.~~

3.1. Data preparation

3.1.1. Groundwater spring inventory map

In ~~any spatial prediction modeling such as~~ groundwater modeling, spatial relationship between ~~occurrence of~~ groundwater springs and ~~the~~ conditioning factors should be analyzed and assessed to determine the best subset of these factors. In Koohdasht-Nourabad plain, a total of 2463 springs were provided by selected from documentary source (Iranian Water Resources Management) ~~and considered for modeling.~~ In which, Mmost of the spring locations were checked using during extensive field surveys with GPS hand hole.

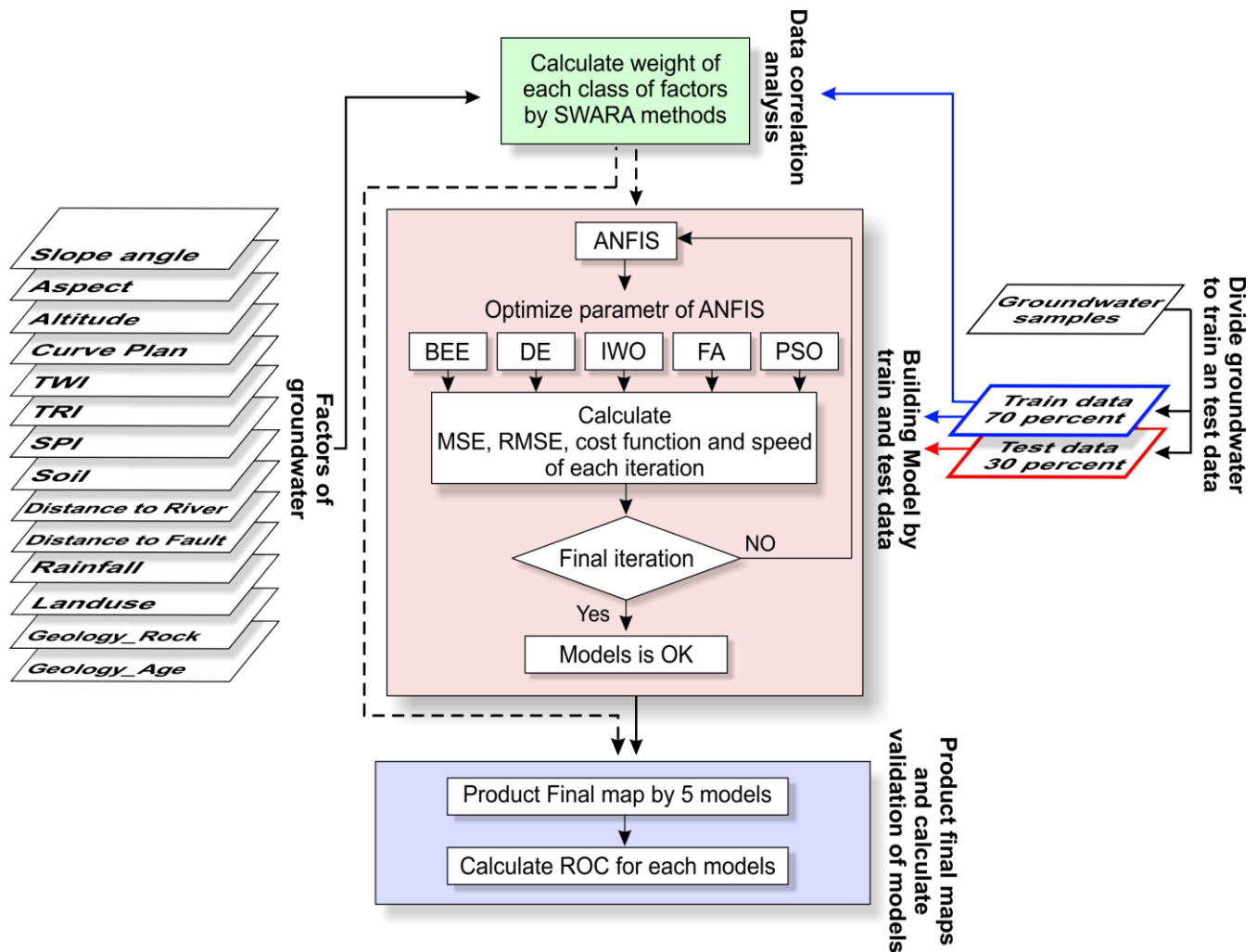


Fig.2. Conceptual modelling adopted in the current study

3.1.2. Construction of the training and validation datasets

Spatial prediction of groundwater potential mapping, using machine learning model, is considered as a binary classification with two classes, ~~because the groundwater potential index is divided into two parts including~~ spring location and non-spring location. Therefore, a total of 2463 non-

spring locations were ~~constructed~~ randomly generated using ~~created~~the random point ~~command~~tool in ArcGIS10.2. According to Chung and Fabbri (Chung and Fabbri, 2003), it is impossible to validate the model performance ~~without using a cross validation method that considering splits~~ the dataset for the two parts (~~Chung and Fabbri, 2003~~). The first part is used for ~~model-building~~ model ~~which is also~~ called training dataset and the other part is utilized for validating ~~or testing~~ the model performance ~~which also called~~ named as testing dataset (Pham et al., 2017a). In this study, a ratio of 70/30 was selected randomly for generating the training and testing the dataset (Pourghasemi et al., 2013a; Pourghasemi et al., 2012; Pourghasemi et al., 2013b; Xu et al., 2012). Accordingly, ~~B~~both spring location and non-spring location have been divided into two groups for the training (1725 location) and the validating (738 location) purposes (Fig 1).

~~For building the training dataset, a total number of 1725 locations were randomly selected for both spring and non-spring location and were then combined with each other, and 738 of the remaining location of springs and non-springs were combined with each other again to construct the testing dataset. Finally, both the training and the testing datasets were converted to raster format and then overlaid with 13 groundwater conditioning factors to extract their attribute values, where. In both training and testing dataset, the spring pixels were assigned to a value of "1" and non-spring pixels were assigned to "0" (Bui et al., 2015).~~

3.1.3. Groundwater conditioning factor analysis

3.1.3.1. Selection of the Groundwater conditioning factor and multi-collinearity analysis

After ~~definition~~ the initial selection of the ~~conditioning~~ effective factors, these ~~conditioning~~ factors should be assessed for multi-collinearity problems. Multi-collinearity takes place when two or more non-independence conditioning factors are highly correlated, or in other words inter-dependent (Li et al., 2010). Several methods have been proposed to ~~multi-collinearity~~ diagnose multi-collinearity, ~~s from and among which them, two methods of~~ Variance Inflation Factor (VIF) and ~~tolerance~~ Tolerance are widely used ~~for multi-collinearity in environmental modeling problem recognition~~ (Bui et al., 2016; O'brien, 2007). ~~The Factors with~~ VIF greater than 5 and tolerance less than 0.1 ~~shows indicate the~~ multi-collinearity problems ~~existed~~ (Bui et al., 2011; O'brien, 2007). Another method namely Information Gain Ratio technique was applied to identification of the importance of the conditioning factor in order and as well as the factors with null effect must be removed to increase the accuracy of the model (Khosravi et al., 2018).

In the current study, 13 conditioning factors have been selected including slope degree, slope aspect, altitude, plan plan curvature, stream power index (SPI), topographic wetness index (TWI), Terrain roughness index (TRI), distance from fault, distance from river, land-use/land-cover, rainfall, soil order, and lithology units. These factors have been ~~selected-determined according to the based~~ literature review, characteristics of the study area, and data availability (Mukherjee, 1996; Nampak et al., 2014; Oh et al., 2011; Ozdemir, 2011a). ~~In fact, -but there isn't any no~~ agreement ~~is reached~~ on which the factors to be used for modeling. The process of converting continuous variables into categorical classes were carried out ~~using expert opinions as well as according to based on our~~ frequency analysis of springs location (Khosravi et al., 2018; Ahmadisharaf et al., 2016) in order to define the class intervals (Bui et al., 2011).

Digital Elevation Model (DEM) has been downloaded from ASTER global DEM with 30x30 m grid size. Based on the DEM, ~~and then~~ slope degree, slope aspect, altitude, plan plan curvature, SPI, TWI and TRI ~~have been constructed using DEM were derived~~. Slope degree of the study areas

varies between 0-64 degree. Slope factor has a direct impact on the runoff generation and ~~therefore~~ groundwater recharge. ~~as~~ As the lower the slope, the lower runoff generation and the higher groundwater recharge. The slope degree has been divided in five categories using the quantile classification scheme (Tehrany et al., 2013; Tehrany et al., 2014), including 0-5.5, 5.5-12.11, 12.11-19.4, 19.4-28.7, 28.7-64.3 degree (Fig 3a). Slope aspect is ~~selected another factor that has because it~~ affects the groundwater potential through solar radiation. In the study area, since the north aspect receives a lower sun light, and as a result, is less wet ~~or has and~~ low evapotranspiration. The slope aspect has been provided in 5 different classes including, flat, north, west, south and east (Fig 3b). The third conditioning factor is altitude. ~~It~~ Altitude ~~has been was~~ divided into five classes using the quantile classification scheme, including 531-1070, 1070-1385, 1385-1703, 1703-2068 and 2068-3175 m (Fig.3c). ~~plan~~ Curvature ~~Plan curvature factor has been constructed using DEM and finally used used with divided into~~ three classes, namely concave (≤ -0.05), flat ($-0.05-0.05$), and convex (>0.05) (Fig.3d) (Pham et al.2017). SPI is ~~the measurement of related to~~ erosive power of surface runoff, ~~whreas and~~ TWI shows links onto amount of the flow that accumulates at any point in the catchment. ~~TRI, topographic roughness or terrain ruggedness calculates the sum of change in elevation between a grid cell and its neighborhood.~~ SPI, TWI and TRI ~~have been were~~ constructed ~~in the system for using the~~ Automated Geoscientific Analyses tool in (SAGA-GIS 2.2) software and finally divided into five classes. ~~that They~~ are 0-48664, 48664-227099, 227099-583969, 583969-1330153, 1330153-4136452 (Fig.3e) for SPI. For TWI, these classes are, 2.1-4.6, 4.6-5.6, 5.6-6.6, 6.6-7.9, 7.9-11.9 (Fig.3f) ~~for TWI,~~ and finally for TRI, these classes are 0-8.7, 8.7-18.2, 18.2-29.9, 29.9-46.6, 46.6-185 (Fig.3g) ~~for TRI.~~

Distance from fault and river factors have been ~~provided generated~~ using fault and river of the study area ~~via using the~~ multiple ring-buffer ~~toole command~~ in ArcGIS10.2, ~~software which is finally divided into with~~ five classes including: 0-200, 200-500, 500-1000, 1000-2000 and >2000 m (Fig. 3h and Fig. 3i). Lithology plays a key role in determining the groundwater potential occurrences due to different infiltration rate of formation that has been considered in some previous studies (Adiat et al., 2012; Nampak et al., 2014; Pradhan, 2009). Land-use/land-cover of the study area has been provided through Landsat 7 Enhanced Thematic Mapper plus (ETM+) images downloaded from the US Geological Survey (USGS) and supervised image classification techniques (Lillesand et al., 2014). Finally, the accuracy of the land-use/land-cover map has been controlled by filed surveys.

~~Twenty five~~ For the case of land-use/land-cover, twenty five types were recognized including agriculture, garden, dense-forest, good rangeland, poor forest, waterway, mixture of garden and agriculture, mixture of agriculture with dry farming, mixture of agriculture with poor-garden, dry farming, follow, dense rangeland, very poor forest, mixture of waterway and vegetation, mixture of moderate forest and agriculture, mixture of moderate rangeland and agriculture, mixture of poor rangeland and follow, mixture of low forest and follow, wood-land, moderate forest, moderate rangeland, poor rangeland, bare soil and rock, urban and residential, mixture of very poor forest, and rangeland have been identified. and assigned to code 1 to 25 respectively ~~and assign to code of 1 to 25 respectively~~ (Fig.3j).

As the major source of recharge to the groundwater, rainfall has been provided via mean annual historical rainfall data of past 15 years (2000–2015) using 4 rain-gauge stations in the study area. Inverse distance weighted (IDW) method has been used for ~~the preparation of deriving~~ the rainfall map ~~due to lower RMSE than other methods and then, rainfall map of the study area has been~~

~~divided into~~ with five categories including: 300-400, 400-500, 500-600, 600-700, 700-800 mm (Fig 3k). The soil properties directly affect the water infiltration rate as well as groundwater recharge. The 1:50,000 soil map of Lorestan province obtained from the Iranian Water Resources Department (IWRD) has been used for the analysis. The soil map was in a polygon format which needed to be converted to grid. The most dominant feature of the study area is rock outcrop/Entisols, rock outcrop/Inceptisols, Inceptisols, Inceptisols/Vertisols and Badlands (Fig.3l).

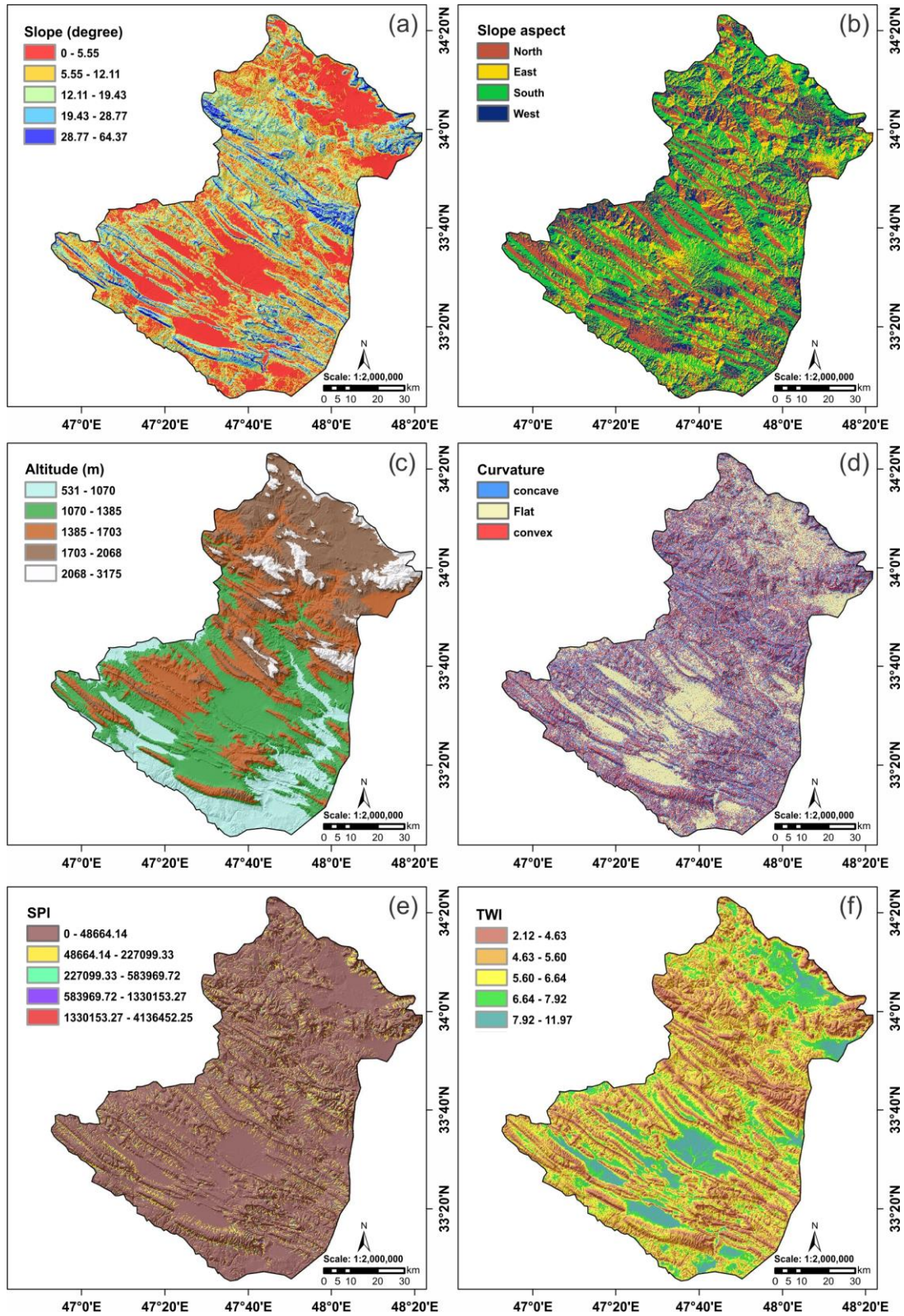
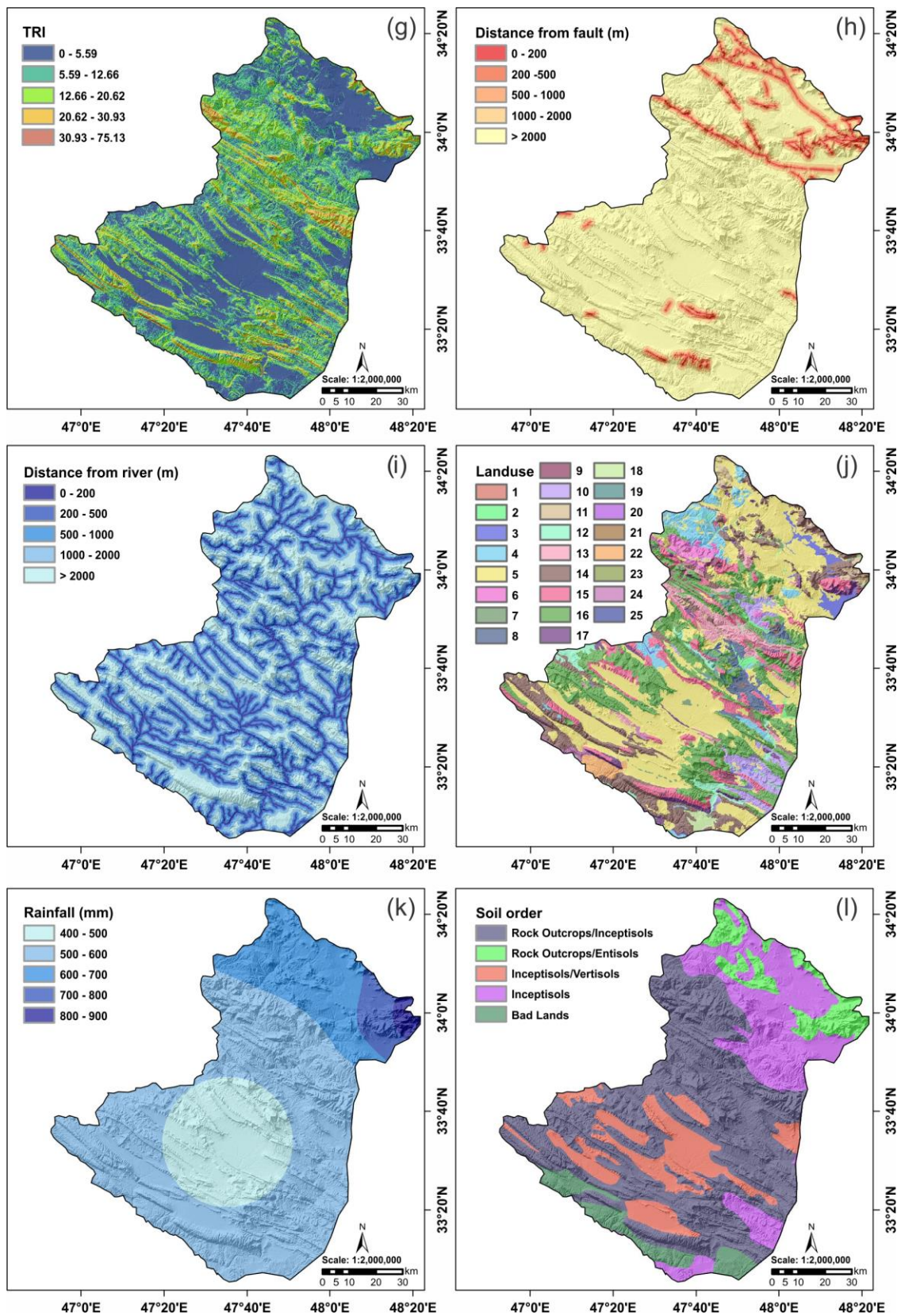


Fig.3. Thematic Groundwater conditioning factor in the study area: slope degree(a), slope aspect (b), altitude (c), plan curvature (d), SPI (e), TWI (f), TRI (g), distance from fault (h), distance from river (i), land-use/land-cover (j), rainfall (k), soil order (l), and lithology units (m).



1392

1393 Fig.3.Continued

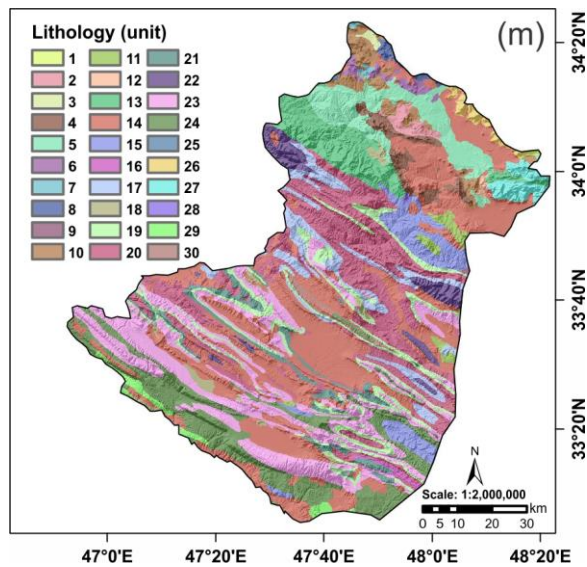


Fig.3. Continued

Finally, all the aforementioned groundwater conditioning factors for modeling purposes were converted to a raster grid with $30\text{ m} \times 30\text{ m}$ pixel-size in the ArcGIS 10.2 software. Lithology (unit) has a high influence on infiltration; thus, it has been considered in the current study. Lithology for the study area has been constructed in scale of 1:100000, which was created-provided by Iranian Department of Geology Survey (IDGS). Accordingly, and divided-into-thirty classes were used including: OMq, PeEf, PIQc, K1bl, Plc, pd, TRKubl, TRJvm, MPIfgp, OMql, Plbk, E2c, TRKurl, Qft2, MuPlaj, KEpd-gu, Kgu, Qft1, Ekn, KPeam, PeEtz, Kbgp, EMas-sb, Mgs, TRJlr, Klsol, JKbl, Kur, OMas and Mmn and assigned to code 1 to 30 respectively and assign to code of 1 to 30 respectively (Fig.3m).

3.2. Spatial relationship between spring location and conditioning factors

Step-wise Assessment Ratio Analysis (SWARA), as a Multi-Criteria Decision Making (MCDM) was first introduced by Keršulienė in 2010 for the first time (Keršulienė et al., 2010) as a Multi-Criteria Decision Making (MCDM). Since was used this method is due to both simple and rooted on experts' views, SWARA it has received drawn a lot of great attention in diverse-various fields in the last five years (Alimardani et al., 2013; Hong et al., 2017).

In SWARA, The-the specialist-expert allocates respectively the highest and lowest rank from the most and least valuable criterion, respectively. Afterwards, the all-inclusive ranks are specified by the average value of ranks. The phases of method are as the following:

Phase one (for evolving decision making models); first, the experts define the problem solving criteria. By using the practical knowledge of the experts, the priority for each criteria are determined as well and the criteria are organized in descending order finally.

Phase two (regarding to each parameter's ranking); the following trend is employed for calculation of the weight in each criteria:

Starting from the second criterion, the respondent explains the relative importance of the criterion j in relation to the $(j - 1)$ criterion, and for each particular criterion as well. As Keršuliene mentioned ~~in his article~~, this process specifies the Comparative Importance of the Average Value, S_j as follows (Keršuliene et al., 2010):

$$S_j = \frac{\sum_i^n A_i}{n} \quad (1)$$

Where n is the number of experts; A_i explicates the offered ranks for each factor by the experts; j stands for the number of the factor.

Subsequently, the coefficient K_j is determined as follows:

$$K_j = \begin{cases} 1 & j = 1 \\ S_j + 1 & j > 1 \end{cases} \quad (2)$$

Recalculation of weight Q_j is as the following:

$$Q_j = \frac{X_{j-1}}{K_j} \quad (3)$$

The relative weights of the evaluation criteria are calculated by the following equation:

$$W_j = \frac{Q_j}{\sum_{j=1}^m Q_j} \quad (4)$$

Where W_j shows the relative weight of j -th criterion, and m stands for the total criteria number.

3.3. Groundwater spring prediction modelling

In this research, five new hybrid models namely ANFIS-DE, ANFIS-IWO, ANFIS-FA, ANFIS-PSO, ANFIS-BA were utilized for the analysis of determination of groundwater potential zonation in the study areas and for comparison between their prediction capabilities.

3.3.1. Adaptive Neuro-Fuzzy Inference System

Adaptive Neuro-Fuzzy Inference System (ANFIS) is obtained from the combination of Artificial Neural Network (ANN) and fuzzy logic (Jang, 1993). ANFIS ~~is has been proven~~ more efficient than the two mentioned models ~~in various fields~~ (Bui et al., 2016). ~~Therefore This is because,~~ ANN has the automatic ability but is not able to explain how to get the output from decision making. Fuzzy logic, on the other hand, is the reverse of ANN by generating output from fuzzy logical decision without the ability of self-operating learning (Aghdam et al., 2017; Chen et al., 2017b; Phootrakornchai and Jiriwibhakorn, 2015). ~~Consequently,~~ ANFIS was proposed ~~by Jang in 1993~~ (Jang, 1993) to solve nonlinear and complex problems in one framework (Rezakazemi et al., 2017). This model has been used in date processing, fuzzy control and others fields (Zengqiang et al., 2008). The members of ANFIS are the function parameters from dataset for describing the system behavior (Jang, 1993). ANFIS applies to Takagi-Sugeno-Kang (TSK) fuzzy model with two rules of “If-Then” with two inputs x_1 and x_2 , and one output f (Takagi and Sugeno, 1985), as follows:

Rule2 1: if x_1 is A_1 and x_2 is B_1 , then $f_1 = p_1x_1 + q_1x_2 + r_1$ (5)

Rule 1: if x_2 is A_2 and x_2 is B_2 , then $f_2 = p_2x_2 + q_2x_2 + r_2$ (6)

Jang's ANFIS consists of feed-forward neural network with six distinct layers. [Detailed description of ANFIS model described in details at can be seen in \(Jangs, 1993\).](#)

3.3.2. Meta-heuristic optimization

The main goal of this phase is to find the optimal antecedent and the consequent parameters of the ANFIS model using IWO, DE, FA, PSO, and Bee algorithms. [Fig.4 illustrates a general methodological flow of ANFIS](#) [The processing in MATLAB software is shown in Fig 4.](#)

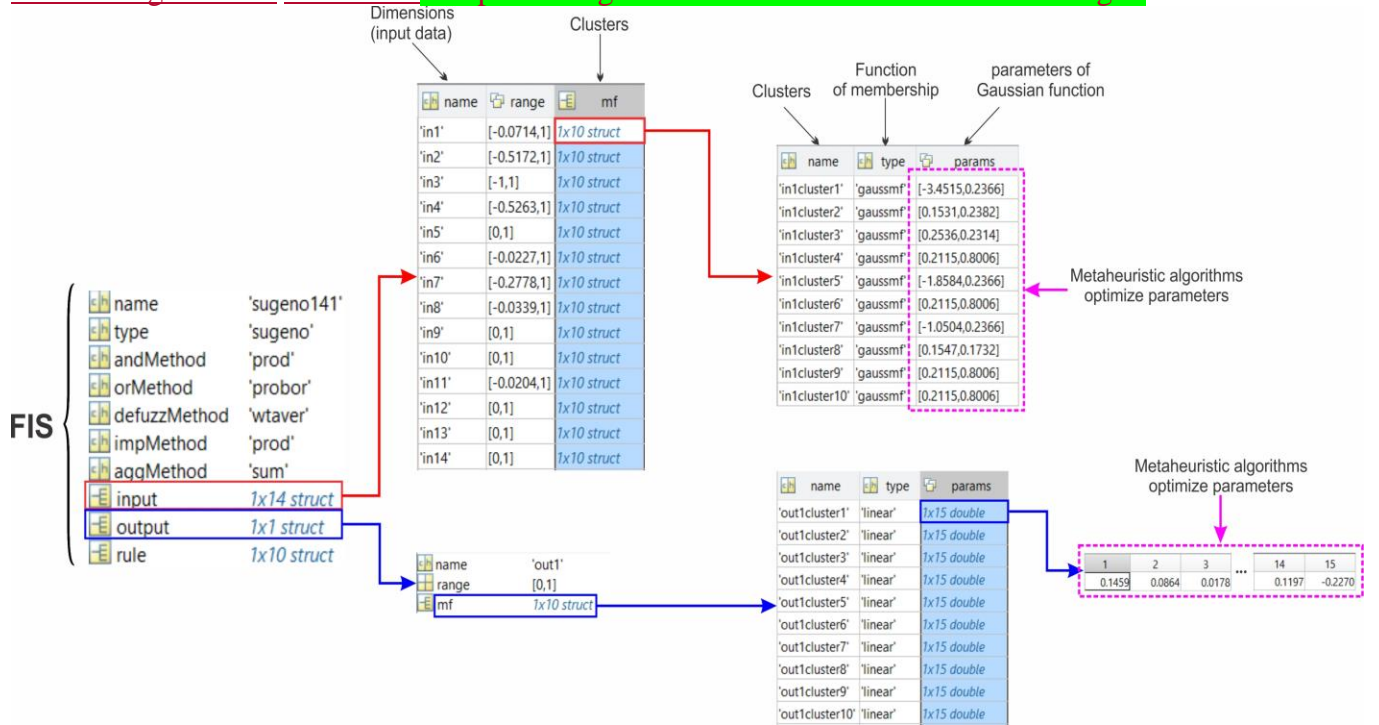


Fig.4. General methodological flow of ANFIS processing of ANFIS hybrid model

3.3.2.1. IWO algorithm

Invasive weed optimization (IWO) is one of the metaheuristic algorithms which mimics the colonizing behavior of weeds. Its design is based on the way to find proper place for growth and reproduction of weeds by Mehrabian and Locus (Mehrabian and Lucas, 2006). One characteristic of this algorithm is its simplified structure; the number of input parameters is low and has strong robustness. Furthermore, it is easy to understand and the same merit causes it to be used for solving difficult nonlinear optimization problems (Ghasemi et al., 2014; Naidu and Ojha, 2015; Zhou et al., 2015). Moreover, by comparing the results of IWO algorithm and other algorithms like SFLA and PSO for solving optimization problems, IWO algorithm can compete with other ones (Ghasemi et al., 2014). This algorithm consists of 4 parts as following:

1- Initialization

Random spread of some limited weeds in searching area with dimension D is considered as the initial population of solutions.

2- Reproduction

Weeds are able to reproduce some seeds in accordance with their fitness during their growth. In other words, the number of produced seeds from S_{\min} value for weeds starts with Worst fitness and then increases in linear fashion to S_{\max} for them with best fitness.

3- Spatial dispersal

Produced seeds are distributed in the searching area randomly in a way that is located close to their families with normal distribution, their mean equal to zero, and different variances. Moreover, standard deviation decreases in each iteration from σ_{\min} to σ_{\max} and is calculated by the following non-linear equation:

$$\sigma_{iter} = \frac{(iter_{max}-iter)^n}{(iter_{max})^n} (\sigma_{min} - \sigma_{max}) + \sigma_{max} \quad (7)$$

Where $iter_{max}$ is the last iteration, σ_{iter} is the standard deviation of iteration, and n is the non-linear index considered between 2 and 3 (Saravanan et al., 2013).

4- Competitive exclusion

All weeds and their seeds combine in order to make up the population of next generation. If the population exceeds a definite maximum, those weeds with lower fitness will be removed. The reproduction mechanism and the competition provide breeding opportunity for proper weeds. If they generate fitter offspring, the offspring can survive the competition.

5- Termination Condition

Step 2 to 4 ~~were repeated in order for the iteration~~ to reach its maximum defined value and the weeds with the best fitness will be the nearest condition to optimal solution.

3.3.2.2. DE algorithm

DE is another popular algorithm used as an evolutionary algorithm in recent years used for finding global optimal answers in a problem with continuous space (Chen et al., 2017a; Das et al., 2009). This method was first introduced by Storn and Price (Storn and Price, 1997). It is very similar to genetic algorithm that produces next optimum generation by three operators: mutation, crossover, and selection. This algorithm starts by producing random population in which each individual of population is a symbol of solution to the problem. Vector $X_i^G = (x_{1,i}^G, x_{2,i}^G, x_{3,i}^G, \dots, x_{D,i}^G)$ shows each individual of population $i = \{0,1,2, \dots, NP\}$ is a number of each individual, in which D stands for the search dimension or in other words, is a component problem and $G = \{0,1,2, \dots, G_{max}\}$ generation time that G_{max} is the total number of generations. By assuming the maximum and minimum of every dimension of searching space, there are $X_L = \{x_{1,L}, x_{2,L}, \dots, x_{D,L}\}$ and $X_U = \{x_{1,U}, x_{2,U}, \dots, x_{D,U}\}$, respectively; initial population is defined as the following (Storn and Price, 1997):

$$x_{j,i}^0 = x_{j,L} + rand(0,1). (x_{j,U} - x_{j,L}) \quad (8)$$

Where $\text{rand}(0,1)$ is a uniformly distributed random number in $[0, 1]$

3.3.2.2.1. Mutation

The first operator in DE algorithm is mutation, which produces mutant vector $V_i^G = (V_i^G, V_2^G, \dots, V_D^G)$ by using each individual which is called target vector. Four well-known mutant operators that are used are as the following:

$$\text{DE/rand/1} : V_i^G = X_{r1}^G + F \cdot (X_{r2}^G - X_{r3}^G)$$

$$\text{DE/rand/2} : V_i^G = X_{r1}^G + F \cdot (X_{r2}^G - X_{r3}^G) + F \cdot (X_{r4}^G - X_{r5}^G)$$

$$\text{DE/best/1} : V_i^G = X_{best}^G + F \cdot (X_{r1}^G - X_{r2}^G)$$

$$\text{DE/best/2} : V_i^G = X_{best}^G + F \cdot (X_{r1}^G - X_{r2}^G) + F \cdot (X_{r3}^G - X_{r4}^G)$$

$$\text{DE/current-to-rand/1} : V_i^G = X_i^G + F \cdot (X_{r1}^G - X_i^G) + F \cdot (X_{r2}^G - X_{r3}^G)$$

$$\text{DE/current-to-rand/1} : V_i^G = X_i^G + F \cdot (X_{best}^G - X_i^G) + F \cdot (X_{r1}^G - X_{r2}^G) \quad (9)$$

$r1, r2, r3, r4$, are the integer numbers that have been chosen randomly from $[0, NP]$ and the condition of $r1 \neq r2 \neq r3 \neq r4$ exists. F is the Scale factor that determines the mutation scale. It is generally selected as a random number from $[0,1]$. X_{best}^G is an individual that has the best fitness value in G generation.

3.3.2.2.2. Crossover

The purpose of this step is to produce trail vector (U_{ij}). Thus, this operator is defined by replacing some elements of the target vector X_i^G with mutant vector V_i^G as the following (Storn and Price, 1997):

$$U_{ij} = \begin{cases} V_{ij}^G & \text{if } \text{rand}[0,1] \leq CR \text{ or } j = j_{rand} \\ X_{ij}^G & \text{otherwise} \end{cases} \quad (10)$$

Where $i \in \{1, 2, \dots, NP\}$, $j \in \{1, 2, \dots, D\}$, j_{rand} , is a random number from $[1, D]$ and CR is the crossover rate which is uniformly distributed random number in $[0,1]$.

3.3.2.2.3. Selection

Selection is characterized by comparing fitness value of U_{ij} trail vector with the target vector (X_i^G) and choosing the best ones as the next generation (Storn and Price, 1997).

$$X_i = \begin{cases} U_i^G & \text{if } f(U_i^G) \leq f(X_i^G) \\ X_i^G & \text{otherwise} \end{cases} \quad (11)$$

3.3.2.3. FA algorithm

~~Researches always try to design powerful evolutionary algorithms by utilization of swarm social behavior of animals, insects, and plants to use them for problem solving (Poursalehi et al., 2015).~~ Firefly algorithm has been defined by Yang in Cambridge University (Yang, 2009) as an evolutionary algorithm. In recent years, many researches in different fields have taken advantage of this algorithm for optimization. ~~The results of using FA algorithm in different problems, which require optimization, have been better than other algorithms such as SA, GA, PSO, and HAS (Alweshah and Abdullah, 2015).~~ This algorithm is known as meta-heuristic algorithm that is originated from flashing and communication behavior of fireflies (Yang, 2009; Yang, 2010). ~~Somewhere in the region of 2000, special firefly species exist that most of which produce short and rhythmic flashes (Zeng et al., 2015).~~ Like in every other swarm intelligence algorithm, where their components are known as solutions for the problems, in this algorithm each firefly is a solution and its light intensity is the objective function value. In other words, a firefly with more light intensity is known as a solution. On the other hand, this firefly attracts more fireflies.

Generally, ~~FA~~firefly algorithm follows three idealized rules as below:

-1- All firefly species are unisex, with each of them attracting other fireflies without considering their gender (Amiri et al., 2013).

2- Attractiveness of a firefly is related to its light intensity. Thus, from two flashing firefly species, the one with lower light intensity moves toward the other one with higher light intensity. It should be noted that the distance between fireflies is significant because the farther they are from each other, the dimmer the light gets and the attractiveness declines exponentially (Gandomi et al., 2013). Moreover, if the light intensity of fireflies were the same; they would move randomly (Senapati and Dash, 2013).

3- Light intensity of a firefly is defined as an objective function value and must be optimized.

In order to design FA, two substantial issues are needed to be defined: light intensity variation (I) and the attractiveness' formulation(β). Fireflies' attractiveness is determined by their light intensity or brightness. In addition, brightness is associated with the objective function. The light intensity $I(r)$ varies with the distance r monotonically and exponentially as:

$$I(r) = I_0 e^{-\gamma r^2} \quad (12)$$

where I is the original light intensity, γ is the fixed light absorption coefficient and r is the distance between the two fireflies. Also, attractiveness rate is defined as below:

$$\beta = \beta_0 e^{-\gamma r^2} \quad (13)$$

where β_0 is the attractiveness when $r=0$. Also, the distance between two fireflies i and j with X_i and X_j is determined by the following equation:

$$r_{ij} = \|X_i - X_j\| = \sqrt{\sum_{k=1}^d (X_{i,k} - X_{j,k})^2} \quad (14)$$

where d is the number of the problem dimensions and $X_{i,k}$ is the k - th element of the i - th firefly. Also, the movement of a firefly i which is attracted to another attractive firefly j , is determined by (Yang, 2009):

$$X_i = X_i + \beta_0 e^{-r_{ij}^2} (X_j - X_i) + \alpha (rand - \frac{1}{2}) \quad (15)$$

In Eq. (21), the first and the second terms determines the attraction. However; the third term is regarded as a randomization with α , which is the step parameter, and ultimately, the rand is a random number generator which is uniformly distributed in a range from 0 to 1.

3.3.2.4. PSO algorithm

~~As a Meta-heuristic algorithm~~, PSO was first designed by Eberhart and Kennedy (Eberhart and Kennedy, 1995). Sensible characteristics of this algorithm include being powerful for optimizing the non-linear problems, its quick convergence, and relatively low calculations. These characteristics have made distinctions between this algorithm and other algorithms (Cheng et al., 2010). Thus, PSO algorithm in those problems that need optimization has a special place among researches. This algorithm has been inspired by the way the birds and fish use their collective intelligence for finding the best way to get food (Kennedy, 2011; Kennedy and Eberhart, 1995). Therefore, each bird implemented in this algorithm acts as a particle that is in fact a representative of solution to problems. These particles find the optimum answers for the problem by searching in "n" dimension space whereas "n" is the number of problem's parameters. For this purpose, particles were scattered randomly in considered space at the beginning of algorithm implementation. Then, the positioning in each iteration can improve by using equation 1 and 2 and finding better situations in that iteration and the best position of particles vector addition. Assuming that $x_i^t = (x_{i1}^t, x_{i2}^t, \dots, x_{in}^t)$ and $v_i^t = (v_{i1}^t, v_{i2}^t, \dots, v_{in}^t)$ are the position and velocity of the "i - th" particle in "t th" iteration, respectively. Then, position and velocity of "i th" particle in "(i + 1) th" iteration is calculated by summing equation 1-2 (Eberhart and Kennedy 1995).

$$\begin{aligned} v_i^{t+1} &= \omega v_i^t + c_1 r_1 (p_i^t - x_i^t) + c_2 r_2 (g_i^t - x_i^t) \quad \text{with } -v_{max} \leq v_i^{t+1} \leq v_{max} \\ x_i^{t+1} &= x_i^t + v_i^{t+1} \end{aligned} \quad (16)$$

where x_i^t is the last position of "i th" particle, p_i^t the best found position by "i th" particle, g_i^t the best found location by particles, r_1, r_2 the random number between 1 and 0. ω, c_1 and c_2 the inertia weight, cognitive coefficient, and social coefficient, respectively. In order to value them, many papers have been presented (Olsson, 2010) and finally the following equation has been used (Nieto et al., 2015).

$$\omega = \frac{1}{2 \ln 2} \quad \text{and} \quad c_1 = c_2 = 0.5 + \ln 2 \quad (17)$$

It is noteworthy that the algorithm continues until the best found position by each particles unifies with the best found position of particles. In other words, all particles accumulate in one position and actually the answer to the problem is optimized.

3.3.2.5. Bee algorithm

One of the meta-heuristic algorithms designed according to bee swarm-based is Bee Algorithm. This algorithm which was first introduced by Pham (Pham et al., 2005; Pham et al., 2011) is inspired by foraging behavior of bees' colonies in search of food sources (flower patches) located near the hive. In the beginning, evenly distributed scout bees are scattered randomly in different directions to identify flower patches.

After that, scout bees come back to hive and start a specific dance called waggle dance. This dance is for communicating with others in order to share the information of discovered flower patches. This information indicates direction, distance, and nectar quality of the flower patches. All the information helps the colony to have proper evaluation of all flower patches. After evaluation, scout bees come back to the location of discovered flower patches with other bees named recruit bees. Regarding the distance and the amount of nectar, different number of recruit bees are assigned to each flower patch. In other words, those flower patches with better nectar quality dedicate more recruit bees to themselves. Following that, recruit bees evaluate the quality of flower patches when performing the harvest process so that they leave the flower patches if they have low quality. Conversely, if the flower patch quality is good, it will be announced during the next waggle dance. Before implementing the BA algorithm, the following parameters need to be defined:

The number of scout bees (n), the number of patches selected out of n visited points (m), the number of best patches out of m selected patches (e), the number of bees recruited for e best patches (ne_p), the number of bees recruited for other ($m-e$) selected patches (ns_p), the size of patches (ng_h) and the stopping criterion.

At first, “ n ” number of scout bees with uniform distribution is scattered in search space randomly. Then, the algorithm starts to evaluate the fitness of those seen places by scout bees in order to define and select suitable bees as elite bees.

The sites of elite bees are selected from local search and the algorithm implements the neighborhood searches within the selected bees’ sites for the best ones where more bees exist. Only the proper bee is chosen to survive the next bee population in each site and other bees are allocated around the search space randomly to find new potential solutions. These steps continue until the algorithm convergences.

3.4. Model’s performance assessment

Forecasting error as the quantitative approaches, define as the difference between the observed and estimated values which have been used for determination of the accuracy of the performed models. In the current study the model prediction capabilities for each hybrid model in terms of spatial groundwater prediction was evaluated using Mean Squared Error (MSE) as follows (Tien Bui et al, 2016):

$$MSE = \frac{\sum_{i=1}^n (O_i - E_i)^2}{N} \quad (18)$$

~~Where~~where O_i and E_i are observation (target) and prediction (output) values in both training and testing dataset and N is the total samples in the training or the testing dataset.

3.5. Model’s performance validation and comparisons

According to Chung and Fabbri (Chung and Fabbri, 2003), validation is one of the most important steps in any spatial prediction modeling and without validation, the result of the models do not have any scientific significance. Prediction capability of

these five spatial groundwater models must be evaluated using both success-rate and prediction-rate curves (Hong et al., 2015). Success-rate curves show how suitable the built model is for the groundwater potential assessment or for the evaluation of the goodness of fit (Gaprindashvili et al., 2014). Success-rate curves have been constructed using groundwater potential maps and the number of spring locations used in training dataset (Pradhan et al. 2010). Prediction rate curves which show the probabilities of the groundwater occurrences demonstrate how good the model is or evaluate the prediction power of the models. Therefore, it can be used for model prediction capabilities (Brenning, 2005). The construction procedure of prediction rate is similar to the success rate which the testing dataset (were not used in the training phase) has been used for instead of training dataset. The area under the curve (AUC) of success and prediction rate is the base for evaluation of model prediction power or assessment accuracy of the groundwater potential models quantitatively (Khosravi et al., 2016a; Khosravi et al., 2016b; Pham et al., 2017b). The AUC value varies from 0.5 to 1; the higher the AUC, the better the prediction capability of models.

3.6. Inferential statistics

3.6.1-Freidman test

As the conditioning factors have been classified into different classes, non-parametric test has been used in the current study. Non-parametric statistical procedures such as Freidman test (Friedman, 1937) have been used regardless of statistical assumptions (Derrac et al., 2011) and do not need the data to be normally distributed. The main aim of this test is to find whether there is a significant difference between the performed models or not. In other words, performing multiple comparisons to detect significant differences between the behaviors of two or more models (Beasley and Zumbo, 2003). The null hypothesis (H_0) is that there are no differences among the performance of the groundwater potential models. The higher the P-value, the higher the probability that the null hypothesis is not true since if the p-value is less than the significance level ($\alpha=0.05$), the null hypothesis will be rejected.

3.6.2 Wilcoxon signed-rank test

The most important drawback of Freidman test is that it only illustrates whether there is any difference between the models or not, and does not have the ability to show pairwise comparisons among performed model. Therefore, another non-parametric statistical test named Wilcoxon signed-rank test have been performed. To evaluate the significance of differences between the performed groundwater potential models, the P value and Z value have been used.

4. Result and analysis

4.1. Multi-collinearity diagnosis

Result of multi-collinearity analysis is shown in Table 1. Result has revealed that as VIF is less than 5 and the tolerance is greater than 0.1, there isn't any multi-collinearity problem among conditioning factors and all of factors are independent.

1693

Table.1. Multi-collinearity analysis for conditioning factors

No	Groundwater conditioning factors	Collinearity Statistics	
		Tolerance	VIF
1	Slope degree	0.231	2.401
2	Slope aspect	0.206	4.270
3	Altitude	0.801	2.097
4	plan Curvature <u>Plan curvature</u>	0.513	1.446
5	SPI	0.410	1.689
6	TWI	0.541	2.113
7	TRI	0.328	1.939
8	Distance from fault	0.408	2.25
9	Distance from river	0.212	3.126
11	Land-use/land-cover	0.296	3.891
12	Rainfall	0.298	1.686
13	Soil order	0.205	4.039
10	Geology (Unit)	0.215	4.150

1694

1695

4.2. Determination of the most important parameters

1696 The most common method of information gain ratio (IGR) was applied to identification of the
 1697 most important conditioning factors. Also result of the IGR technique Result shows that all thirteen
 1698 conditioning factors are effective on groundwater occurrences as the land-use/landcover factor has
 1699 the most important impact on groundwater (IGR=0.502) followed by lithology (IGR=0.465),
 1700 rainfall (IGR=0.421), TWI (IGR=0.400), soil (IGR=0.370), TRI (IGR=0.337), slope degree
 1701 (IGR=0.317), altitude (IGR=0.287), distance to river (IGR=0.139), aspect (IGR=0.066), plan
 1702 curvature (IGR=0.0548), distance to fault (IGR=0.0482) and SPI (IGR=0.0323).

1703

1704

4.2.3. Spatial relationship between springs and the conditioning factors by SWARA method

1705 The spatial correlation between springs and the conditioning factor has been shown in Table 2. For
 1706 the slope, the class of 0-5.5 degree shows the highest probability (0.45) on spring groundwater
 1707 occurrences and there is a contrary correlation between slope degree and SWARA values. As the
 1708 slope degree increases, the probability of spring occurrence has reduced. In the case of slope
 1709 aspect, the east aspect (0.44) has the most impact on spring occurrences followed by north (0.22),
 1710 west (0.177), south (0.15) and flat (0.12) in the Koohdasht- Nourabad plain. According to
 1711 calculated results, in terms of altitude, the springs are the most abundant in the altitude of 1703-
 1712 2068 m (0.6) and the least abundant in the altitude of 1070-1385 m (0.04). The SWARA model is
 1713 high in flat areas (0.4), followed by concave (0.38) and convex (0.2). For SPI, the highest SWARA

value is found for the classes of 583969-1330153 (0.46), followed by the classes of 227099-583969(0.0.23) and 48664-227099 (0.19). In the case of the TWI, the SWARA values decrease when the TWI reduces, while the highest TWI belongs to the classes of 6.6-7.9 (0.47), and the lowest is for 2.1-4.6 (0.02). There is an adverse relationship between TRI and SWARA value, and as the TRI increases, the SWARA value reduces. The highest and the lowest values of SWARA also belongs to classes 0-8.7 (0.54) and 46.6-185 (0.001), respectively. For distance from the fault, distance less than 2000 m has the highest impact on spring occurrences and with increase in the distance (greater than 2000 m), the probability of spring occurrences has reduced. The highest SWRA value belongs to distance from the fault of 500-1000 m (0.29) and the lowest value is for greater than 2000 m (0.1). For the distance to river, it can be seen that the class of 0-200 m has the highest correlation with the spring occurrence (0.46) and there is a contrary relationship between spring occurrence and SWARA values; as the more the distance from the river, the lower the spring occurrence probability. In the case of land use, the highest SWARA values are shown for garden areas (0.219), followed by mixture of garden and agriculture (0.17), agricultural areas (0.12), whereas the lowest SWARA is for bare soil and rock (0.00063). The rainfall between 500 and 600 mm has the highest SWARA value with 0.61 and the lowest SWARA belongs to 300-400 mm (0.02). The Inceptisols have the highest SWARA values (0.5) followed by rock outcrop/Entisols (0.39), rock outcrop/Inceptisols (0.056), Inceptisols/Vertisols (0.028), and Badlands (0.014). The highest probability respectively belongs to the highly porous and very good water reservoir karstic oligomiocene and cretaceous pure carbonate formation (OMq and K1bl), the young and poorly consolidated highly porous detrital rock units (PeEf and Plq) and the unconsolidated quaternary alluvium (PIQc).

Table.2. Spatial correlation between conditioning factors and the spring locations by SWARA methods

Factors	Classes	Comparative importance of average value K_j	Coefficient $K_j = S_j + 1$	$w_j = (X(j-1))/k_j$	weight $w_j / \text{sigma } w_j$
Slope (degree)	0 - 5.55		1.000	1.000	0.454
	5.55 - 12.11	0.300	1.300	0.769	0.349
	12.11 - 19.43	1.500	2.500	0.308	0.140
	19.43 - 28.77	2.000	3.000	0.103	0.047
	28.77 - 64.37	3.500	4.500	0.023	0.010
Slope aspect	East		1.000	1.000	0.448
	North	1.000	2.000	0.500	0.224
	West	0.300	1.300	0.385	0.172
	South	0.100	1.100	0.350	0.156
	Flat	0.8	1.05	0.31	0.121
Altitude (m)	1703 - 2068		1.000	1.000	0.608
	1385 - 1703	2.200	3.200	0.313	0.190
	2068 - 3175	0.800	1.800	0.174	0.106

	531 - 1070	1.000	2.000	0.087	0.053
	1070 - 1385	0.200	1.200	0.072	0.044
	Flat		1.000	1.000	0.408
	concave	0.050	1.050	0.952	0.388
	convex	0.900	1.900	0.501	0.204
	583969.72 - 1330153.27		1.000	1.000	0.466
	227099.33 - 583969.72	1.000	2.000	0.500	0.233
SPI	48664.14 - 227099.33	0.200	1.200	0.417	0.194
	0 - 48664.14	1.000	2.000	0.208	0.097
	1330153.27 - 4136452.25	10.000	11.000	0.019	0.009
	6.64 - 7.92		1.000	1.000	0.471
	5.60 - 6.64	0.700	1.700	0.588	0.277
TWI	7.92 - 11.97	1.300	2.300	0.256	0.120
	4.63 - 5.60	0.100	1.100	0.233	0.110
	2.12 - 4.63	4.000	5.000	0.047	0.022
	0 - 5.59		1.000	1.000	0.544
	5.59 - 12.66	0.800	1.800	0.556	0.302
TRI	12.66 - 20.62	1.500	2.500	0.222	0.121
	20.62 - 30.93	3.000	4.000	0.056	0.030
	30.93 - 75.13	10.000	11.000	0.005	0.003
	0 - 200		1.000	1.000	0.242
	200 - 500	0.050	1.050	0.952	0.231
Distance from fault (m)	500 - 1000	0.100	1.100	0.866	0.210
	1000 - 2000	0.050	1.050	0.825	0.200
	> 2000	0.700	1.700	0.485	0.118
	0 - 200		1.000	1.000	0.464
	200 - 500	1.900	2.900	0.345	0.160
Distance from river (m)	500 - 1000	0.050	1.050	0.328	0.152
	1000 - 2000	0.300	1.300	0.253	0.117
	> 2000	0.100	1.100	0.230	0.107
	Garden		1.000	1.000	0.219

Land- use/land- cover	mixture of garden and agriculture	0.282	1.282	0.780	0.171
	agriculture	0.340	1.340	0.582	0.128
	mixture of poor rangeland and follow	0.419	1.419	0.410	0.090
	follow	0.233	1.233	0.333	0.073
	mixture of moderate rangeland and agriculture	0.294	1.294	0.257	0.056
	mixture of very poor forest	0.124	1.124	0.229	0.050
	mixture of waterway and vegetation	0.549	1.549	0.148	0.032
	moderate forest	0.205	1.205	0.122	0.027
	mixture of agriculture with dry farming	0.064	1.064	0.115	0.025
	wood-land	0.030	1.030	0.112	0.024
	good rangeland	0.043	1.043	0.107	0.023
	rangeland	0.333	1.333	0.080	0.018
	poor rangeland	0.030	1.030	0.078	0.017
	poor forest	0.210	1.210	0.065	0.014
	moderate rangeland	0.281	1.281	0.050	0.011
	bare soil and rock	0.237	1.237	0.041	0.009
	dense rangeland	0.278	1.278	0.032	0.007
	dense-forest	10.000	11.000	0.003	0.001
	waterway	0.000	1.000	0.003	0.001
	mixture of agriculture with poor-garden	0.000	1.000	0.003	0.001
	very poor forest	0.000	1.000	0.003	0.001
	mixture of moderate forest and agriculture	0.000	1.000	0.003	0.001
	mixture of low forest and follow,	0.000	1.000	0.003	0.001
	urban and residential	0.000	1.000	0.003	0.001
	600 - 700		1.000	1.000	0.617
	700 - 800	2.200	3.200	0.313	0.193
	800 - 900	0.600	1.600	0.195	0.121

Soil order	500 - 600	1.500	2.500	0.078	0.048
	400 - 500	1.300	2.300	0.034	0.021
	Rock Outcrops/Entisols		1.000	1.000	0.509
	Rock Outcrops/Inceptisols	0.300	1.300	0.769	0.392
	Inceptisols	5.900	6.900	0.111	0.057
	Inceptisols/Vertisols	1.000	2.000	0.056	0.028
	Bad Lands	1.000	2.000	0.028	0.014
	OMq		1.000	1.000	0.133
	PeEf	0.309	1.309	0.764	0.101
	PlQc	0.253	1.253	0.610	0.081
	K1bl	0.113	1.113	0.548	0.073
	Plc	0.014	1.014	0.541	0.072
	pd	0.059	1.059	0.511	0.068
	TRKubl	0.223	1.223	0.417	0.055
	TRJvm	0.027	1.027	0.406	0.054
	MPlfgp	0.048	1.048	0.388	0.051
Lithology (unit)	OMql	0.015	1.015	0.382	0.051
	Plbk	0.081	1.081	0.353	0.047
	E2c	0.291	1.291	0.274	0.036
	TRKurl	0.059	1.059	0.258	0.034
	Qft2	0.335	1.335	0.194	0.026
	MuPlaj	0.100	1.100	0.176	0.023
	KEpd-gu	0.080	1.080	0.163	0.022
	Kgu	0.566	1.566	0.104	0.014
	Qft1	0.064	1.064	0.098	0.013
	Ekn	0.109	1.109	0.088	0.012
	KPeam	0.027	1.027	0.086	0.011
	PeEtz	0.328	1.328	0.065	0.009
	Kbgp	0.445	1.445	0.045	0.006
	EMas-sb	0.310	1.310	0.034	0.005
	Mgs	0.626	1.626	0.021	0.003

TRJlr	10.000	11.000	0.002	0.000
Klsol	0.000	1.000	0.002	0.000
JKbl	0.000	1.000	0.002	0.000
Kur	0.000	1.000	0.002	0.000
OMas	0.000	1.000	0.002	0.000
Mmn	0.000	1.000	0.002	0.000

4.34. Application of ANFIS ensemble models and model's assessment

In the current study, hybrids of ANFIS model and five meta-heuristic algorithms were designed, constructed and implemented in MATLAB 8.0 software. These models are trained according to the data of other intelligent models and the amount of training and optimization is tested by using other data. All thirteen spring occurrence using conditioning factors and the training dataset were applied in building the model. Methods of these models are like this: gained weights by SWARA method for each conditioning factor was fed as the input for Training-training dataset. was used for finding the correlation between SWARA values of conditioning factor and springs (were assigned to 1), and non-springs (were assigned to 0). Also, the spring and non-springs were assigned to 1 and 0 respectively. These weights entered into a hybrid model as an output. It can find and model the relationships between input and output data and the modeling accuracy is calculated by statistical methods. The prediction ability of the five hybrid models with training dataset as a target and estimated springs pixel as an output (in a training phase) and testing dataset (in a validation phase) was shown in Fig.4-5 and Fig.56.

The MSE parameter indicates how much output of each hybrid's model is close to real rate. As it can be seen in Fig. 45, MSE values of ANFIS-IWO, ANFIS-DE, ANFIS-FA, ANFIS-PSO, and ANFIS-BA have been calculated for the training step 0.066, 0.066, 0.066, 0.049, and 0.09, respectively. This shows that compared to other models, ANFIS-PSO had the best performance while ANFIS-BA had the worst one for training step. However, it should be noted that training step is not adequate for determining the best model for MSE optimization, and MSE level for testing phase needs to be reviewed. According to the results shown in Fig.45, values of MSE – 0.060, 0.060, 0.060, 0.045, and 0.09 – relate to the hybrid models; ANFIS-IWO, ANFIS-FA, ANFIS-PSO, and ANFIS-BEE have been calculated and indicate that the best performance is for ANFIS-PSO, the worst for ANFIS-BA.

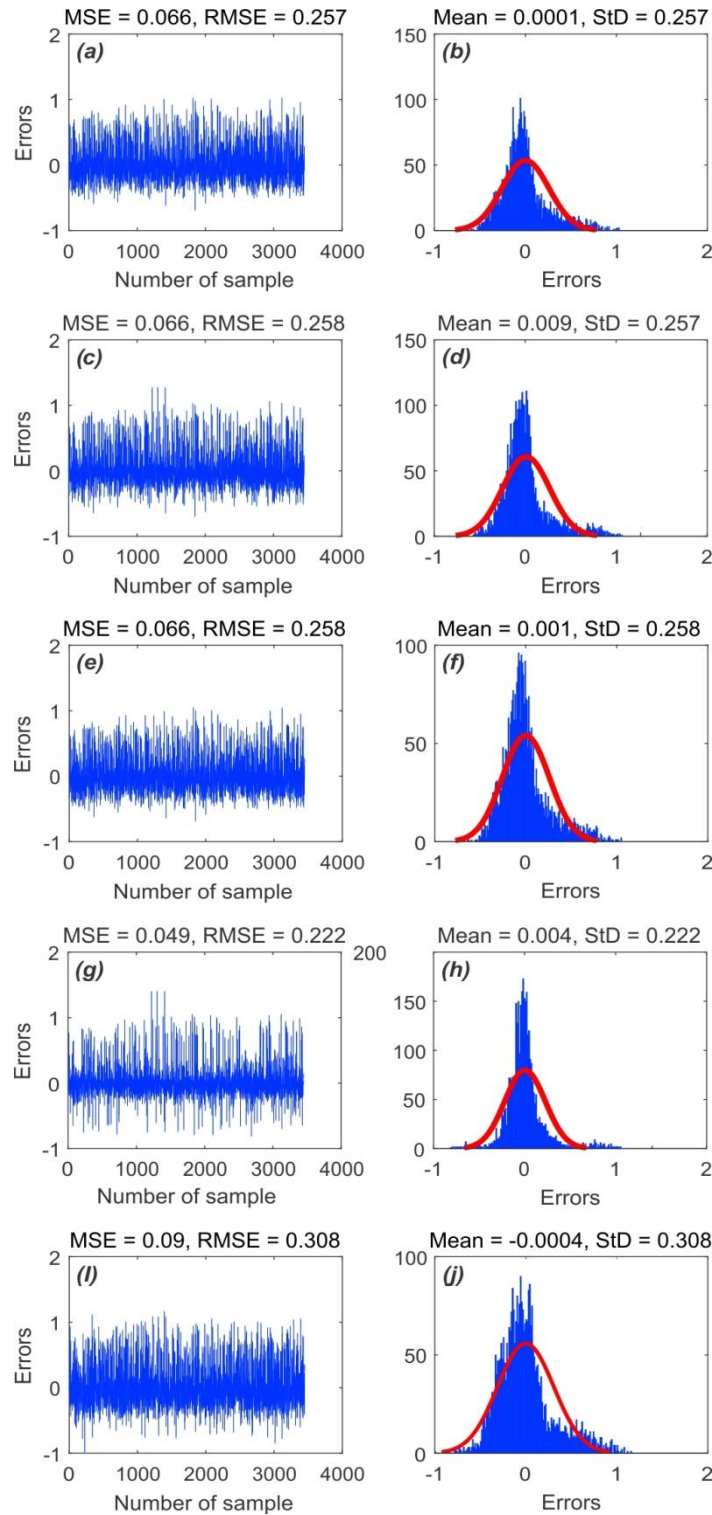


Fig.-54. MSE and RMSE values of the training data set samples of: a) ANFIS-IWO, c) ANFIS-DE, e) ANFIS-FA, g) ANFIS-PSO i) ANFIS-BA frequency errors of train data samples of b) ANFIS-IWO, d) ANFIS-DE, f) ANFIS-FA, h) ANFIS-PSO j) ANFIS-BA

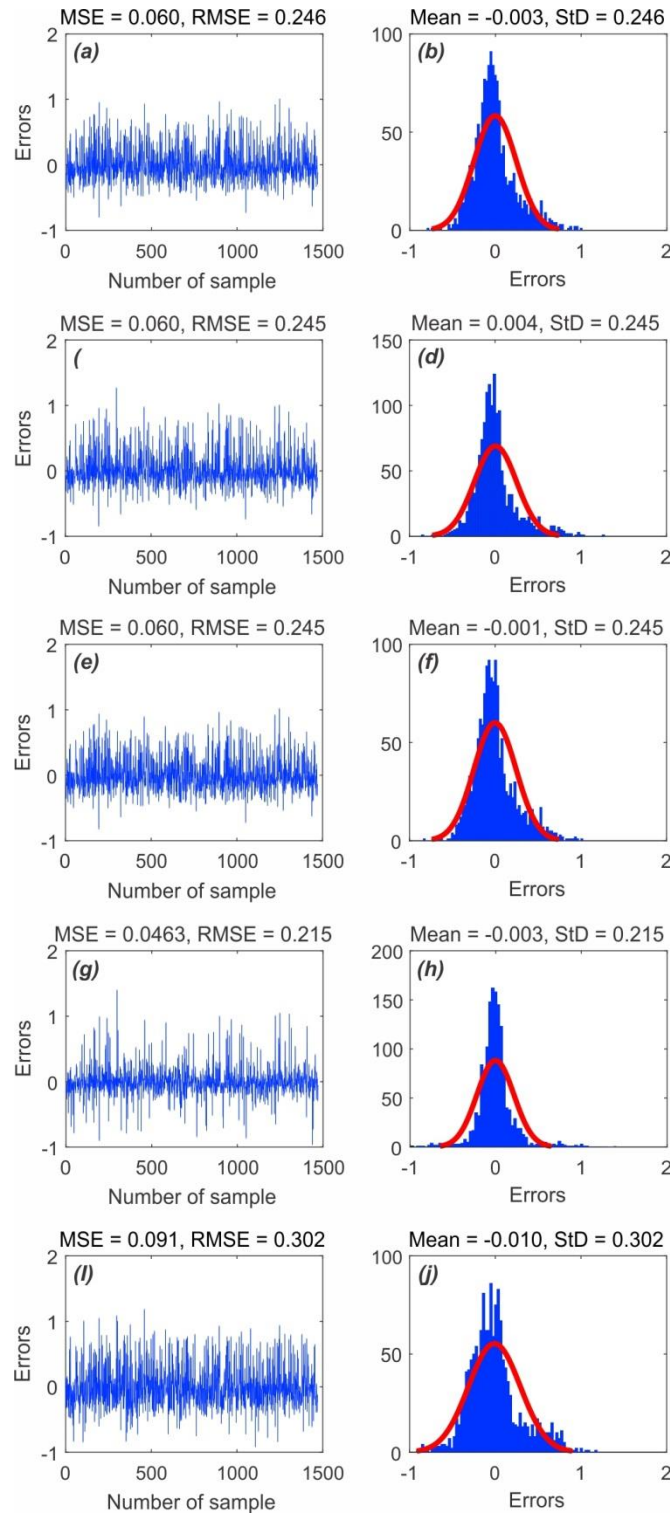


Fig.56. MSE and RMSE values of the validation data samples of a) ANFIS-IWO, c) ANFIS-DE, e) ANFIS-FA, g) ANFIS-PSO l) ANFIS-BA frequency errors of test data samples of b) ANFIS-IWO, d) ANFIS-DE, f) ANFIS-FA, h) ANFIS-PSO j) ANFIS-BA

However, it must be noticed that in addition to accuracy, determining the speed of used models has recently found significance. To accomplish this, therefore, the processing time of 1000 iteration is calculated for each model where the amounts of 8036, 547, 22111, 1050, and 6993 seconds are related to ANFIS-IWO, ANFIS-DE, ANFIS-FA, ANFIS-PSO, and ANFIS-BA, respectively (Fig. 67). As a result, it can be concluded that ANFIS-DE has had the minimum time of processing speed compared to other models and ANFIS-FA has had the maximum time.

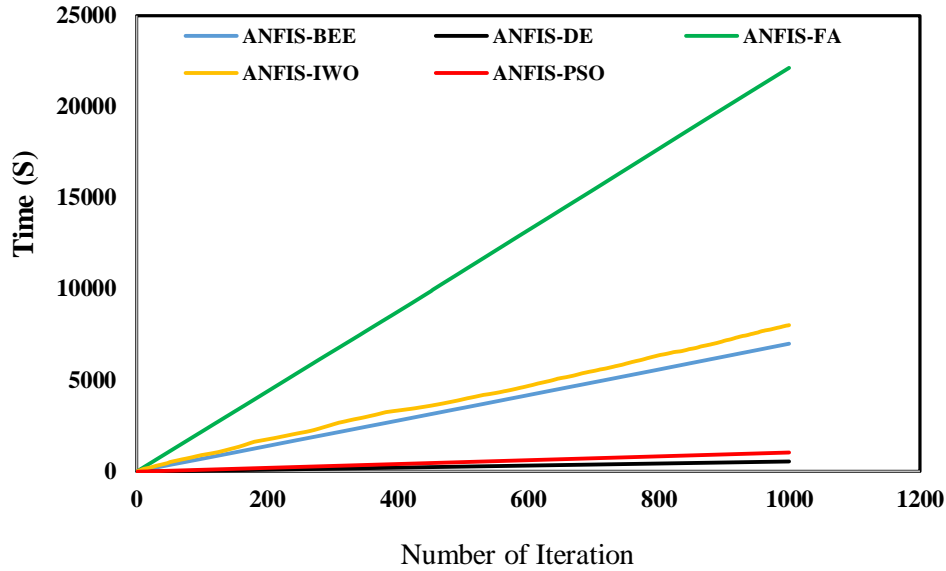


Fig. 67. Cumulative curve for speed processing of methods Processing time used for training the models

On the other hand, it is possible to test how each model achieves convergence in learning. By drawing a diagram, cost function values have been calculated in each iteration of convergence graph for all five models as depicted in Fig. 78. The results show that cost function values of ANFIS-DE and ANFIS-BA become constant in 30 and 95 iterations. This indicates a rapid convergence of every model. On the other side, ANFIS-PSO, ANFIS-IWO, and ANFIS-FA achieved convergence in 650, 650, and 360 iterations, respectively that indicates the low speed of these methods in reaching convergence.

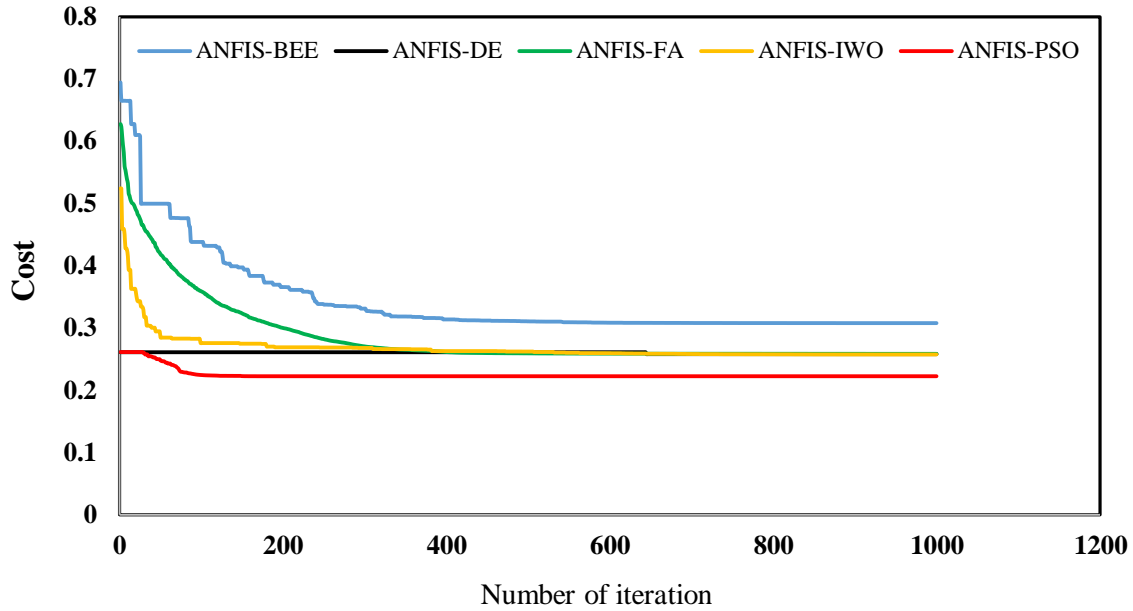


Fig. 78. Convergence plot of ~~methods~~the models

4.45. Preparation of groundwater spring potential maps using ANFIS hybrid models

In this study, SWARA values were standardized between 0-1 and were then transformed to MATLAB software. Following that, ANFIS hybrid models of ANFIS with IWO, DE, FA, PSO and BA algorithms were constructed using training dataset and standardized SWARA values. In the next step, the built models were used for estimating the groundwater spring index (GSI), which was assigned to whole the pixels of the study area and finally, the groundwater spring potential mapping was developed from groundwater spring indices. At first, each pixel was assigned to a unique groundwater spring index. In second step, all indices were exported in ArcGIS10.2 software and were utilized in the construction of the groundwater spring potential mapping. Ultimately, the archived maps were divided into five potential classes, namely very low, low, moderate, high and very high based on quantile classification scheme. Therefore, based on the five hybrid model, five maps of groundwater spring potential were prepared (Figs. 8-9 a-e). There are six methods, namely manual, equal interval, geometric interval, quantile, natural break and standard deviation for classification based on the different purposes. The selection of the best method depends on the characteristics of the data and the distribution of the groundwater spring indexes in a histogram (Ayalew and Yamagishi, 2005). If the distribution of the indexes in the histogram is normal or close to normal, two methods of Equal interval and standard deviation are used. However, if the indexes have a positive or negative skewness, the quantile or natural break classification is proper for indexes classification (Akgun, 2012). In this research, the histogram was checked and the results revealed that quantile method was better than other methods for indexes classification.

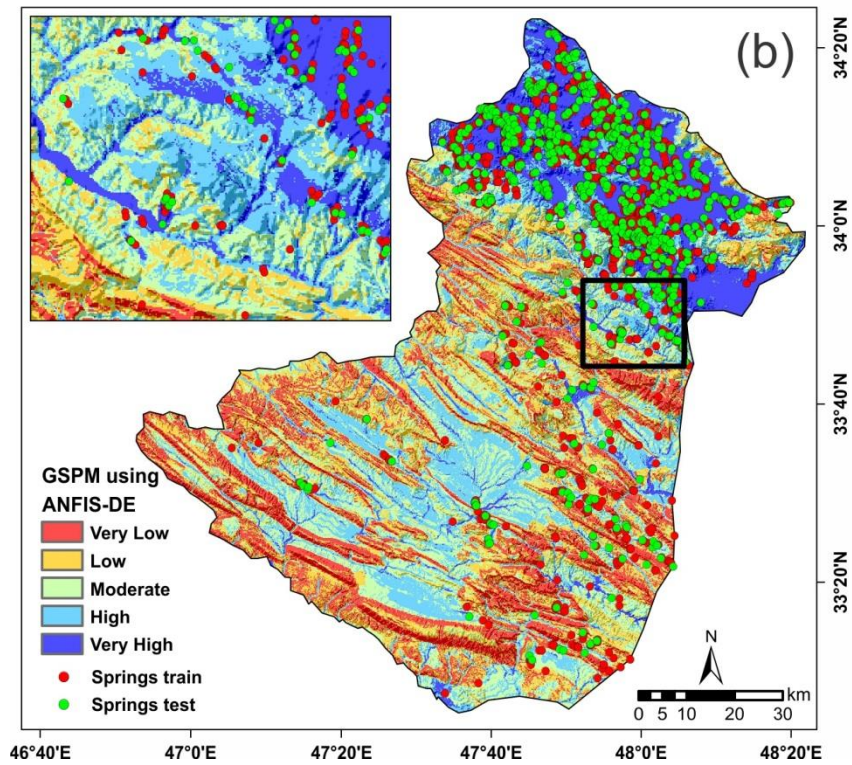
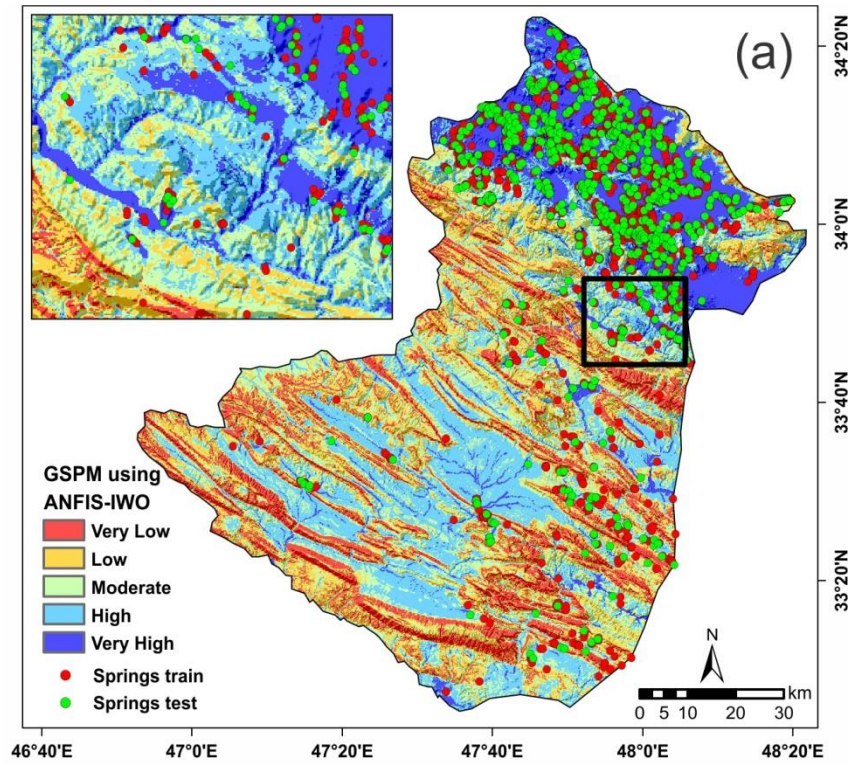
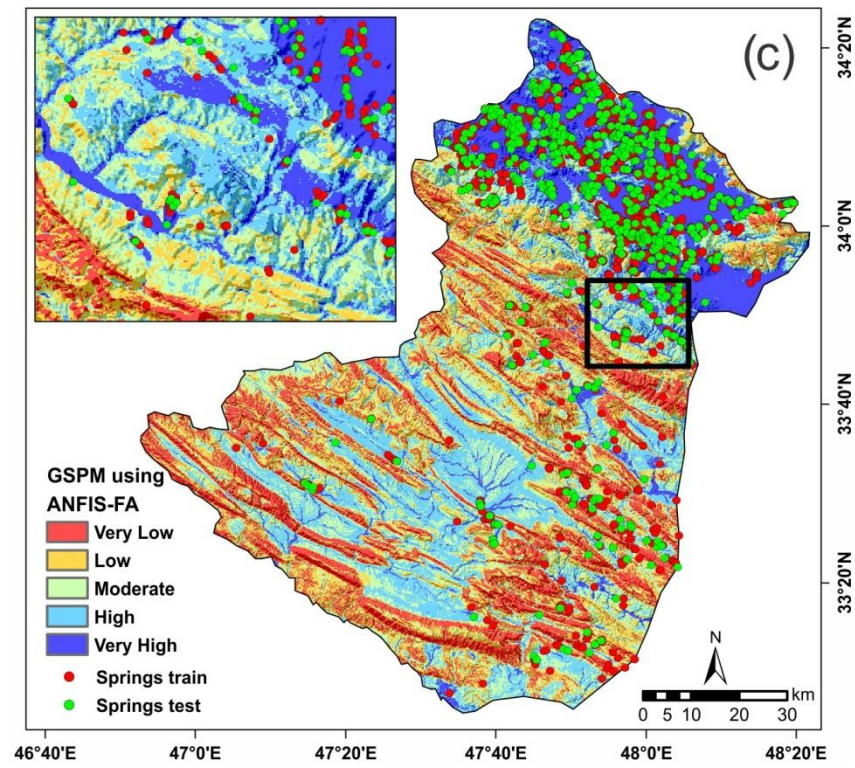
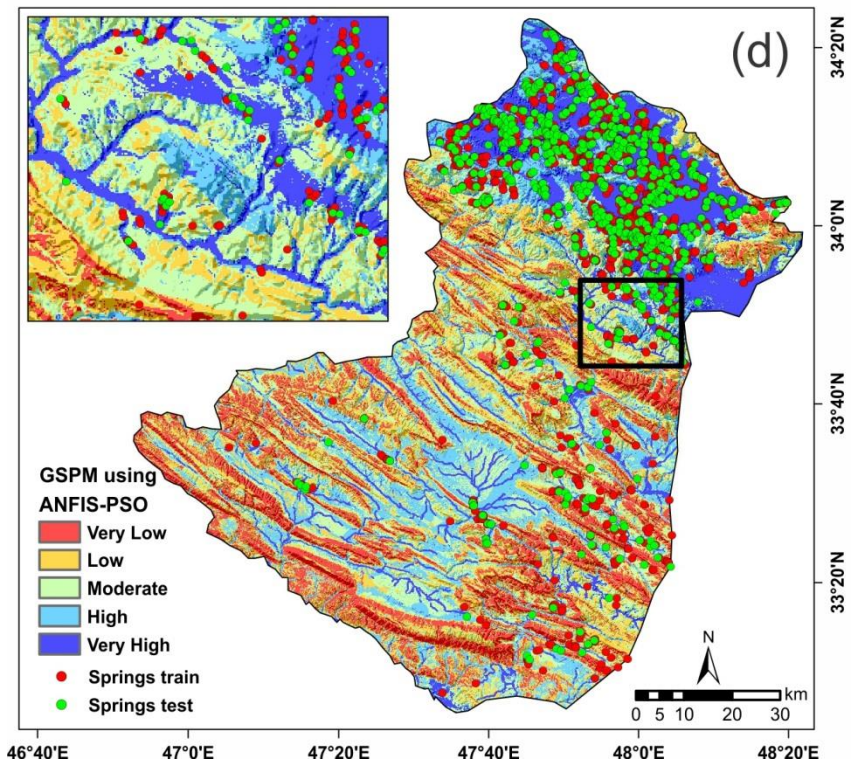


Fig. 89. Groundwater spring potential mapping using ANFIS-IWO (a), ANFIS-DE (b), ANFIS-FA (c), ANFIS-PSO (d) and ANFIS-BA (e).

1813



1814



1815

Fig.89. Continued

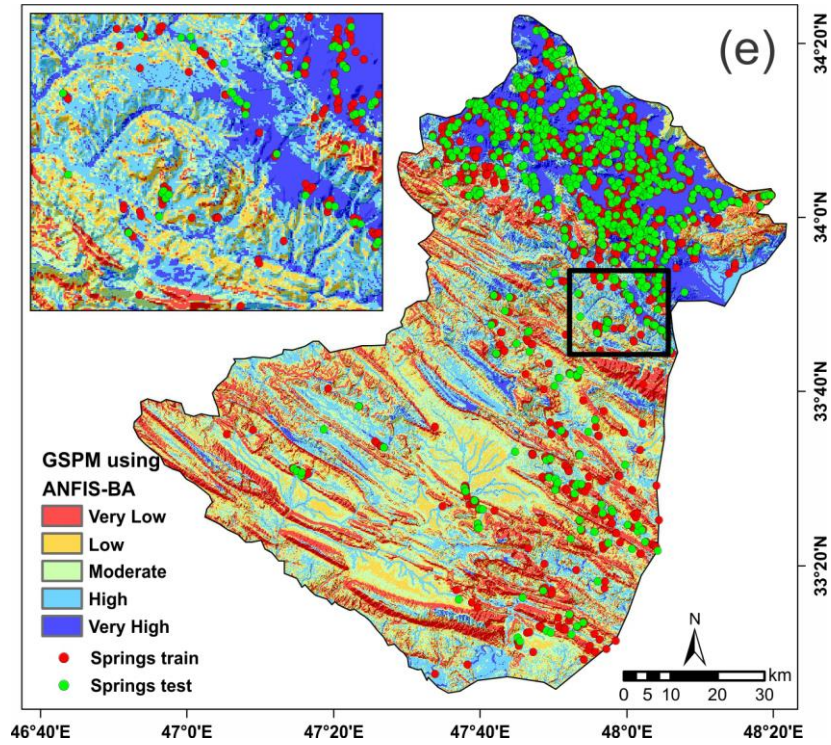


Fig.89. Continued

4.56. Validation and comparisons of the groundwater spring potential map

The prediction ability and reliability of the five achieved maps have been evaluated by both the training and the testing-validating dataset. The results of the success rate revealed that the ANFIS-DE had the highest AUC value of 0.883 followed by ANFIS-IWO and ANFIS-FA (0.882), ANFIS-PSO (0.871) and ANFIS-BA (0.852) (Fig.9a10a). The results exhibited that all five models had a very good prediction capability but the ANFIS-DE has the highest prediction rate (0.873) followed by NFIS-IWO and ANFIS-FA (0.873), ANFIS-PSO (0.865) and ANFIS-BA (0.839), respectively (Fig.9b10b).

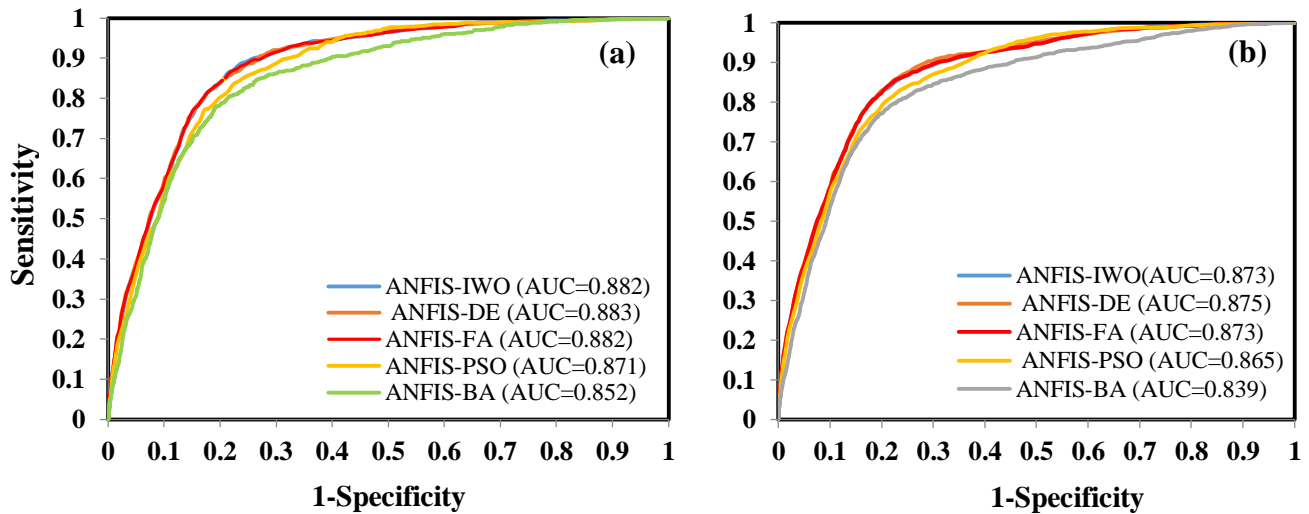


Fig.9.10. Success rate (a) and prediction rate (b) curves for the five performed models

4.67. Non-parametric statistical tests

The two tests of Freidman and Wilcoxon signed rank have been performed to determine whether there are any statistically significant differences between the models performance or not. The result of Freidman test revealed that (Table.3) as Sig and chi-square values were less than 0.05 and greater than 3.84, respectively, null hypothesis has been rejected. The result also indicated that there was statistically a significant difference between prediction capabilities of these five models.

Table.3. The result of Freidman test

NO	Performed models	Mean rank	Chi-square	Sig
1	ANFIS-DE	3.04	64.84	0.00
2	ANFIS-IWO	3.13		
3	ANFIS-FA	2.98		
4	ANFIS-PSO	2.72		
5	ANFIS-BA	3.12		

To show the pairwise differences between models performance, the Wilcoxon signed rank test was carried out and result were shown in Table 4. Result of the Wilcoxon signed-rank test showed that both P-values and z were far from the standard values of 0.05 and (from -1.96 to + 1.96), respectively except for ANFIS-FA vs. ANFIS-DE and ANFIS-PSO vs. ANFIS-DE. This indicates that there are statistically significant differences between models performance except for ANFIS-FA vs. ANFIS-DE and ANFIS-PSO vs. ANFIS-DE.

Table.4. The result of Wilcoxon signed rank test

NO	Pairwise comparison	Z-Value	P-Value	Significance
1	ANFIS-DE vs. ANFIS-BA	-3.97	0.00	Yes
2	ANFIS-FA vs. ANFIS-BA	-2.37	0.017	Yes
3	ANFIS-IWO vs. ANFIS-BA	-2.35	0.018	Yes
4	ANFIS-PSO vs. ANFIS-BA	-3.04	0.002	Yes
5	ANFIS-FA vs. ANFIS-DE	-1.32	0.185	No
6	ANFIS-IWO vs. ANFIS-DE	-3.96	0.00	Yes
7	ANFIS-PSO vs. ANFIS-DE	-0.841	0.41	NO
8	ANFIS-IWO vs. ANFIS-FA	-3.19	0.001	Yes
9	ANFIS-PSO vs. ANFIS-FA	-1.90	0.057	Yes

10	ANFIS-PSO vs. ANFIS-IWO	-2.44	0.015	Yes
----	-------------------------	-------	-------	-----

4.78. Percentage area

The percentage area of each class of final map resulting from five hybrid models has been represented in Fig.4011. According to results, as ANFIS-DE is more accurate in groundwater spring prediction capabilities, the percentage areas of very low, low, moderate, high and very high groundwater spring potential are about 19.06, 19.88, 21.72, 20.55 and 18.78 % of the study area, respectively.

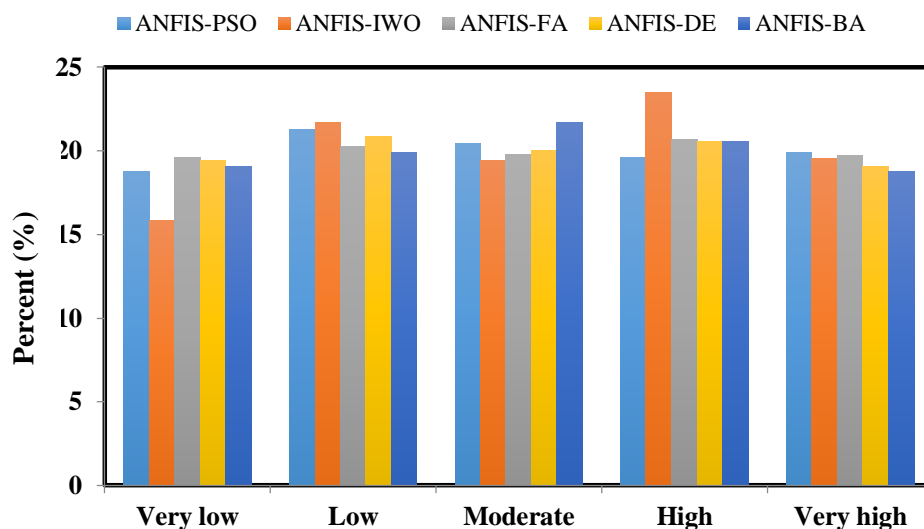


Fig.4011. Percentage areas of different groundwater spring potential classes for five models

5. Discussion

5.1. The impact of conditioning factor's classes on GSPM

~~The classification~~Assessment of conditioning factor is a necessary step in finding the correlation analysis between spring and conditioning factor. It should be noted that ~~there isn't anyno~~ universal guideline ~~is available for regarding~~ the number and size of the classes as well as selecting the conditioning factors. ~~and t~~They ~~were selected~~ mostly ~~depend-based~~ on ~~some factors including~~ characteristics of the study area and previous similar studies (Xu et al., 2013). As the slope increase, the probability of the water infiltration reduces and runoff generation will increase. Thus, the more the slope, the lowest the spring occurrence probability. According to the result of the SWARA method, the springs almost occur in a middle altitude or mountain slopes (but wells are dug in a low-land area). The flat curvature class retains and infiltrates rainfall. Therefore, the amount of groundwater in these areas is higher than concave or convex curvature. The east aspect has more springs than other aspects. These results are in accordance with Pourtaghi and Pourghasemi (Pourtaghi and Pourghasemi, 2014), that had explained most springs occurred in the elevation of 1600-1900 m and east slope aspect (with FR method). TWI shows the amount of wetness, and it is obvious that the more the TWI, the higher the springs probability occurrence is. Terrain Roughness Index (TRI) or topographic roughness or terrain ruggedness calculates the sum

of change in elevation between a grid cell and its neighborhood, and as the lowest the roughness, the highest spring potential mapping. The SPI shows the erosive power of the water and mountainous area is higher than plain area. So, As the SPI increases, the spring potential occurrence increases. Rivers are one of the most important sources of groundwater recharge and the nearer to river, the higher probability to springs occurrences. Also, as the rainfall increases, the higher springs incident, but in the current study, some other conditioning factors affected the spring occurrences.

Most of the springs were located in the garden land-use/land-cover. Therefore, it can be stated that the gardens have been established near the springs. Pliocene-Quaternary formation in a geologic time scale is newer and Quaternary formation has a high potential to groundwater springs incident due to high permeability. The fault is discontinuity in a volume of rock. Thus, the nearer to the fault, the higher the spring occurrence probability will be. Inceptisols soils are relatively new and are characterized by having only the weakest appearance of horizons, the most abundant on the Earth (<https://www.britannica.com/science/Inceptisol>) and mostly formed from colluvial and alluvial materials. So, due to high permeability and high rainfall infiltration, they have a high potential for springs occurrences. In the case of lithological unit, there are four suitable rock type as water reservoir based on physical phenomena such as porosity and permeability that consist of: 1. unconsolidated sands and gravels; 2. sandstones; 3. Lime-stones; and 4. basaltic lava flows. In this study area lithological units include sedimentary rocks mostly carbonate and detrital rocks with cover of alluvium and minor soil.

5.2. Advantages/disadvantages of the models and performance analysis

The highest accuracy based on the RMSE in both training and testing dataset belonged to the ANFIS-PSO model. However, -but based on the AUC for success and prediction rate, the ANFIS-DE model had-has the highest prediction capability. The problem with RMSE comes from the fact that, it is based on the error assessment. But the models should be acted upon holistically based on the abilities. AUC for Receiver operating characteristic (ROC) curves (success and prediction rate curves) is based on the true positive (TP), true negative (TN), false positive (FP) and false negative (FN), it is more accurate than RMSE for comparison (Termeh et al., 2018). The two axes of the ROC curves are (Negnevitsky, 2005):

$$X = 1 - \text{specificity} = 1 - (TN / (TN + FP)) \quad (19)$$

$$Y = \text{sensitivity} = (TP / (TP + FN)) \quad (20)$$

ANFIS ~~model~~ is one of the machine learning algorithms that is proper for natural phenomenon modeling due to its non-linear structure. The ANFIS model, which is based on Takagi–Sugeno fuzzy inference system, is a hybrid of ANNs and fuzzy logic. Therefore, it has a potential to capture the benefits of both in a single framework and can be considered as a robust model. The predictions in ANFIS model are based on learning the “if–then” rules between groundwater spring locations and conditioning factors.

Polykretis et al. (Polykretis et al., 2017), applied ANFIS for landslide susceptibility mapping (LSM) in Peloponnese peninsula, Grece and stated that ANFIS model was a robust model. Vahidinia et al. (Vahidinia et al., 2010), applied ANFIS model to LSM in the Mazandaran Province, Iran, and revealed that ANFIS was a flexible and non-linear model and was completely appropriate

for building a framework of easy inferences. Isanta Navarro (Isanta Navarro, 2013), applied ANFIS to stability augmentation of an airplane and stated that ANFIS had some advantages including: (1) much better learning ability, (2) need for fewer adjustable parameters than those required in other neural network structure and (3) allowing a better integration with other control design methods by its networks.

Despite several advantages of ANFIS ~~model~~, non-adjustancy of membership function is the biggest disadvantage of this model. Finding the optimal parameter for neural fuzzy model in a membership function is difficult; therefore, the best parameter should be finding other optimization models. This problem was addressed in this paper for being solved by five meta-heuristic algorithms, namely Invasive Weed Optimization, Differential Evolution, Firefly, Particle Swarm Optimization and Bees algorithms. The aim of any optimization is to find values of the variable to gratify the restriction by minimizing or maximizing the objective function. These optimization algorithms are completely new in environmental modeling (especially in groundwater potential mapping) and have been used for natural hazards assessment by a few researchers in landslide susceptibility assessment (Chen et al., 2017a) as well as in flood susceptibility mapping (Bui et al., 2016; Termeh et al., 2018).

In the current study, the results showed that DE algorithm optimized the parameter for neural fuzzy model better than four other algorithms. The main DE algorithm's advantage is its simplicity as it consists of only three parameters called N (size of population), F (mutation parameter) and C (crossover parameter) for controlling the search process (Tvrđik, 2006). Advantages of DE algorithm can be explained as follows: (1) Ability to handle non-differentiable, nonlinear and multimodal cost functions, (2) Parallelizability to cope with computation intensive cost functions, (4) good convergence properties, i.e. consistent convergence to the global minimum in consecutive independent trials, and (5) random sampling and combining vectors in the present population for creating vectors for the next generation.

Finally, it should be noted that each algorithm has some advantages or disadvantages according to the optimization problems which can be summarized as:

Some of the advantages of IWO in comparison to other evolutionary algorithms include the way of reproduction, spatial dispersal, and competitive exclusion (Mehrabian and Lucas, 2006) as well as the fact that seeds and their parents are ranked together and those with better fitness survive and become reproductive (Ahmed et al., 2014). This algorithm can benefit from combined advantages of retaining the dominant poles and the error minimization (Abu-Al-Nadi et al., 2013) and there is no need for continuity or differentiability of the objective function.

Bees algorithm doesn't employ any probability approach, but utilizes fitness evaluation to drive the search (Yuce et al., 2013). This algorithm is implemented with several optimization problems or in other words, BA uses a set of parameters including the number of scout bees in the selected patches, the number of best patches in the selected patches, the number of elite patches in the selected best patches, the number of recruited bees in the elite patches, the number of recruited bees in the non-elite best patches, the size of neighborhood for each patch, the number of iterations and the difference between the value of first and last iterations that makes it powerful. BA also has both local and global search capability and the local search step of the algorithm covers the best locations. BA is really easy to use and available for hybridization combination with other algorithms (Yuce et al., 2013). Another advantage is hiring smart bees since bees (artificial insects)

can memorize the location of the best food source and its quality which has been found before. If the new solution has a lower fitness than the best-saved solution in the SB memory, it is replaced with new candidate solution (Gorji-Bandpy and Mozaffari, 2012).

Firefly Algorithm's (FA) advantages are summarized as: (1) handling highly non-linear, multi-modal optimization problems efficiently, (2) not utilizing velocities (3) very high speed of convergence in finding the global optimized answer (4) ability to be integrated with other optimization techniques as a flexible method, and finally (5) not needing a good initial solution to beginning of its iteration process.

Advantages of Particle Swarm Optimization (PSO) algorithm can be summarized as follows: (1) Particles update themselves with the internal velocity; (2) particles have a memory important to the algorithm, (3) the 'best' particle gives out the information to others, (4) it often produces quality solutions more rapidly than alternative methods, (5) this algorithm simulates bird flocking behavior to achieve a self-evolution system, (6) it automatically searches for the optimum solution in the solution space, (7) (Wan, 2013).

As a result, there isn't any algorithm which works perfectly for all optimization problems, and each algorithm has a different performance accuracy based on different data. New algorithms, therefore, should be applied, tested and finally the most powerful algorithm should be selected; as the conclusion of the research demands.

5.3. Previous works and future work proposal

Some research has been ~~done-carried out~~ in groundwater well or spring potential mapping using bivariate statistical models (Al-Manmi and Rauf, 2016; Guru et al., 2017; Nampak et al., 2014) using random forest (Rahmati et al., 2016) and using boosted regression tree and classification and regression tree (Naghbi et al., 2016). The ANFIS-metaheuristic hybrid models ~~have not seen are not~~ used in groundwater potential mapping. However, these hybrid models and are only used have proven efficient in flood susceptibility mapping (Bui et al., 2016; Termeh et al., 2018) and landslide susceptibility mapping (Chen et al., 2017a). Tien Bui et al. (Bui et al., 2016) ensemble the ANFIS using two optimization models, namely Genetic (GA) and PSO for the identification of flood prone areas in Vietnam. Razavi Termeh et al. (Termeh et al., 2018), used ANFIS-Ant Colony Optimization, ANFIS-GA and ANFIS-PSO in flood susceptibility mapping of Jahrom basin and stated that ANFIS-PSO had higher prediction capabilities than the two other models. Chen et al (2017) applied three hybrid models, namely ANFIS- Genetic Algorithm (GA), ANFIS-Differential Evolution (DE) and ANFIS-Particle Swarm Optimization (PSO) for identifying the areas prone to landslides in Hanyuan County, China. The results showed that ANFIS-DE had a higher performance (AUC=0.84) followed by ANFIS-GA (AUC=0.82) and ANFIS-PSO (AUC=0.78).

GenerallyIn general, the ~~mentioned~~ results of the present study and different researchers revealed that by applying hybrid models, better results could be achieved for any spatial prediction modeling including groundwater potential mapping. The ensembles of ANFIS by meta-heuristic algorithms can be proposed for any spatial prediction modeling such as groundwater potential mapping, flood susceptibility mapping, landslide susceptibility assessment, gully occurrences susceptibility mapping and other endeavors at a regional scale and in other areas.

For future work, it is recommended that (1) the water quality of the Koohdasht-Nourabad plain be investigated and the water quality of areas with high potential be determined for different aspects such as drinking, agricultural and industrial activities, and (2) the groundwater vulnerability assessment should be applied by some common methods including DRASTIC model for which the zones with high potential to groundwater occurrences should be preserved against pollution.

6. Conclusion

Groundwater is the most important natural resource in the world and about 25 percent of all fresh water is estimated as groundwater. Thus, the groundwater potential mapping has been considered as one of the most effective ~~methods~~tools for the management of groundwater resources for better exploitation. The conservation and the maps with high accuracy is necessary for decisions. As the natural phenomena are complex, the simple method and statistical models do not have an appropriate result in modeling of the natural phenomena. To solve the problem, the artificial intelligence models have been used for having a reasonable result but these model have some weaknesses, especially in modeling process. To resolve this problem, this study verifies the five new hybrid models of ANFIS with metaheuristic algorithms namely IWO, DE, FA, PSO and BA to increase the prediction capability of the spatial prediction of groundwater potential mapping (1) for solving the weakness of the artificial intelligence models and (2) using non-linear structure of these models which are better for modeling of the complex natural phenomena such as groundwater modeling. The result of this modeling has been evaluated using prediction rate ROC curves and the results showed that all models had very good reasonable results. However, the ANFIS-DE had the highest prediction power (0.875) followed by ANFIS-IWO and ANFIS-FA (0.873), ANFIS-PSO (0.865) and ANFIS-BA (0.839). Thus, the results revealed that the metaheuristic algorithms could optimize the weights parameters of the ANFIS model with high accuracy as the highest advantage of these algorithms

According to the results of the SWARA method, most springs existed in an altitude of 1703-2068 m, flat curvature, east aspect, TWI of 6.6-7.9, TRI of 0-8.7, SPI of 583969-1330153, Inceptisols soil, slope of 0-5.5 degree, 0-200 m distance from river, 500-1000 m distance from fault, rainfall between 500-600 mm, in a garden, in a Pliocene-Quaternary lithological age and OMq lithology unit.

The results of the current study is helpful for Iran Water Resources Management Company (IWRMC) for sustainable management of the groundwater resources. Overall, the maps resulting from these hybrid artificial intelligence algorithms can be applied for better management of the groundwater resources in the study area, and can be used for other areas for groundwater potential assessment or mapping of gully, flood, landslide and other susceptibility uses in the world due to its high precision.

References

Abu-Al-Nadi DI, Alsmadi OM, Abo-Hammour ZS, Hawa MF, Rahhal JS. Invasive weed optimization for model order reduction of linear MIMO systems. *Applied Mathematical Modelling* 2013; 37: 4570-4577.

2035 Adiat K, Nawawi M, Abdullah K. Assessing the accuracy of GIS-based elementary multi criteria decision
 2036 analysis as a spatial prediction tool—A case of predicting potential zones of sustainable
 2037 groundwater resources. *Journal of Hydrology* 2012; 440: 75-89.
 2038 Aghdam IN, Pradhan B, Panahi M. Landslide susceptibility assessment using a novel hybrid model of
 2039 statistical bivariate methods (FR and WOE) and adaptive neuro-fuzzy inference system (ANFIS)
 2040 at southern Zagros Mountains in Iran. *Environmental Earth Sciences* 2017; 76: 237.
 2041 Ahmed A, Al-Amin R, Amin R. Design of static synchronous series compensator based damping controller
 2042 employing invasive weed optimization algorithm. *SpringerPlus* 2014; 3: 394.
 2043 Akgun A. A comparison of landslide susceptibility maps produced by logistic regression, multi-criteria
 2044 decision, and likelihood ratio methods: a case study at İzmir, Turkey. *Landslides* 2012; 9: 93-106.
 2045 Al-Manmi DAM, Rauf LF. Groundwater potential mapping using remote sensing and GIS-based, in
 2046 Halabja City, Kurdistan, Iraq. *Arabian Journal of Geosciences* 2016; 9: 357.
 2047 Alimardani M, Hashemkhani Zolfani S, Aghdaie MH, Tamošaitienė J. A novel hybrid SWARA and VIKOR
 2048 methodology for supplier selection in an agile environment. *Technological and Economic*
 2049 *Development of Economy* 2013; 19: 533-548.
 2050 Alley WM, Reilly TE, Franke OL. Sustainability of ground-water resources. Vol 1186: US Department of
 2051 the Interior, US Geological Survey, 1999.
 2052 Alweshah M, Abdullah S. Hybridizing firefly algorithms with a probabilistic neural network for solving
 2053 classification problems. *Applied Soft Computing* 2015; 35: 513-524.
 2054 Amiri B, Hossain L, Crawford JW, Wigand RT. Community detection in complex networks: Multi-
 2055 objective enhanced firefly algorithm. *Knowledge-Based Systems* 2013; 46: 1-11.
 2056 Ayalew L, Yamagishi H. The application of GIS-based logistic regression for landslide susceptibility
 2057 mapping in the Kakuda-Yahiko Mountains, Central Japan. *Geomorphology* 2005; 65: 15-31.
 2058 Beasley TM, Zumbo BD. Comparison of aligned Friedman rank and parametric methods for testing
 2059 interactions in split-plot designs. *Computational statistics & data analysis* 2003; 42: 569-593.
 2060 Berhanu B, Seleshi Y, Melesse AM. Surface Water and Groundwater Resources of Ethiopia: Potentials
 2061 and Challenges of Water Resources Development. Nile River Basin. Springer, 2014, pp. 97-117.
 2062 Brenning A. Spatial prediction models for landslide hazards: review, comparison and evaluation. *Natural*
 2063 *Hazards and Earth System Science* 2005; 5: 853-862.
 2064 Bui DT, Lofman O, Revhaug I, Dick O. Landslide susceptibility analysis in the Hoa Binh province of
 2065 Vietnam using statistical index and logistic regression. *Natural hazards* 2011; 59: 1413.
 2066 Bui DT, Pradhan B, Nampak H, Bui Q-T, Tran Q-A, Nguyen Q-P. Hybrid artificial intelligence approach
 2067 based on neural fuzzy inference model and metaheuristic optimization for flood susceptibility
 2068 modeling in a high-frequency tropical cyclone area using GIS. *Journal of Hydrology* 2016; 540:
 2069 317-330.
 2070 Bui DT, Pradhan B, Revhaug I, Nguyen DB, Pham HV, Bui QN. A novel hybrid evidential belief function-
 2071 based fuzzy logic model in spatial prediction of rainfall-induced shallow landslides in the Lang
 2072 Son city area (Vietnam). *Geomatics, Natural Hazards and Risk* 2015; 6: 243-271.
 2073 Chang F-J, Tsai M-J. A nonlinear spatio-temporal lumping of radar rainfall for modeling multi-step-ahead
 2074 inflow forecasts by data-driven techniques. *Journal of Hydrology* 2016; 535: 256-269.
 2075 Chen W, Panahi M, Pourghasemi HR. Performance evaluation of GIS-based new ensemble data mining
 2076 techniques of adaptive neuro-fuzzy inference system (ANFIS) with genetic algorithm (GA),
 2077 differential evolution (DE), and particle swarm optimization (PSO) for landslide spatial
 2078 modelling. *CATENA* 2017a; 157: 310-324.
 2079 Chen W, Pourghasemi HR, Panahi M, Kornejady A, Wang J, Xie X, et al. Spatial prediction of landslide
 2080 susceptibility using an adaptive neuro-fuzzy inference system combined with frequency ratio,
 2081 generalized additive model, and support vector machine techniques. *Geomorphology* 2017b;
 2082 297: 69-85.

2083 Cheng Z, Zhou H, Yang H. Research on MPPT control of PV system based on PSO algorithm. Control and
2084 Decision Conference (CCDC), 2010 Chinese. IEEE, 2010, pp. 887-892.

2085 Chenini I, Mammou AB. Groundwater recharge study in arid region: an approach using GIS techniques
2086 and numerical modeling. Computers & Geosciences 2010; 36: 801-817.

2087 Chung C-JF, Fabbri AG. Validation of spatial prediction models for landslide hazard mapping. Natural
2088 Hazards 2003; 30: 451-472.

2089 Clapcott J, Goodwin E, Snelder T. Predictive Models of Benthic Macroinvertebrate Metrics. Prepared for
2090 Ministry for the Environment. Cawthron Report, 2013.

2091 Das S, Abraham A, Chakraborty UK, Konar A. Differential evolution using a neighborhood-based
2092 mutation operator. IEEE Transactions on Evolutionary Computation 2009; 13: 526-553.

2093 David Keith Todd, Mays LW. Groundwater Hydrology, 2nd Edition. Wiley, New York 1980.

2094 Derrac J, García S, Molina D, Herrera F. A practical tutorial on the use of nonparametric statistical tests
2095 as a methodology for comparing evolutionary and swarm intelligence algorithms. Swarm and
2096 Evolutionary Computation 2011; 1: 3-18.

2097 Eberhart R, Kennedy J. A new optimizer using particle swarm theory. Micro Machine and Human
2098 Science, 1995. MHS'95., Proceedings of the Sixth International Symposium on. IEEE, 1995, pp.
2099 39-43.

2100 Fashae OA, Tijani MN, Talabi AO, Adedeji OI. Delineation of groundwater potential zones in the
2101 crystalline basement terrain of SW-Nigeria: an integrated GIS and remote sensing approach.
2102 Applied Water Science 2014; 4: 19-38.

2103 Fitts CR. Groundwater science: Academic press, 2002.

2104 Friedman M. The use of ranks to avoid the assumption of normality implicit in the analysis of variance.
2105 Journal of the american statistical association 1937; 32: 675-701.

2106 Gandomi AH, Yang X-S, Talatahari S, Alavi AH. Firefly algorithm with chaos. Communications in Nonlinear
2107 Science and Numerical Simulation 2013; 18: 89-98.

2108 Gaprindashvili G, Guo J, Daorueang P, Xin T, Rahimy P. A new statistic approach towards landslide
2109 hazard risk assessment. International Journal of Geosciences 2014; 5: 38.

2110 Ghalkhani H, Golian S, Saghaian B, Farokhnia A, Shamseldin A. Application of surrogate artificial
2111 intelligent models for real-time flood routing. Water and Environment Journal 2013; 27: 535-
2112 548.

2113 Ghasemi M, Ghavidel S, Akbari E, Vahed AA. Solving non-linear, non-smooth and non-convex optimal
2114 power flow problems using chaotic invasive weed optimization algorithms based on chaos.
2115 Energy 2014; 73: 340-353.

2116 Gorji-Bandpy M, Mozaffari A. Multiobjective optimization of irreversible thermal engine using mutable
2117 smart bee algorithm. Applied Computational Intelligence and Soft Computing 2012; 2012: 5.

2118 Güçlü YS, Şen Z. Hydrograph estimation with fuzzy chain model. Journal of Hydrology 2016; 538: 587-
2119 597.

2120 Guru B, Seshan K, Bera S. Frequency ratio model for groundwater potential mapping and its sustainable
2121 management in cold desert, India. Journal of King Saud University-Science 2017; 29: 333-347.

2122 Hong H, Panahi M, Shirzadi A, Ma T, Liu J, Zhu A-X, et al. Flood susceptibility assessment in Hengfeng
2123 area coupling adaptive neuro-fuzzy inference system with genetic algorithm and differential
2124 evolution. Science of The Total Environment 2017.

2125 Hong H, Pradhan B, Xu C, Bui DT. Spatial prediction of landslide hazard at the Yihuang area (China) using
2126 two-class kernel logistic regression, alternating decision tree and support vector machines.
2127 Catena 2015; 133: 266-281.

2128 Isanta Navarro R. Study of a neural network-based system for stability augmentation of an airplane.
2129 2013.

2130 Israil M, Al-Hadithi M, Singhal D. Application of a resistivity survey and geographical information system
 2131 (GIS) analysis for hydrogeological zoning of a piedmont area, Himalayan foothill region, India.
 2132 Hydrogeology journal 2006; 14: 753-759.
 2133 Jang J-S. ANFIS: adaptive-network-based fuzzy inference system. IEEE transactions on systems, man, and
 2134 cybernetics 1993; 23: 665-685.
 2135 Jha MK, Chowdary V, Chowdhury A. Groundwater assessment in Salboni Block, West Bengal (India) using
 2136 remote sensing, geographical information system and multi-criteria decision analysis
 2137 techniques. Hydrogeology journal 2010; 18: 1713-1728.
 2138 Jha MK, Chowdhury A, Chowdary V, Peiffer S. Groundwater management and development by
 2139 integrated remote sensing and geographic information systems: prospects and constraints.
 2140 Water Resources Management 2007; 21: 427-467.
 2141 Kaliraj S, Chandrasekar N, Magesh N. Identification of potential groundwater recharge zones in Vaigai
 2142 upper basin, Tamil Nadu, using GIS-based analytical hierarchical process (AHP) technique.
 2143 Arabian Journal of Geosciences 2014; 7: 1385-1401.
 2144 Kennedy J. Particle swarm optimization. Encyclopedia of machine learning. Springer, 2011, pp. 760-766.
 2145 Kennedy J, Eberhart R. Particle swarm optimization, IEEE International of first Conference on Neural
 2146 Networks. Perth, Australia, IEEE Press, 1995.
 2147 Keršulienė V, Zavadskas EK, Turskis Z. Selection of rational dispute resolution method by applying new
 2148 step-wise weight assessment ratio analysis (SWARA). Journal of business economics and
 2149 management 2010; 11: 243-258.
 2150 Khosravi K, Nohani E, Maroufinia E, Pourghasemi HR. A GIS-based flood susceptibility assessment and its
 2151 mapping in Iran: a comparison between frequency ratio and weights-of-evidence bivariate
 2152 statistical models with multi-criteria decision-making technique. Natural Hazards 2016a; 83:
 2153 947-987.
 2154 Khosravi K, Pourghasemi HR, Chapi K, Bahri M. Flash flood susceptibility analysis and its mapping using
 2155 different bivariate models in Iran: a comparison between Shannon's entropy, statistical index,
 2156 and weighting factor models. Environmental monitoring and assessment 2016b; 188: 656.
 2157 Khosravi K, Pham B.T, Chapi K, Shirzadi A, Shahabi H, et al. 2018. A comparative assessment of decision
 2158 trees algorithms for flash flood susceptibility modeling at Haraz watershed, northern Iran.
 2159 Science of the Total Environment 627, 744-755.
 2160 Lee M-J, Choi J-W, Oh H-J, Won J-S, Park I, Lee S. Ensemble-based landslide susceptibility maps in Jinbu
 2161 area, Korea. Environmental Earth Sciences 2012; 67: 23-37.
 2162 Li Y-F, Xie M, Goh T-N. Adaptive ridge regression system for software cost estimating on multi-collinear
 2163 datasets. Journal of Systems and Software 2010; 83: 2332-2343.
 2164 Lillesand T, Kiefer RW, Chipman J. Remote sensing and image interpretation: John Wiley & Sons, 2014.
 2165 Lohani A, Kumar R, Singh R. Hydrological time series modeling: A comparison between adaptive neuro-
 2166 fuzzy, neural network and autoregressive techniques. Journal of Hydrology 2012; 442: 23-35.
 2167 Mehrabian AR, Lucas C. A novel numerical optimization algorithm inspired from weed colonization.
 2168 Ecological informatics 2006; 1: 355-366.
 2169 Mukerji A, Chatterjee C, Raghuwanshi NS. Flood forecasting using ANN, neuro-fuzzy, and neuro-GA
 2170 models. Journal of Hydrologic Engineering 2009; 14: 647-652.
 2171 Mukherjee S. Targeting saline aquifer by remote sensing and geophysical methods in a part of Hamirpur-
 2172 Kanpur, India. Hydrogeol J 1996; 19: 53-64.
 2173 Naghibi SA, Moghaddam DD, Kalantar B, Pradhan B, Kisi O. A comparative assessment of GIS-based data
 2174 mining models and a novel ensemble model in groundwater well potential mapping. Journal of
 2175 Hydrology 2017; 548: 471-483.

2176 Naghibi SA, Pourghasemi HR, Dixon B. GIS-based groundwater potential mapping using boosted
 2177 regression tree, classification and regression tree, and random forest machine learning models
 2178 in Iran. *Environmental monitoring and assessment* 2016; 188: 44.

2179 Naghibi SA, Pourghasemi HR, Pourtaghi ZS, Rezaei A. Groundwater qanat potential mapping using
 2180 frequency ratio and Shannon's entropy models in the Moghan watershed, Iran. *Earth Science*
 2181 *Informatics* 2015; 8: 171-186.

2182 Naidu YR, Ojha A. A hybrid version of invasive weed optimization with quadratic approximation. *Soft*
 2183 *Computing* 2015; 19: 3581-3598.

2184 Nampak H, Pradhan B, Manap MA. Application of GIS based data driven evidential belief function model
 2185 to predict groundwater potential zonation. *Journal of Hydrology* 2014; 513: 283-300.

2186 Nayak P, Sudheer K, Rangan D, Ramasastri K. Short-term flood forecasting with a Neurofuzzy model.
 2187 *Water Resources Research* 2005; 41.

2188 Negnevitsky M. *Artificial intelligence: a guide to intelligent systems*: Pearson Education, 2005.

2189 Nieto PG, García-Gonzalo E, Fernández JA, Muñiz CD. Hybrid PSO-MARS-based model for forecasting a
 2190 successful growth cycle of the *Spirulina platensis* from experimental data in open raceway
 2191 ponds. *Ecological engineering* 2015; 81: 534-542.

2192 Nosrati K, Van Den Eeckhaut M. Assessment of groundwater quality using multivariate statistical
 2193 techniques in Hashtgerd Plain, Iran. *Environmental Earth Sciences* 2012; 65: 331-344.

2194 O'brien RM. A caution regarding rules of thumb for variance inflation factors. *Quality & Quantity* 2007;
 2195 41: 673-690.

2196 Oh H-J, Kim Y-S, Choi J-K, Park E, Lee S. GIS mapping of regional probabilistic groundwater potential in
 2197 the area of Pohang City, Korea. *Journal of Hydrology* 2011; 399: 158-172.

2198 Olsson AE. *Particle swarm optimization: Theory, techniques and applications*: Nova Science Publishers,
 2199 Inc., 2010.

2200 Ozdemir A. GIS-based groundwater spring potential mapping in the Sultan Mountains (Konya, Turkey)
 2201 using frequency ratio, weights of evidence and logistic regression methods and their
 2202 comparison. *Journal of Hydrology* 2011a; 411: 290-308.

2203 Ozdemir A. Using a binary logistic regression method and GIS for evaluating and mapping the
 2204 groundwater spring potential in the Sultan Mountains (Aksehir, Turkey). *Journal of Hydrology*
 2205 2011b; 405: 123-136.

2206 Pham BT, Bui DT, Pourghasemi HR, Indra P, Dholakia M. Landslide susceptibility assessment in the
 2207 Uttarakhand area (India) using GIS: a comparison study of prediction capability of naïve bayes,
 2208 multilayer perceptron neural networks, and functional trees methods. *Theoretical and Applied*
 2209 *Climatology* 2017a; 128: 255-273.

2210 Pham BT, Khosravi K, Prakash I. Application and comparison of decision tree-based machine learning
 2211 methods in landside susceptibility assessment at Pauri Garhwal Area, Uttarakhand, India.
 2212 *Environmental Processes* 2017b; 4: 711-730.

2213 Pham D, Ghanbarzadeh A, Koc E, Otri S, Rahim S, Zaidi M. The bees algorithm. Technical note.
 2214 *Manufacturing Engineering Centre, Cardiff University, UK* 2005: 1-57.

2215 Pham D, Ghanbarzadeh A, Koc E, Otri S, Rahim S, Zaidi M. The bees algorithm-A novel tool for complex
 2216 optimisation. *Intelligent Production Machines and Systems-2nd I* PROMS Virtual International*
 2217 *Conference* (3-14 July 2006). sn, 2011.

2218 Phootrakornchai W, Jiriwibhakorn S. Online critical clearing time estimation using an adaptive neuro-
 2219 fuzzy inference system (ANFIS). *International Journal of Electrical Power & Energy Systems* 2015;
 2220 73: 170-181.

2221 Polykretis C, Chalkias C, Ferentinou M. Adaptive neuro-fuzzy inference system (ANFIS) modeling for
 2222 landslide susceptibility assessment in a Mediterranean hilly area. *Bulletin of Engineering*
 2223 *Geology and the Environment* 2017: 1-15.

2224 Pourghasemi H, Moradi H, Aghda SF. Landslide susceptibility mapping by binary logistic regression,
 2225 analytical hierarchy process, and statistical index models and assessment of their performances.
 2226 Natural hazards 2013a; 69: 749-779.

2227 Pourghasemi HR, Beheshtirad M. Assessment of a data-driven evidential belief function model and GIS
 2228 for groundwater potential mapping in the Koohrang Watershed, Iran. Geocarto International
 2229 2015; 30: 662-685.

2230 Pourghasemi HR, Pradhan B, Gokceoglu C. Application of fuzzy logic and analytical hierarchy process
 2231 (AHP) to landslide susceptibility mapping at Haraz watershed, Iran. Natural hazards 2012; 63:
 2232 965-996.

2233 Pourghasemi HR, Pradhan B, Gokceoglu C, Mohammadi M, Moradi HR. Application of weights-of-
 2234 evidence and certainty factor models and their comparison in landslide susceptibility mapping at
 2235 Haraz watershed, Iran. Arabian Journal of Geosciences 2013b; 6: 2351-2365.

2236 Poursalehi N, Zolfaghari A, Minuchehr A. A novel optimization method, Effective Discrete Firefly
 2237 Algorithm, for fuel reload design of nuclear reactors. Annals of Nuclear Energy 2015; 81: 263-
 2238 275.

2239 Pourtaghi ZS, Pourghasemi HR. GIS-based groundwater spring potential assessment and mapping in the
 2240 Birjand Township, southern Khorasan Province, Iran. Hydrogeology Journal 2014; 22: 643-662.

2241 Pradhan B. Groundwater potential zonation for basaltic watersheds using satellite remote sensing data
 2242 and GIS techniques. Open Geosciences 2009; 1: 120-129.

2243 Rahmati O, Pourghasemi HR, Melesse AM. Application of GIS-based data driven random forest and
 2244 maximum entropy models for groundwater potential mapping: a case study at Mehran Region,
 2245 Iran. Catena 2016; 137: 360-372.

2246 Rahmati O, Samani AN, Mahdavi M, Pourghasemi HR, Zeinivand H. Groundwater potential mapping at
 2247 Kurdistan region of Iran using analytic hierarchy process and GIS. Arabian Journal of Geosciences
 2248 2015; 8: 7059-7071.

2249 Rezaeianzadeh M, Tabari H, Yazdi AA, Isik S, Kalin L. Flood flow forecasting using ANN, ANFIS and
 2250 regression models. Neural Computing and Applications 2014; 25: 25-37.

2251 Rezakazemi M, Dashti A, Asghari M, Shirazian S. H 2-selective mixed matrix membranes modeling using
 2252 ANFIS, PSO-ANFIS, GA-ANFIS. International Journal of Hydrogen Energy 2017.

2253 Sander P, Chesley MM, Minor TB. Groundwater assessment using remote sensing and GIS in a rural
 2254 groundwater project in Ghana: lessons learned. Hydrogeology Journal 1996; 4: 40-49.

2255 Saravanan B, Vasudevan E, Kothari D. A solution to unit commitment problem using invasive weed
 2256 optimization algorithm. Power, Energy and Control (ICPEC), 2013 International Conference on.
 2257 IEEE, 2013, pp. 386-393.

2258 Senapati MR, Dash PK. Local linear wavelet neural network based breast tumor classification using firefly
 2259 algorithm. Neural Computing and Applications 2013; 22: 1591-1598.

2260 Shu C, Ouarda T. Regional flood frequency analysis at ungauged sites using the adaptive neuro-fuzzy
 2261 inference system. Journal of Hydrology 2008; 349: 31-43.

2262 Siebert S, Henrich V, Frenken K, Burke J. Update of the digital global map of irrigation areas to version 5.
 2263 Rheinische Friedrich-Wilhelms-Universität, Bonn, Germany and Food and Agriculture
 2264 Organization of the United Nations, Rome, Italy 2013.

2265 Singh AK, Prakash SR. An integrated approach of remote sensing, geophysics and GIS to evaluation of
 2266 groundwater potentiality of Ojhala sub-watershed, Mirzapur district, UP, India. Asian conference
 2267 on GIS, GPS, aerial photography and remote sensing, Bangkok-Thailand, 2002.

2268 Storn R, Price K. Differential evolution—a simple and efficient heuristic for global optimization over
 2269 continuous spaces. Journal of global optimization 1997; 11: 341-359.

2270 Takagi T, Sugeno M. Fuzzy identification of systems and its applications to modeling and control. IEEE
 2271 transactions on systems, man, and cybernetics 1985: 116-132.

2272 Tehrany MS, Pradhan B, Jebur MN. Spatial prediction of flood susceptible areas using rule based
 2273 decision tree (DT) and a novel ensemble bivariate and multivariate statistical models in GIS.
 2274 Journal of Hydrology 2013; 504: 69-79.

2275 Tehrany MS, Pradhan B, Jebur MN. Flood susceptibility mapping using a novel ensemble weights-of-
 2276 evidence and support vector machine models in GIS. Journal of hydrology 2014; 512: 332-343.

2277 Termeh SVR, Kornejady A, Pourghasemi HR, Keesstra S. Flood susceptibility mapping using novel
 2278 ensembles of adaptive neuro fuzzy inference system and metaheuristic algorithms. Science of
 2279 the Total Environment 2018; 615: 438-451.

2280 Tvrdík J. Competitive differential evolution and genetic algorithm in GA-DS toolbox. Technical Computing
 2281 Prague, Praha, Humusoft 2006: 99-106.

2282 Umar Z, Pradhan B, Ahmad A, Jebur MN, Tehrany MS. Earthquake induced landslide susceptibility
 2283 mapping using an integrated ensemble frequency ratio and logistic regression models in West
 2284 Sumatera Province, Indonesia. Catena 2014; 118: 124-135.

2285 Vahidnia MH, Alesheikh AA, Alimohammadi A, Hosseinali F. A GIS-based neuro-fuzzy procedure for
 2286 integrating knowledge and data in landslide susceptibility mapping. Computers & Geosciences
 2287 2010; 36: 1101-1114.

2288 Waikar M, Nilawar AP. Identification of groundwater potential zone using remote sensing and GIS
 2289 technique. Int J Innov Res Sci Eng Technol 2014; 3: 1264-1274.

2290 Wan S. Entropy-based particle swarm optimization with clustering analysis on landslide susceptibility
 2291 mapping. Environmental earth sciences 2013; 68: 1349-1366.

2292 Xu C, Dai F, Xu X, Lee YH. GIS-based support vector machine modeling of earthquake-triggered landslide
 2293 susceptibility in the Jianjiang River watershed, China. Geomorphology 2012; 145: 70-80.

2294 Xu C, Xu X, Dai F, Wu Z, He H, Shi F, et al. Application of an incomplete landslide inventory, logistic
 2295 regression model and its validation for landslide susceptibility mapping related to the May 12,
 2296 2008 Wenchuan earthquake of China. Natural hazards 2013; 68: 883-900.

2297 Yang X-S. Firefly algorithms for multimodal optimization. International symposium on stochastic
 2298 algorithms. Springer, 2009, pp. 169-178.

2299 Yang X-S. Nature-inspired metaheuristic algorithms: Luniver press, 2010.

2300 Yuce B, Packianather MS, Mastrocinque E, Pham DT, Lambiasi A. Honey bees inspired optimization
 2301 method: the bees algorithm. Insects 2013; 4: 646-662.

2302 Zehtabian G, Khosravi H, Ghodsi M. High demand in a land of water scarcity: Iran. Water and
 2303 Sustainability in Arid Regions. Springer, 2010, pp. 75-86.

2304 Zeng Y, Zhang Z, Kusiak A. Predictive modeling and optimization of a multi-zone HVAC system with data
 2305 mining and firefly algorithms. Energy 2015; 86: 393-402.

2306 Zengqiang M, Cunzhi P, Yongqiang W. Road safety evaluation from traffic information based on ANFIS.
 2307 Control Conference, 2008. CCC 2008. 27th Chinese. IEEE, 2008, pp. 554-558.

2308 Zhou Y, Luo Q, Chen H, He A, Wu J. A discrete invasive weed optimization algorithm for solving traveling
 2309 salesman problem. Neurocomputing 2015; 151: 1227-1236.

2310

2311

2312

2313